An Introduction to Local Multipoint Distribution Services with an Investigation into the Effects of Vegetation on the Radio Channel

by

Edward P. Manning

Thesis submitted to the Faculty of the Virginia Polytechnic Institute and State University in partial fulfillment of the requirements of the degree of

Master of Science

in

Electrical Engineering

APPROVED:

Charles W. Bostian, Chairman

William A. Davis

Tim Pratt

January 13, 1999
Blacksburg, Virginia

Keywords: Local Multipoint Distribution Services, LMDS, Vegetative Fading, Propagation

An Introduction to Local Multipoint Distribution Services with an Investigation of the Effects of Vegetation on the Radio Channel

Edward P. Manning

(ABSTRACT)

This thesis takes the reader through an overview of issues pertinent to Local Multi-point Distribution Services (LMDS). The reader will first learn what LMDS is and then review the system architectures that are made available for LMDS technologies. After summarizing the basics of LMDS, we will compare it with some competing technologies.

The reader will then be guided through the aspects of millimeter (mm) wave radio link design. This should be a good lead into the experiment section, since it is suspected that the reader would want to be aware of what design techniques are involved in mm-wave radio link design and what issues may pose potential problems and how they may be mitigated.

Of the potential problems posed in the mm-wave radio link design section, one will be further investigated experimentally. This is the investigation of the effect of vegetation on the magnitude, phase and error vector magnitude (EVM) performance of an LMDS channel. The motivation for this experiment came from the review earlier work, which showed an unexpected relationship between carrier to noise ratio (C/N) and bit error rate BER.

Table of Contents

List of Figures

List of Tables

Acknowledgements

I would like to thank my advisor, Dr. Charles Bostian, and my committee members, Dr. William Davis and Dr. Tim Pratt. Dr. Bostian has been an exceptional advisor. Throughout my graduate studies, he has been consistently patient and approachable. Furthermore, I have benefited tremendously from his technical knowledge and experiences. I am grateful to Dr. Pratt and to Dr. Davis for providing guidance throughout my research and for reviewing my thesis.

Many people and organizations have contributed directly to this research. I wish first of all to thank Hewlett Packard, mm-Tech, the Center for Wireless Telecommunications (CWT), and Dr. Warren Stutzman for lending me the transmission and test equipment needed to complete the studies discussed in this paper. Additionally, I would like to express my gratitude to the people who invested both their time and effort to assist me in taking the propagation measurements. These include Dr. Bostian, Dr. Pratt, Woody Farley, Katina Reece, Eric Johnson, Ben Grady, and Mannin Dodd.

I would also like to thank another group of people who have contributed to my graduate studies in both direct and indirect ways. These include John Nichols and the staff at CNS; Dr. Dennis Sweeney, Woody Farley, Angie Rutledge, and Melanie George of the CWT; and my friends and colleagues I met while here at Virginia Tech.

Finally, but most importantly, I wish to thank my family for their continuous support and encouragement.

Chapter 1.0 Introduction

This thesis will educate the reader about LMDS. Specifically it will address LMDS issues, architectures, and services seen to be competitive with the technology. It will then guide the reader through mm-wave radio link design. This should provide the tools necessary for the reader to approach the implementation of an LMDS radio link successfully.

We then picked one of the design topics to investigate further; this happened to be the effects of vegetation on the radio channel.

Chapter 2.0 What is LMDS?

LMDS stands for Local Multi-point Distribution Services. The acronym LMDS is derived from the following [1]:

> L (local) — denotes that propagation characteristics of signals in this frequency range limit the potential coverage area of a single cell site; ongoing field trials conducted in metropolitan centers place the range of an LMDS transmitter at up to 5 kilometers.
>
> M (multipoint) — indicates that signals are transmitted in a point-to-multipoint or "broadcast" method; the wireless return path, from subscriber to the base station, is a point-to-point transmission
>
> D (distribution) — refers to the distribution of signals, which may consist of simultaneous voice, data, Internet, and video traffic
>
> S (service) — implies the "subscriber" nature of the relationship between the operator and the customer; the services offered through an LMDS network are entirely dependent on the operator's choice of business

This broadband wireless millimeter wave technology operates in the 27 – 31GHz region in the US. The frequency bands of operation for the US and other countries are listed in Table 2.1 below.

Table 2.1. LMDS/LMCS (Local Multi-point Communications System) Frequency Allocations for the USA and Other Countries [2]

Country	Frequency Range (GHz)	Bandwidth (MHz)
USA (LMDS)	27.50 - 28.35	850
	29.10 - 29.25	150
	31.00 - 31.30	300
Venezuela (LMDS)	27.50 - 28.50	1000
	28.50 – 29.50	1000
	31.00 – 31.30	300
Argentina (LMCS)	25.35 – 26.35	1000
	26.35 – 27.35	1000
	27.35 – 28.35	1000
	29.10 – 29.25	150
	31.00 – 31.15	150
	31.15 – 31.30	150
Canada (LMCS)	25.85 – 26.35	500
	26.35 – 26.85	500
	26.85 – 27.35	500
	27.35 – 27.85	500
	28.35 – 28.85	500
	28.85 – 29.35	500
	29.35 – 29.85	500
Romania (LMCS)	27.50 – 28.00	500
	28.00 – 28.50	500
South Korea (LMCS)	24.25 – 24.75	500
	25.50 – 26.70	1200
	26.70 – 27.50	800
France (LMDS)	27.50 – 29.50	2000
Philippines (LMDS)	25.35 – 26.35	1000
	26.35 – 27.35	1000
	27.35 – 28.35	1000
Russia (LMDS)	27.50 – 29.50	2000

In the US this frequency spectrum was put up for sale in 493 basic trading areas (BTA's). This was the most spectrum ever auctioned. The frequency band was split into A and B blocks. The A block spans the 27.500 – 28.350 GHz, 29.100 – 29.250 GHz, and 31.075 – 31.225 GHz frequency bands, while the B block spans the 31.000 – 31.075 GHz and 31.225 – 31.300 GHz frequency bands. This equates to a total of 1300 MHz with 1150 MHz being allocated to the A block and 150MHz being allocated to the B block.

Chapter 2.1 Why LMDS?

Why is there a need for LMDS? In the last decade PC's have become crucial communications tools, now found in many businesses and US households. Most of these PC's are limited by the speed at which they

can communicate to the outside world even though network backbones have been upgraded to accommodate higher data rates [3].

Network backbones are made up of fiber optic cables that can provide $N \times Gbps$ capacity. They were originally designed to support low data rate voice traffic, but are now required to support the increased capacity required for data services (Internet, video conferencing, etc.). These networks have been or are being upgraded to handle the capacity requirements, but the benefactors of the increase in capacity are typically large corporate customers, not the private and small corporate customer. Large corporate customers typically have fiber optic cabling needed for high capacity requirements at their facilities; this is not the case for the private and small commercial customer. In the case of the private and small commercial customer, the backbone network branches off to local exchanges which in turn supply service to the end user. The network that supports the end user within the "local loop" has a data rate limited by the capacity of the copper cabling that provides the "last mile" service. The problem is that the end customer has limited data rate service due to the problem of the fiber optic system interfacing with the data rate limited medium of copper cabling [4].

This is where LMDS fits in. It can make symmetric high data rate communication services affordable to and realistic for the private and small commercial customer. It has the capability to provide various, scalable, and flexible types of broadband system architectures to the local loop. The various architectures that are available through LMDS include point-to-point, point-to-multi-point, and hybrid point-to-multi-point; these will be described later in the thesis. Scalable network architectures provide up front capital cost savings by allowing the build out to occur as the customer base increases. The flexibility of the system really has to do with how wired networks are standardizing to the Asynchronous Transfer Mode (ATM) protocol with LMDS following this trend. Since this is the case, LMDS to land based network integration issues should be made simpler and more cost effective. Also, with ATM the provider will be able to provide flexibility of services since ATM supports certain levels of quality of service (QoS) which will provide the metrics needed to support simultaneous voice, video, and data traffic over the network.

The aforementioned providers will not be the incumbent local exchange carriers (ILEC). This was an FCC mandate to stimulate competition in the local loop; the providers discussed here are normally referred to as competitive local exchange carriers (CLEC).

2.2 CLEC vs. ILEC via LMDS

One would ask how can a CLEC compete with an ILEC that has paid for its infrastructure. The answer is LMDS can act as a bypass to the local loop. The LMDS services provided by the CLEC's have to exceed

the quality and pricing of existing services; advanced services not being offered by ILEC's need to be offered as well at superior quality and competitive pricing.

LMDS has the capacity to deliver all the video, Internet, and voice services that carriers anticipate will be in demand. It also avoids the unprofitable practice of passing each home with broadband lines whether they use the service or not; this gives RF transmission a competitive edge. The engineering firm of Hicks & Ragland of Lubbock, TX estimated that carriers will spend between $2000 and $2750 per subscriber to establish LMDS service. Their conclusion is that LMDS remains less costly per subscriber than any other networking approach when the network penetrates 35% or less of a given area. This implies to the competing service provider that if they are anticipating low market penetration either at present or for years to come, then they are better off in choosing a broadband wireless service like LMDS [5].

2.3 Lessons Learned from LMDS First Deployment

The first provider of LMDS services in the US was CellularVision USA under a pioneer's preference A-block license. Their initial offering was one-way video service, in competition with existing cable franchise. This was Cellular Vision's mistake.

CellularVision made the decision to install analog video service because the up front cost for the head end equipment was a lot lower than digital head end equipment. Estimates from Hicks & Ragland are that it costs between $0.8 - $1 million to build an analog cable TV head end and the same digital head end would cost between $4.5 million to $5.5 million [5]. This decision meant that CellularVision was simply trying to match the cable service that already existed and not provide superior services. This did not attract much of a customer base.

The other mistake had to do with the advent of business data and high speed Internet access. CellularVision's investors had shifted their focus from wireless cable television to these type services. By the time CelluarVision was able to get such services in place (June 1997) they did not attract much attention since most other vendors of LMDS equipment were taking that approach [5]. This caused CellularVision to lose its spot as an LMDS leader and not have the capital to even participate in the LMDS auctions.

What happened to CellularVision should be heeded by all in the LMDS industry. As was mentioned earlier if an LMDS service provider wants to compete against existing services, the LMDS service offerings must be of higher quality and competitive pricing. Advanced service offerings should be a high priority for LMDS; this may be the key to enticing new customers.

Chapter 3.0 LMDS System Architectures

There are three predominant architectures for the provision of LMDS and other terrestrial wireless communications. These architectures are "termed" point-to-point, point-to- multipoint, and hybrid point-to-multipoint.

A brief definition of each architecture should help in understanding the above-mentioned terminology.

- Point-to-point: A communications system where the terminals at either end of the transmission path are dedicated to communicating with each other.
- Point-to-multipoint: A communications system where a hub terminal at one end of the transmission path communicates with many other terminals. These "many" terminals in the reverse direction communicate with the single hub terminal. The coverage area in this type of system is sectorized and usually covers 90°/sector. The customer base typically ranges from 250-1000 users per sector.
- Hybrid point-to-multipoint: A communications system where a hub terminal at one end of the transmission path communicates with a few other terminals. These "few" terminals in the reverse directions communicate with the single hub terminal. The coverage area in this type of system is sectorized and usually covers 15°-30°/sector. The customer base typically ranges from 1-12 users per sector.

There are technical, fiscal, and logistical tradeoffs to each of these architectures. The technical tradeoffs basically come down to: how many customers can services be provided at a given data rate, and what type of services can be provided to them. The fiscal tradeoff is based on being competitive with local services. If you cannot be competitive with local services or offer an improvement to that service then there is no use in doing the deployment. This forces the designer to find a niche market for the technology or to come up with a mechanism for delivering services that will beat any competitors. The logistical tradeoff being the availability of equipment and necessary lead-time to meet project deadlines is determined by contacting LMDS equipment vendors. In contacting these vendors it is typically found that they are focused on providing one of the architectures mentioned above. The other issue that is addressed at that time is whether they have the equipment for sale in production volumes. The answer to this, in most cases, is "not at the present, but maybe by the second quarter of 1999". This tells us that many of the system vendors are not going to be prepared to sell equipment for some time, and when they are, initial pricing will be high.

Chapter 4.0 Competitive Services

The services which seem to be in direct competition with LMDS at present are cable modems, Asymmetric Digital Subscriber Line (ADSL) and Multi-Channel Multipoint Distribution Services (MMDS). The intent of this section is to give the reader a high level technical understanding of each of the mentioned technologies. From this it is hoped that the reader can see that LMDS is not the only solution to solving the

"local loop" problem, but one within a suite of services that may stand on its own or integrate with others to solve this problem.

4.1 Cable Modems

The cable television (CATV) system was originally designed to provide television services, but is now being used to provide other services; for example telephone , Internet, etc. It operates over the existing cable television infrastructure.

The basic structure of a CATV system (Figure 4.1) in which a cable modem operates consists of five parts[6]:

1. The headend.
2. The main line or trunk cable.
3. The distribution or bridged cable into the neighborhood.
4. The drop cable to the home and in-house wiring.
5. The consumer electronics equipment within the home.

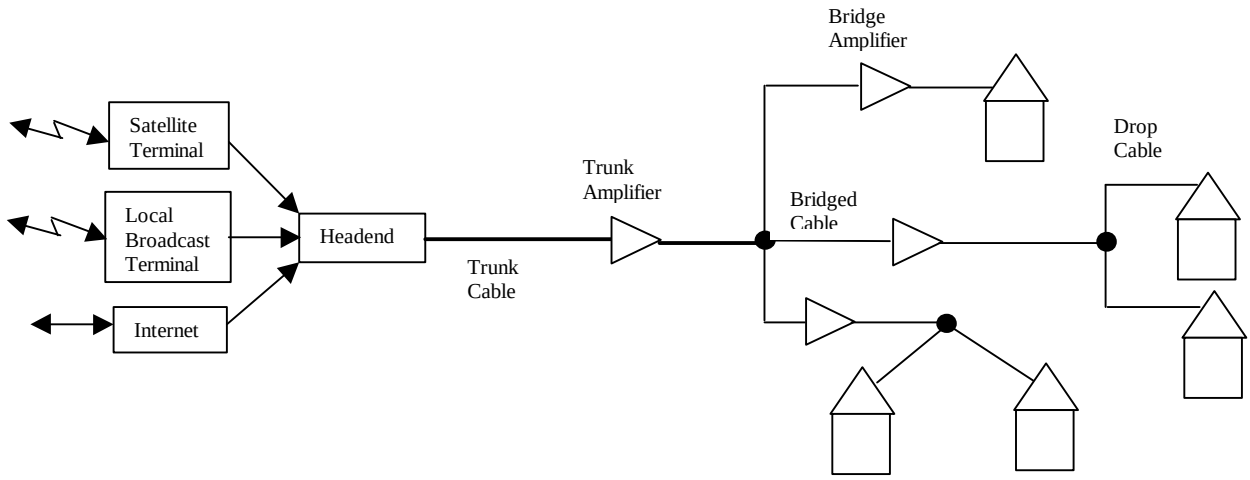

Figure 4.1 Basic Structure of a Cable Television System [7]

The headend receives and in turn retransmits satellite and local broadcasts and acts as an Internet service provider (ISP). To achieve area wide coverage the trunk cables from the head end are branched ("bridged") like a tree into a neighborhood. The bridged line, as it passes houses, is then split again - this time in the form of a drop line to a house. As the signals travel from the headend they are attenuated; to overcome this attenuation amplifiers are put in line. To provide for two-way communication over the cable

plant the amplifiers implemented in the system must include circuitry to separate and amplify upstream and downstream signals. If this can't be done, then the CATV systems will only allow for downstream traffic, and the upstream traffic must be handled over a dial-up connection. This may be a CATV systems owner's alternative if an upgrade for two directions is seen as cost prohibitive.

The cable modem modulates and demodulates data to and from the cable system "network". It sends modulated data in the downstream direction, from the headend to the user location, on a 6MHz television carrier between 42MHz and 750MHz. The modulation schemes used in the downstream are typically QPSK (≤ 10Mbps) or 64QAM (≤36Mbps). This signal can be placed in a 6MHz channel with adjacent television signals on either side without causing interference to the television signals [6].

The upstream direction is harder to implement than the downstream direction. This is not only due to the electronics that need to be implemented for two way communication, but the band in which it is transmitted (5-40MHz) allows for only about four usable channels. Users will contend for much less bandwidth in the upstream than in the downstream, requiring the implementation of multiple access TDMA, CSMA, etc [7]. In this band electromagnetic interference (EMI) also tends to be a problem. The EMI is generated from sources like amateur radio, impulse noise from house appliances, etc. It is introduced easily through the home due to factors such as loose connections and poor cabling. All the generated noise is added together in the upstream direction, due to the tree architecture of the CATV system. This is causing manufacturers to provide modems with QPSK implemented for the upstream modulation scheme. Although QPSK offers a lower data rate than other modulation schemes such as 16QAM or 64QAM, it is more robust to noise [6].

4.2 Asymmetric Digital Subscriber Line (ADSL)

The public switched telephone network (PSTN) was originally designed for a high level of voice calls averaging 3-5 minutes. Analog modem calls are treated like voice calls by local and long distance carriers. The problem is that these calls typically last 20 minutes instead of 5 minutes. This is causing the PSTN to overload. Carriers could either upgrade the complete system or move data traffic to a separate network. They are deciding to move the data to a separate network; this is where ADSL comes in (Figure 4.2) [8].

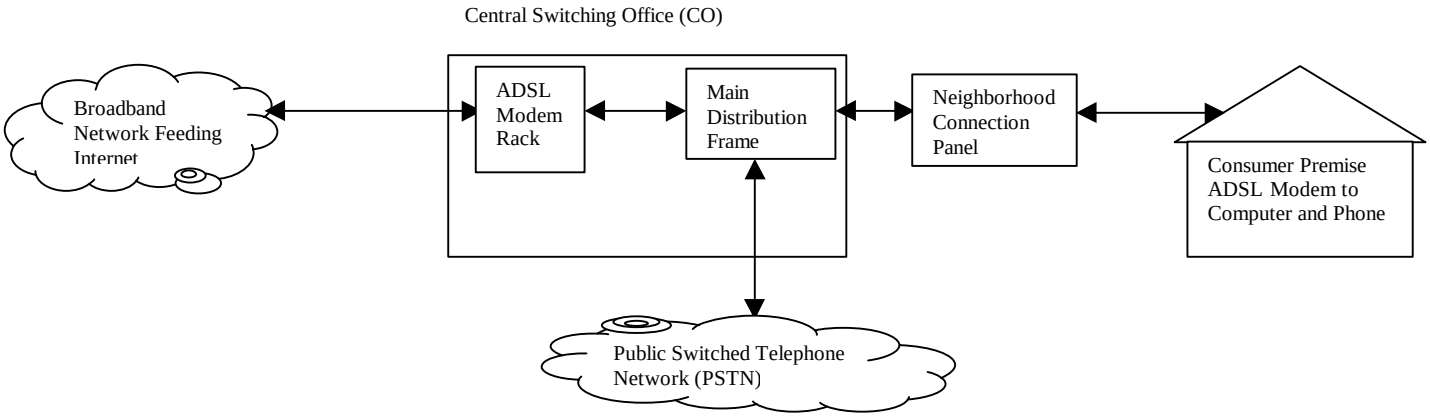

Figure 4.2 ADSL Implementation within Public Switched Telephone Network (PSTN)

ADSL delivers greater bandwidth while utilizing the existing wired infrastructure. It can provide both plain old telephone service (POTS) and data over the same unconditioned twisted pair wire [9]. The customer base it targets is residential, since it provides higher data rates in the downstream than in the upstream.

This comes with some limitations. In ADSL as the distance from the central switching office (CO) increases, the data rate that can be provided decreases (Table 4.1). Other factors that impact performance include gauge of the line, number of times the line is bridged, and cross coupling interference [10]. The maximum distance at which ADSL service can support users from the CO is 18000 feet, which is approximately 75% of all lines in the U.S.

Table 4.1 Data Rate vs. Distance for ADSL Downstream and Upstream Data Paths [8, 10, 11]

Distance (ft.)	Downstream Data Rate (Mbps)	Upstream Data Rate (kbps)
18000	1.544	16
16000	2.048	Insufficient Data
12000	6.312	Insufficient Data
9000	8.448	640

Two line coding techniques have been developed for ADSL. They are Discrete Multi-tone (DMT) and Carrierless Amplitude and Phase (CAP) modulation. Both techniques use algorithms to adjust the data rate relative to the condition of the specific line. Of the two line codes DMT was determined by the ANSI T-1 committee to be the standard line code for ADSL transmission [9]. Considering this, DMT will be the line code which will be looked at more in depth.

DMT divides the channel into a number of sub-channels, referred to as tones, each of which is QAM modulated on a separate carrier (Figure 4.3). The carrier frequencies are a multiple of one base frequency.

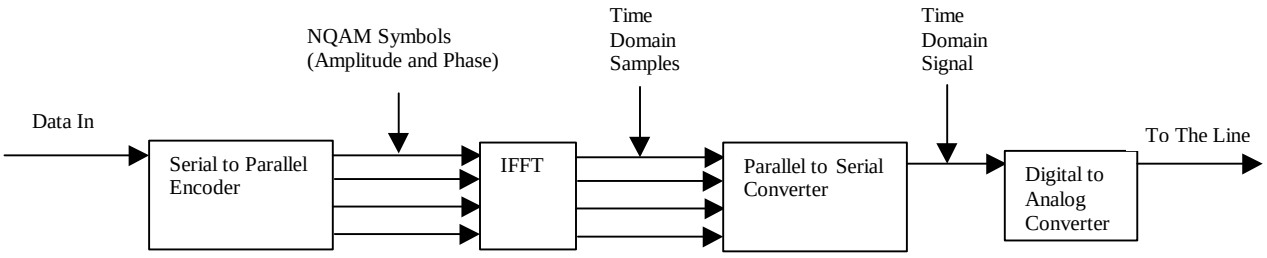

Figure 4.3 DMT Basic Block Diagram

The available spectrum ranges from about 20kHz – 1.104MHz with the spectrum below 20kHz being set aside for voice traffic. The system uses 256 channels for the downstream and 32 channels for the upstream. All channels have a bandwidth of 4.3125kHz and the frequency difference between two successive channels is 4.3125kHz [9]. To support duplex channels ADSL modems use frequency division multiplexing (FDM) for the upstream and downstream communication.

4.3 Multi-channel Multipoint Distribution Services (MMDS)

Multi-channel Multipoint Distribution Services' (MMDS) original application was for a wireless "cable like" television service and distance learning. Since this was the application at the time, the FCC ruled that the MMDS channel was only able to provide a downstream data path. This in recent years has been a hindrance to the success of the MMDS industry. There are a number of factors that caused this to be a hindrance, but two stand out. The first has to do with the wireless cable television service that MMDS provides. This market is an extremely difficult one. If the wireline providers are having a difficult time convincing customers to pay more for service, how is MMDS going to get customers to pay a similar price for less service. The second has to do with the increased need for high data rate services in the "local loop". MMDS was not positioned to provide two-way high data rate services, since it was ruled as being a one way service. It looked like wireline and wireless services threatened to drive MMDS out of business.

As of 9/25/98 the FCC changed its ruling and now allows for two-way transmission on the MMDS radio channel [12]. This may be seen as a savior for the MMDS industry.

MMDS operates in the 2500MHz – 2686MHz band; it is split into 31 6MHz channels. These 6MHz channels may be either subdivided into " subchannels" or combined into " superchannels". The MMDS frequency band has better propagation characteristics than other wireless technologies. Typical cell sizes range to 30 miles with the ability to extend specific cells up to 50 miles with repeater hardware. The system architecture is similar to LMDS point-to-multi-point. Each sector is typically capable of providing data rates of 10Mbps or more [13]. The target market would be for MMDS companies to act as the ISP providing higher data rates at a lower price than could be provided by an ISP depending on T-1 lines.

Chapter 5.0 Terrestrial Millimeter (mm) Wave Radio Link Design

This section of the thesis will take the reader through a high level overview of the information needed to understand the important issues in mm-wave radio link design and therefore LMDS radio link design. Specific items related to LMDS are also included.

5.1 The Generic Digital Radio Terminal

The generic digital radio terminal is typically made up of a transmitter and receiver subsystem (Figure 5.2 and 5.3 [14]). The transmitter subsystem building blocks are the modulator, upconverter with local oscillator, and power amplifier (PA). The receiver subsystem building blocks are the low noise amplifier (LNA), downconverter with local oscillator, and demodulator. The antenna in most cases is shared by both the transmitter and receiver subsystems, but in some cases, separate antennas are used. Baseband conditioning is used to condition the incoming data before it is sent to a modulator. The steps that are typically followed in baseband conditioning are in Figure 5.1 [16]. In order to provide a digital radio link the baseband conditioning steps of sampling, quantization, and digital to analog conversion must be followed. The other steps are optional, but are implemented to provide performance gains within the digital radio link. Some of these will be elaborated on later in the thesis.

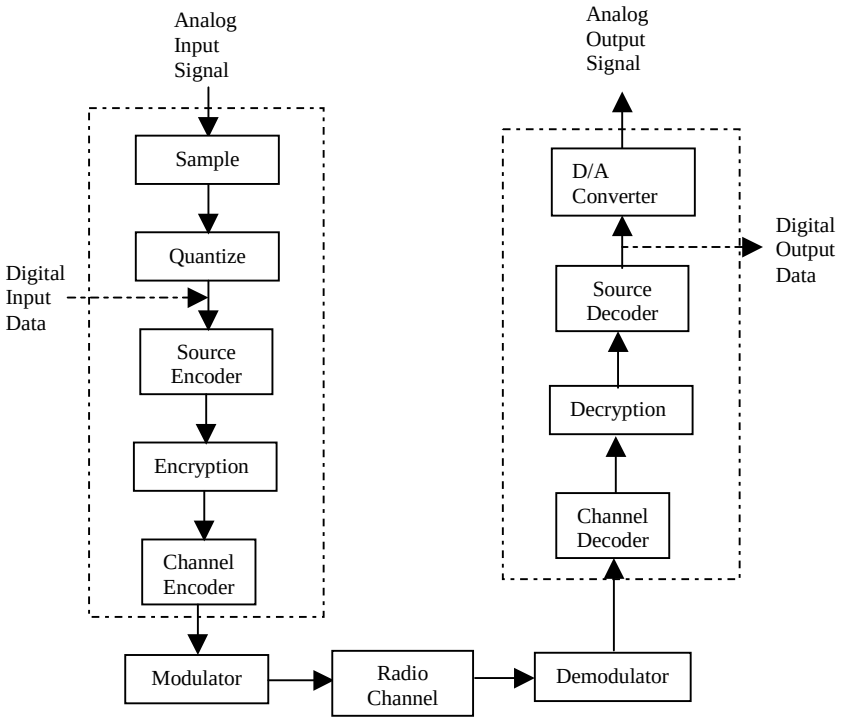

Figure 5.1 Typical Steps Followed in Baseband Conditioning

Both the transmitter and receiver in Figures 5.2 – 5.3 use conventional single-conversion architecture.

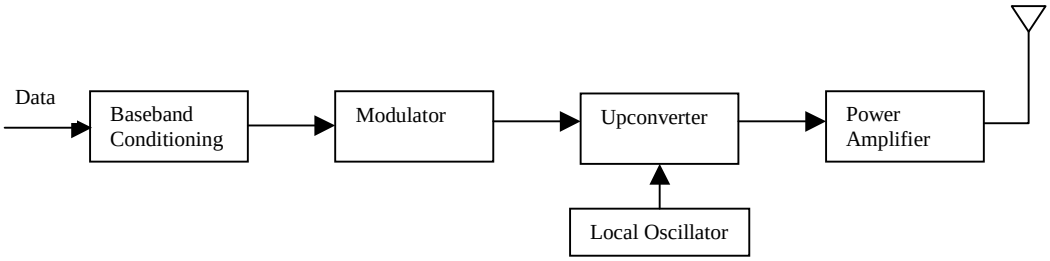

Figure 5.2 Transmitter Section of a Generic Digital Radio Terminal (Single Conversion)

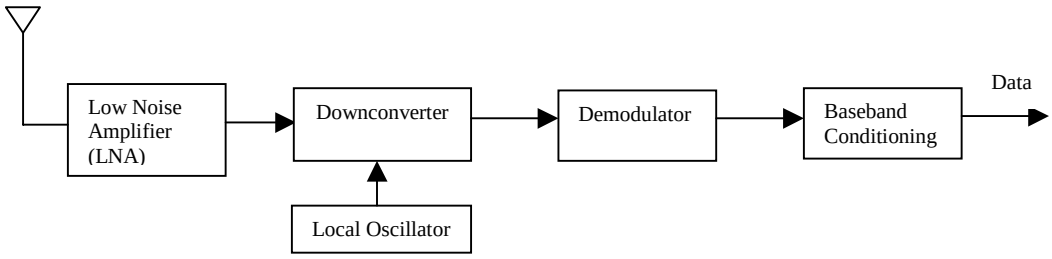

Figure 5.3 Receiver Section of a Generic Digital Radio Terminal (Single Conversion)

5.2 Free Space Model and the Friis Transmission Formula

The Friis transmission formula is the most basic formula that describes the transmission characteristics of a radio link. The formula is as follows:

$$P_r = P_t G_t G_r \left[\frac{\lambda}{4\pi R} \right]^2 \qquad (5.1)$$

The power received at the receiver is signified by P_r. It is equated to the product of the transmitted power P_t, transmitting antenna gain G_t, receiving antenna gain G_r, divided by the free space path loss.

$$pl = \left[\frac{4\pi R}{\lambda}\right]^2 \tag{5.2}$$

An isotropic radiator is a hypothetical lossless antenna radiating equal intensity in all directions [14]; it has a gain of 0dBi. The decibel unit of antenna gain is in reference to an isotropic radiator. As an antenna concentrates transmitted energy or received energy over an effective area antenna gain increases with respect to an isotropic radiator; this is evident in the following equation:

$$G = \frac{4\pi A_e}{\lambda^2} \tag{5.3}$$

The expression for path loss is called the "free space" equation (5.2) since it is given an exponent of the second order. It is considered "free space" when there are no other factors in the radio link path loss other than clear air. If there were other factors involved in the path loss other than clear air the path loss exponent would be greater than two. It is evident that path loss is distance dependent, since R is the distance between the transmitter and receiver and is typically measured in meters or kilometers.

The Friis transmission formula equation (5.1) is usually expressed in the form of decibels as are most communications engineering mathematical expressions. It is expressed in the following fashion:

$$P_r = P_t + G_t + G_r - PL \text{ (dBW or dBm)} \tag{5.4}$$

The product of the transmitter power and antenna gain is typically referred to as the effective isotropic radiated power (EIRP).

$$EIRP = 10\log_{10}\left(P_t G_t\right) \tag{5.5}$$

The decibel expression of received antenna gain and free space path loss is as follows:

$$G_r = 10\log_{10}\left(\frac{4\pi A_e}{\lambda^2}\right) \tag{5.6}$$

$$PL = 20\log_{10}\left(\frac{4\pi R}{\lambda}\right)(dB) \tag{5.7}$$

With this mentioned, equation (5.4) can be rewritten as:

$$P_r = EIRP + G_r - PL \text{ (dBW or dBm)} \tag{5.8}$$

This tells the system designer what the received signal power is at the receiving terminal, but system performance is typically determined by the ratio of the received signal power or carrier to the receiving system noise power.

The equation that defines the system noise power is:

$$P_{sn} = kT_s B \tag{5.9}$$

where k = Boltzman's Constant = $1.38 \times 10^{-23}\ J/K = -228.6 dBW/K/Hz$

T_s = System Noise Temperature in Kelvin (K)

B = Bandwidth of Transmitted Waveform in Hertz (Hz)

In decibel form this equation becomes:

$$P_{sn}(dBW) = -228.6 + T_s + B \tag{5.10}$$

The noise temperature of a receiving system is found in the following manner (Figure 5.4-5.6). Determine what elements make up the receiving system, which is shown in Figure 5.4. The receiving system is made up of a receiving antenna, LNA, downconverter (mixer), and IF amplifier.

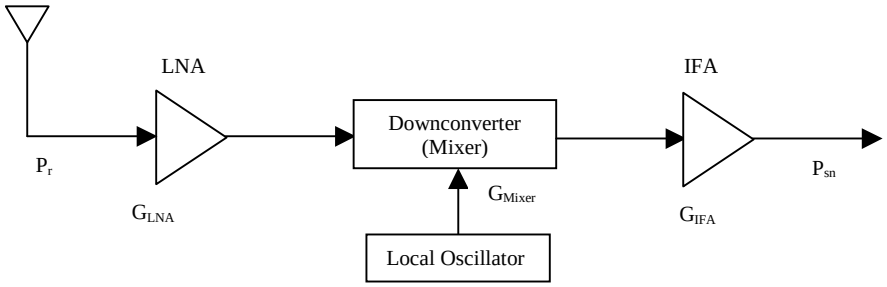

Figure 5.4 System Noise Temperature: Receiving System Block Diagram [18]

Find the noise temperature and gain for each block of the receiving system (Figure 5.5).

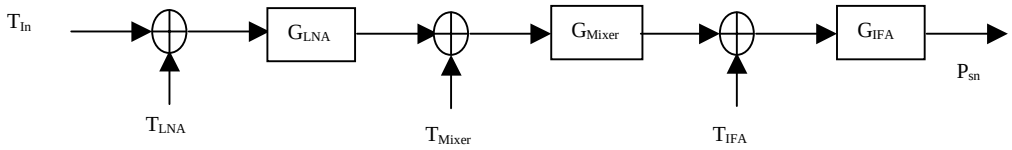

Figure 5.5 System Noise Temperature: Noise Temperature and Gain for Receiving System [18]

The series of equations that relate to Figure 5.5 are as follows:

$$P_{sn} = G_{LNA} G_{Mixer} G_{IFA} k T_s B \tag{5.11}$$

In essence equation (5.11) states that the receiving system noise power (P_{sn}) can be found if Boltzman's constant, the receiving system bandwidth, the gain of each element of the receiving system, and the system noise temperature are known. Let us now move on to determining the system noise temperature.

$$T_s = \left[T_{In} + T_{LNA} + \left(\frac{T_{Mixer}}{G_{LNA}} \right) + \left(\frac{T_{IFA}}{G_{LNA} G_{Mixer}} \right) \right] \tag{5.12}$$

Equation (5.12) shows that the system noise temperature is related to the sum of the noise temperature of the receiving system components multiplied by the gains of the appropriate stages that the noise is going through. By looking at this description Figure 5.5 can be redrawn as:

Figure 5.6 System Noise Temperature: Block Diagram Equivalent of Figure 5.5

The receiver system noise power can now be expressed as:

$$P_{sn} = kT_s BG_s \tag{5.13}$$

When relating the received signal power or carrier to the noise power the gain terms cancel out as can be seen in equation (5.14)

$$\frac{C}{N} = \frac{P_r G_s}{P_{sn} G_s} = \frac{P_r}{kT_s B} \tag{5.14}$$

With this result equation (5.15) expresses the carrier to noise ratio (C/N) in decibel form.

$$\frac{C}{N} = \frac{P_r}{P_{sn}} = EIRP + G_r - PL + 228.6 - T_s - B(dBW) \tag{5.15}$$

An LMDS radio link carrier to noise ratio can be expressed in the following manner equations (5.16-5.18).

$$\frac{C}{N} = EIRP + G_r - \left(20\log_{10} R + 20\log_{10}\left(\frac{4\pi}{\lambda}\right)\right) + 228.6 - T_s - B \tag{5.16}$$

The transmitted frequency of 28GHz corresponds to a wavelength of $\lambda = 0.01071$m. This is found via equation (5.17).

$$\lambda = \frac{c}{f} = \frac{3\times10^8}{28\times10^9} = 0.01071m \tag{5.17}$$

This allows equation (5.16) to be reduced to

$$\frac{C}{N} = EIRP + G_r - 20\log_{10} R(m) + 167.21 - T_s - B \tag{5.18}$$

The carrier to noise ratio is typically a measure of system performance for an analog radio system.

5.2.1 Digital Communications

The measure of performance of a digital radio system is probability of bit error P_e. It is calculated from E_b/N_o, which is the energy per bit divided by the noise power per Hertz.

The relationship between P_e and E_b/N_o depends on the type of digital signaling used [19]. Table 5.1 shows the mathematical relationship between P_e and E_b/N_o for a few types of digital modulation. In presenting this relationship it is seen that P_e is related to E_b/N_o through the argument of the Q function [21].

Table 5.1 Mathematical Relationship between P_e and E_b/N_o

Modulation	Probability of Bit Error (P_e)
BPSK, QPSK	$Q\left[\sqrt{\left(2\frac{E_b}{N_o}\right)}\right]$
16QAM (Gray Coded)	$\frac{3}{4}Q\left[\sqrt{\left(\frac{4E_b}{5N_o}\right)}\right]$
Non-coherent DPSK	$\frac{1}{2}\exp\left(-\frac{E_b}{N_0}\right)$
Coherent FSK	$Q\left[\sqrt{\left(\frac{E_b}{N_o}\right)}\right]$

These relationships can be viewed graphically in Figure 5.7.

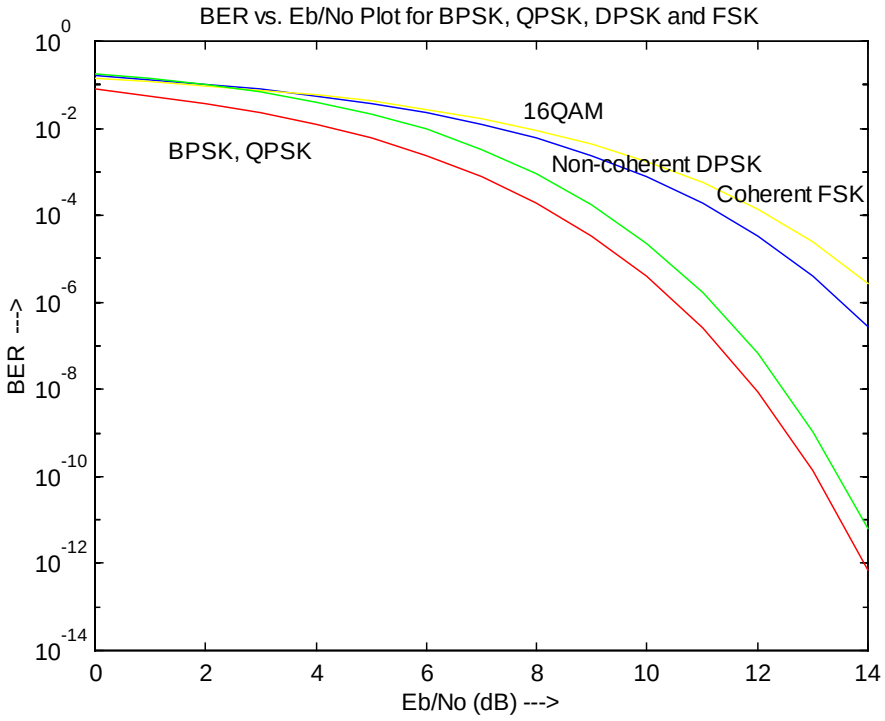

Figure 5.7 Graphical Relationship between Probability Bit Error Rate (P_e) and E_b/N_o

It can be deduced from the mathematical and graphical relationship that, as the BER is lowered, the E_b/N_o needs to be increased to achieve the required level of performance. This measure of performance for a given type of signaling shows how much energy needs to be expended in order to achieve a specific P_e. Another measure of performance for a given type of signaling is the bandwidth efficiency equation (5.20). It measures how efficiently a type of signaling uses bandwidth and it is measured in bits/(second x Hertz).

$$\eta_B = \frac{R_b}{B}(b/sHz)) \tag{5.20}$$

Where R_b is the bit rate and B is the bandwidth of the transmitted waveform. The relationship between R_b and B (equation (5.21-5.24)) is dependent on the type of signaling used (M-ary QAM, M-ary PSK, etc.) and whether the signal is baseband or bandpass.

For baseband signaling:

$$\text{Rectangular pulse shaping: } B = \frac{R_b}{\log_2 M} \tag{5.21}$$

$$\text{Raised cosine pulse shaping: } B = \frac{R_b(1+r)}{2\log_2 M} \tag{5.22}$$

and for bandpass signaling:

$$\text{Rectangular pulse shaping: } B = \frac{2R_b}{\log_2 M} \tag{5.23}$$

$$\text{Raised cosine pulse shaping: } B = \frac{R_b(1+r)}{\log_2 M} \tag{5.24}$$

where M is the number of levels of signaling (e.g. QPSK: M=4).

Some examples of bandwidth and power efficiency for various types of digital signaling are found in Tables 5.2-5.4 [21].

Table 5.2 Bandwidth and Power Efficiency of M-ary PSK Signals [21]

M	2	4	8	16	32	64
η_B	1	2	3	4	5	6
E_b/N_o for BER=10^{-6}	10.5	10.5	14	18.5	23.4	28.5

Table 5.3 Bandwidth and Power Efficiency of M-ary QAM Signals [21]

M	4	16	64	256	1024	4096
η_B	2	4	6	8	10	12
E_b/N_o for BER=10^{-6}	10.5	15	18.5	24	28	33.5

Table 5.4 Bandwidth and Power Efficiency of Coherent M-ary FSK Signals [21]

M	2	4	8	16	32	64
η_B	0.4	0.57	0.55	0.42	0.29	0.18
E_b/N_o for BER=10^{-6}	13.5	10.8	9.3	8.2	7.5	6.9

In reviewing Tables 5.2-5.4, M-ary QAM has the same bandwidth efficiency as M-ary PSK and is more bandwidth efficient than M-ary FSK. M-ary FSK is more energy efficient than both M-ary QAM and PSK with M-ary QAM being more energy efficient than M-ary PSK.

Now refer back to Figure 5.1, which shows the steps followed in baseband signal conditioning. We will now comment briefly upon the processes that provide performance gains within this part of the system.

At the transmitter side the *quantizer* makes the incoming signal discrete in amplitude, but it introduces distortion into the system. Good quantizers are able to use few bits and introduce small distortion [16]. The types of quantizers that perform this optimization of quantization levels are the scalar and vector quantizer. Some of the algorithms used in scalar and vector quantizers to perform this optimization are the Lloyd Max and K-means or Generalized Lloyd Max. *Source coding* compresses digital data to eliminate redundant information. It is like quantization because its goal is to reduce bit rate, but it is unlike quantization since it does not introduce distortion [16]. Two types of source coding are the Improved Lempel Ziv Algorithm and the Huffman Algorithm. *Encryption* is used to ensure data privacy [16]. It provides a coding of data which is difficult to decode unless the receiver has the key to decode the data. *Channel encoding* otherwise referred to as *forward error correction coding* (FEC) provides protection against transmission errors by selectively introducing redundant data into the bit stream [16]. It is defined as a method of error control that employs the adding of systematic redundancy at the transmit end of a link such that many or all of the errors caused by the medium can be corrected at the receiver by means of a decoding algorithm [14]. FEC performance enhancement is referred to as coding gain, which is typically in the range of 2-6dB. The price paid for introducing FEC is an increase in bandwidth due to the introduction of redundant information into the bit stream. This redundancy is reflected upon at the symbol rate (R_s) level. Equation (5.25) shows the relation between symbol rate and bit rate (R_b), where l is the number of bits per symbol and M is the number of levels being used for the modulation chosen (i.e. 16QAM; M=16; l=4).

$$R_s = \frac{R_b}{l}; l = \log_2 M \tag{5.25}$$

The reflected change in R_s is shown in equation (5.26) and the new designation of encoded symbol rate is R_c.

$$R_c = \frac{R_s}{CR} \tag{5.26}$$

The term CR in equation (5.26) is referred to as the code rate. With CR<1 it can be deduced from equation (5.26) that the encoded symbol rate has increased; therefore a bandwidth increase will also take place assuming no change in modulation. Types of FEC that are commonly used in communications links are Reed-Solomon, BCH, Viterbi, etc. At the receive side the *decoder's* job is to choose which transmitted codeword most closely resembles the received sequence of bits [16]. As long as the decoder does its job properly and produces a reliable replication of the bits that where sent the *decryption* device acts like a key to decrypt encrypted information. *Source decoding* would decode what was encoded at the transmitter, basically re-inserting redundant information. The *digital to analog (D/A)* converter would then convert the waveform back to analog.

If a digital data stream, from a computer, were to be the source instead of an analog data stream, from a telephone, data would be input and output at the spots labeled "input digital data" and "output digital data" in Figure 5.1.

The relationship between C/N and E_b/N_o (equation (5.27)) should now be discussed in light of the previous discussion about the relationship between BER and E_b/N_o, efficiency, and processing performance.

$$\frac{C}{N} = \frac{E_b R_b}{N_o B} \tag{5.27}$$

Therefore E_b/N_o is

$$\frac{E_b}{N_o} = \frac{CB}{NR_b} \tag{5.28}$$

Equation (5.29) describes E_b/N_o in decibel form for an LMDS radio link operating at 28GHz.

$$\frac{E_b}{N_o} = EIRP + G_r - 20\log R(m) + 167.21 - T_s - R_b \tag{5.29}$$

5.3 Power or Link Budget

In looking at both the expression for C/N equation (5.18) and E_b/N_o equation (5.29) it can be seen that the computation looks like a budget and is often called a power or link budget [22]. It is typically expressed in tabular form. An example of a clear weather link budget is in Table 5.5. By clear weather it is meant that there are no weather disturbances and that the transmitter has a clear line of site to the receiver.

Table 5.5 Clear Weather Link Budget

	Linear Value	Units	Logarithmic Value	Units
Transmitter Power	1	W	0	dBW
Transmit Antenna Gain			36.0	dB
Receive Antenna Gain			30.0	dB
Path Length	1000	Meters	60.0	dBmeters
Path Loss			121.39	dB
Received Power			-55.39	dB
Receiver Noise Figure			4.0	dB
Receiver Noise Temp.	437.9	K	26.41	dBK
Receiver Antenna Noise Temp.	300.0	K	24.77	dBK
System Noise Temp.	737.9	K	28.68	dBK
Bandwidth	1.5	MHz	61.76	dBHz
Receiver Noise Power			138.16	dBW
Clear Weather C/N			82.77	dB

In reviewing this clear weather link budget it is seen that there is an 82.77dB clear weather C/N. In analog communication radio links a C/N is specified to tell the designer what the minimum is for adequate link performance. The difference between the clear air C/N and the specified C/N is called "margin" (equation (5.30)).

$$\text{Margin} = \frac{C}{N_{cw}} - \frac{C}{N_{spec}}(dB) \qquad (5.30)$$

Therefore if a minimum C/N for the link budget above is specified to be 12dB the margin will be 70.77dB.

The next step is to move to an example clear weather link budget for a digital radio link (Table 5.6). This example will show what E_b/N_o and C/N are required to meet performance minima for a BPSK digital radio link operating at 1.5Mbps. From this a margin will be established.

Table 5.6 Clear Weather Link Budget for a Digital Radio Link

	Linear Value	Units	dB	Units
BER (P_e)	10^{-6}			
Required E_b/N_o			13.5	dB
Required C/N			10.5	dB
Transmitter Power	1	W	0	dBW
Transmit Antenna Gain			36.0	dB
Receive Antenna Gain			30.0	dB
Path Length	1000	Meters	60.0	dBmeters
Path Loss			121.39	dB
Received Power			-55.39	dB
Receiver Noise Figure			4.0	dB
Receiver Noise Temp.	437.9	K		
Receiver Antenna Noise Temp.	300.0	K		
Receiver Noise Temp.	737.9	K	28.68	dBK
Data Rate	1.5	Mbps	61.76	dBbps
Bandwidth	3.0	MHz	64.76	dBHz
Receiver Noise Power			138.16	dBW
Clear Weather E_b/N_o			82.77	dB
Clear Weather C/N			79.77	dB

The clear weather C/N from Table 5.6 is 79.77dB and the required C/N was 10.50dB. Therefore the clear weather margin for this radio link is 69.27dB.

Considering what was just discussed a valid question to be asked would be "why design margin into a radio link if the required C/N or E_b/N_o is already met"? Margin is designed into a radio link because radio links undergo fading and attenuation. Fading and attenuation are described as follows:

Fading is any reduction in clear weather line of sight signal strength [22].

Attenuation is the dB reduction in signal strength due to something in the path that absorbs or obstructs the signal [22].

Attenuation and fading are not synonymous. Attenuation is one cause of fading [22]. Some of the other mechanisms that cause fading will be discussed in upcoming sections of the thesis.

5.4 Tradeoffs in the Link Budget

To achieve an acceptable level of performance in a radio link certain tradeoffs need to be made. These tradeoffs will be addressed in this section and the digital radio link budget (Table 5.6) will the source of our reference data.

We will start by looking at the BER requirement. This requirement will determine the required E_b/N_o and C/N are in order to meet minimum system performance goals as previously mentioned. This is something that really is not adjustable unless a performance specification allows for a varying range of requirements. The transmitter power, transmitter antenna gain, and receiver antenna gain are the parameters of link performance which are most commonly adjusted to meet radio link performance goals, but there are issues relevant to these performance parameters. Transmitter power can be increased but usually not in a linear manner relative to the pricing of the transmitter; this is definitely the case when the link is operating in the 28GHz region as in Table 5.6. The transmitter and receiver antenna gains can also be increased, but as the gain is increased the 3dB beamwidth of the antenna decreases. This can make antenna alignment difficult. A receiver can be designed for a low noise figure, but the limit to which the noise figure can be decreased is governed by the current state of technology and the price that will be paid for it. When given a minimum data rate to support the digital radio link, the designer needs to choose a modulation technique that will fit the data rate within the bandwidth allocated for the channel. One technique that could be used to increase radio link performance relative to data rate would be to use adaptive data rate techniques. This would provide the user with an acceptable nominal data rate when the channel is sensed to be performing in other than a clear weather scenario and would provide a maximum data rate when the channel is sensed to be in a clear weather condition.

When looking at what would need to be done on paper or with a computer to change link performance may seem trivial when in fact it is not. Many topics (pricing, tower loading, system complexity, etc.) not foreseen in the theory need to be addressed in order to make these performance changes.

5.5 Link Availability

Availability is defined as the time a system, link, or terminal is meeting its operational requirements [14]. It is usually expressed as a percentage or decimal (<1). The expression for availability is expressed in equation (5.31).

$$A = \frac{MTBF}{(MTBF + MTTR)} \tag{5.31}$$

Where MTBF stands for mean time between failures and MTTR stands for mean time to repair. Equation (5.32) shows the previous expression with more common terminology

$$A = \frac{uptime}{(uptime + downtime)} \tag{5.32}$$

The expression for unavailability or exceedance is expressed in equation (5.33).

$$U = 1 - A \tag{5.33}$$

There are one way and two way unavailabilities. A one way unavailability can be found via equation (5.33). For a two way unavailability, if each link is considered independent then the total availability is expressed in equation (5.34):

$$A_{Total} = A_{Link1} + A_{Link2} - A_{Link1}A_{Link2} \tag{5.34}$$

Typically the product of A_{Link1} and A_{Link2} is so small that it can be neglected, therefore equation (5.34) becomes:

$$A_{Total} = A_{Link1} + A_{Link2} \tag{5.35}$$

this would then be substituted into equation (5.33) to find the two way unavailability.

For convenience one-way links will be used for the rest of the discussion.

The five major factors that contribute to link availability are [14]:

1. Equipment
    a) Failure/degradation of radio equipment such as modulators and demodulators.
    b) Failure of auxiliary equipment, such as switchover equipment.
    c) Failure of primary power.
    d) Failure of antenna or feeder.
2. Propagation
    a) Excessive precipitation attenuation that is caused mainly by heavy rainfall and, in some cases, heavy snow. Typically the effect lasts 20-30 minutes.
3. Interference: Intermittent noise in excess of a certain limit caused by interference sources that may exist within or outside the system.
4. Support facilities: collapse of towers or buildings in disastrous circumstances.
5. Human error: this includes maintenance downtime/outages.

In referring to the previous listing it would seem logical that unavailability due to equipment failure and propagation effects are dependent upon each other. This is not the case. Equipment failures and propagation effects are independent of each other and should be considered separate. This can be inferred from the high reliability of electronics. Electronic manufacturers design components for low failure rates in which there could be MTBF's of years. The MTTR for an electronic failure could in some instances take days. This would basically make the effort of trying to achieve a high reliability radio link futile. Ways to reduce MTTR and make the high reliability link feasible would be to have automatically switched hot standby backup equipment on site or use Internet based system remote monitoring which could alert a technician prior to a potential system failure. High MTTR's are typically not the case with propagation. It

is something that can be studied and predicted, but humans have no control over certain propagation mechanisms. What we can do as designers is try to design for the worse case predicted effects in an area and hope that our predictions are correct. Availability relative to propagation is measured in hours, minutes, or seconds per year. Propagation outages over a year's period consist of many separate occurrences. The total unavailability time for a 99.999% availability is 87.6×10^{-3} hours or 5.26 minutes per year.

5.6 Refractive Effects and K Factor

Radio waves traveling through the atmosphere do not follow true straight lines; they are refracted or bent (Figure 5.8). This is due to the velocity of an electromagnetic wave being a function of the density of the media through which it travels [15].

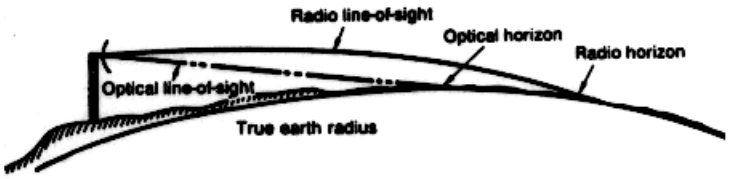

Figure 5.8 Optical Line of Site versus Radio Line of Site [14]

The amount of refraction depends on the gradients of temperature and humidity and is most significant in coastal regions and deserts [22]. This curvature of the rays is taken into account by introducing an effective earth radius factor K, where K=1 relates to the radio waves being on a straight line, K<1 relates to radio waves being bent away from the earth, and K>1 relates to radio waves being bent towards the earth. The K factor comes into effect when plotting path profiles. The curvature of the earth is modified in such a way by the K factor that straight lines can represent the ray paths (Figure 5.9).

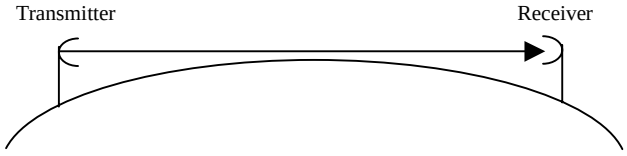

Figure 5.9 K Factor Effect on Ray Path

The curvature of the earth and atmospheric refraction cannot be neglected in path lengths greater than 10km [24]. The earth's bulge at a point in the radio link is approximated by:

$$h_t = \frac{d_1 d_2}{2Kr_t} \times 1000 \qquad (5.36)$$

Where: h_t = the earth's bulge at a point on the path

d_1 = the distance from one side of the radio link labeled point A to the bulge point on the path

d_2 = the distance from the other side of the radio link labeled point B to the bulge point on the path.

K= the effective earth radius factor

r_t = earth's radius

For gross planning of radio links K=4/3 is typically used. This is relative to the refractive effects of a standard atmosphere, making the earth appear flatter by a factor of 1/3 [22].

Since LMDS radio links are typically at a 5km maximum, refractive effects in most cases can be ignored.

5.7 Knife Edge Diffraction and First Fresnel Zone

Diffraction occurs when an obstacle that is large in comparison to the operating wavelength obstructs a radio wavefront. This causes secondary wavefronts or waves to be generated. These waves are present throughout the transmission space and even behind the obstacle, giving rise to a bending of waves around the obstacle, even when a line of site path does not exist between the transmitter and receiver [21] . This provides the opportunity for a receiver to see a transmitter behind an obstacle. Typically this happens at short distances and the non-line-of-site area is called the shadowed area. This incidence with an obstacle or knife edge can be seen in Figure 5.10. Figure 5.10 also shows the first three Fresnel zones, which are cigar shaped volumes that surround the line of site path. By taking a cross section of the transmission space in Figure 5.10 what would be seen is a diffraction pattern or concentric rings similar to age rings when a tree is cross sectioned. The first Fresnel zone is the first volume that surrounds the LOS path and the radial distance that separates the LOS path from the first Fresnel zone is λ/2 or 180°. Similarly additional Fresnel zones are separated by multiples of this distance. Most of the transmitted energy travels in the first Fresnel zone. Thus radio links are most sensitive to objects in the first Fresnel zone.

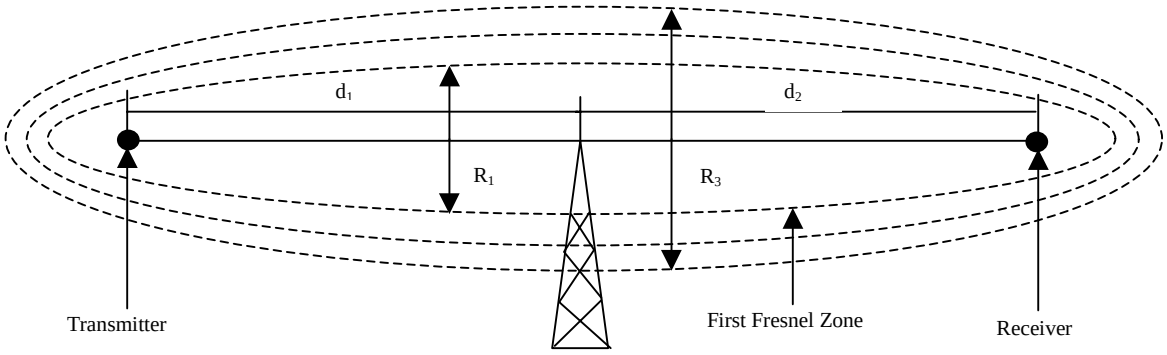

Figure 5.10 Knife Edge Diffraction with Cross Sectional View of First Three Fresnel Zones (h=0)

Equation (5.37) expresses the radius of the nth Fresnel zone

$$R_n \cong 17.3\sqrt{\frac{n}{F_{GHz}}\left(\frac{d_1 d_2}{d_1 + d_2}\right)} \tag{5.37}$$

Where R_n = radius of the nth Fresnel zone in meters

n = order of Fresnel zone

F = the frequency in GHz

d_1 = the distance from the transmitter to the obstacle in kilometers

d_2 = the distance from the receiver to the obstacle in kilometers

If an obstruction does not block 0.6 of the first Fresnel zone layer then attenuation due to that obstacle can be considered minimal. As an illustration of Fresnel zone sizes, the 1.0 and 0.6 first Fresnel zone clearances for a 1km-5km LMDS path are listed in Table 5.7 [22]. In the example distances d_1 and d_2 equal one half the path length.

Table 5.7 1.0 and 0.6 First Fresnel Zone Clearances for a 1km-5km LMDS (F_{GHz}=28GHz) Path

Length, km	1.0 R_1, m	0.6R_1, m
1.0	1.63	0.981
2.0	2.31	1.39
3.0	2.83	1.70
4.0	3.27	1.96
5.0	3.66	2.19

If one was not able to clear 0.6 of the first Fresnel zone, then the following series of equations can be used to calculate attenuation due to diffraction [21].

$$A_d(dB) = 0 \qquad \upsilon \le -1 \tag{5.38}$$

$$A_d(dB) = 20\log(0.5 - 0.62\upsilon) \qquad -1 \le \upsilon \le 0 \tag{5.39}$$

$$A_d(dB) = 20\log(0.5\exp(-0.95\upsilon)) \qquad 0 \le \upsilon \le 1 \tag{5.40}$$

$$A_d(dB) = 20\log\left(0.4 - \sqrt{0.1184 - (0.38 - 0.1\upsilon)^2}\right) \qquad 1 \le \upsilon \le 2.4 \tag{5.41}$$

$$A_d(dB) = 20\log\left(\frac{0.225}{\upsilon}\right) \qquad \upsilon > 2.4 \tag{5.42}$$

Where A_d(dB) is the diffraction attenuation and υ is the Fresnel-Kirchoff diffraction parameter.

Equation (5.43) express this parameter as:

$$\upsilon = h\sqrt{\frac{2(d_1 + d_2)}{\lambda d_1 d_2}} \tag{5.43}$$

In this equation d_1 and d_2 have the same relevance as in equation (5.37) except that they are expressed in meters. Parameter h is the height of the obstruction in meters measured from the straight line between the transmitter and receiver.

5.8 Multipath Fading

Multipath fading occurs when multiple copies of the transmitted signal are received at the receiving antenna. These multiple copies of the transmitted signal arrive by a direct path, if one exists, and by indirect paths (Figure 5.11).

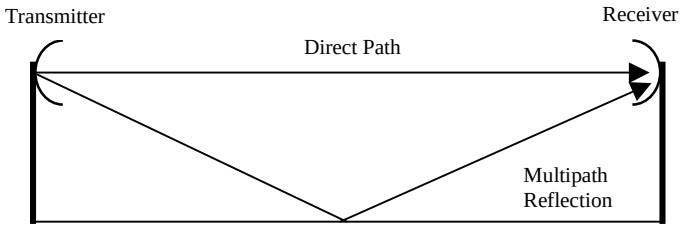

Figure 5.11 Comparison of Direct Ray to Multipath Ground Reflecting Ray

A surface looks smooth or "mirror like" if the following criteria are met in equation (5.44). If this type of reflection occurs it is considered specular reflection. [22]

$$H \leq \frac{\lambda}{8\cos\theta_i} \tag{5.44}$$

Where H =height of the surface irregularity

λ = wavelength

θ_i = angle of incidence (with a 0° measure being perpendicular to the surface and 90° being parallel to the surface)

These reflected waveforms will be delayed in amplitude and phase relative to the direct path waveform, with the phase differences depending upon the differences in path length in relation to the wavelength [24]. When received they will either constructively or destructively interfere with each other. If destructive interference occurs, so will multipath fading.

Mulitpath reflections can be reduced or eliminated by adjusting tower heights, effectively moving the reflection point from an area along the path of greater reflectivity (lakes) to one of lesser reflectivity (forest). If the reflected path is entirely over water or desert, the radio link designer may have to resort to frequency or additional space diversity techniques, since these surfaces typically look smooth most of the time [14].

The reflection point in question is not isolated to one spot but it lies over a range of distance. This is due to the dynamic behavior of the atmosphere, which relates to a varying K value. The procedure for finding the range of reflection points is as follows:

- Determine the transmitter and receiver antenna tower heights and the path length.
- Find the ratio of the tower heights equation (5.45)

$$THR = \frac{h_1}{h_2} \tag{5.45}$$

- From Figure 5.12 find the value of n for K=grazing and K=∞.

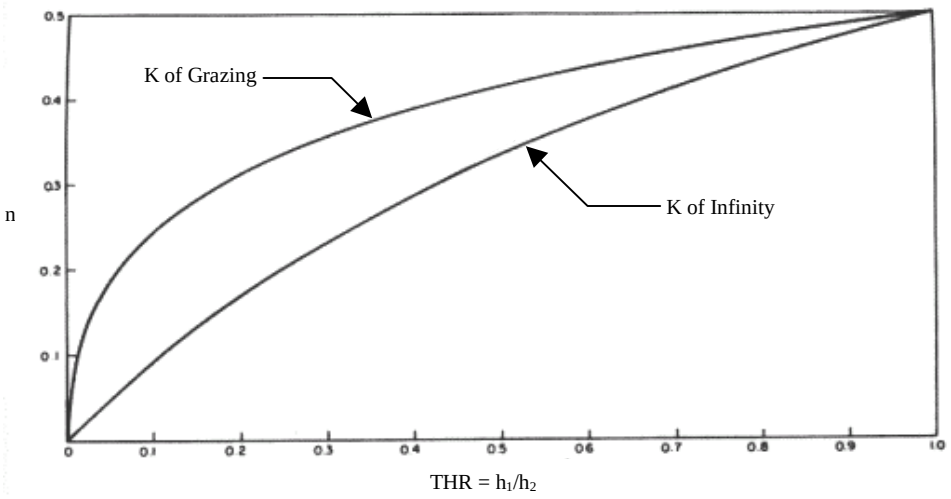

Figure 5.12 Reflection Point Nomogram [14]

- Multiply the path length by the n values found .
- This gives the minimum and maximum range for the reflection point area.

With this information the designer can look at a path profile (discussed later) of the radio link in question and determine whether the reflection point is in a smooth area (lakes). If so antenna heights may need to be changed to put the reflection point into a more desirable area (forest).

At LMDS frequencies multipath problems should be rare because most natural and man made surfaces, excluding chromatic glass, appear to be rough. Measurement results show that these same building materials show that reflected signals are 11.25dB [25] below LOS signals at zero angle of incidence. It

should be noted that at a grazing angle any surface could look smooth; this topic will be addressed on the next page. Additionally, in most applications LMDS transmit and receive antennas will be high gain with narrow beamwidths [22]. An antenna with a narrow beamwidth focuses primarily on the direct ray and eliminates multipath components.

In an urban environment two of the principal reflecting surfaces are the street itself and buildings if the angle of incidence approaches a point where the building surfaces look smooth. Figure 5.13 shows the signal amplitude as a function of range along an asphalt road in a rural area at 28.8GHz [25].

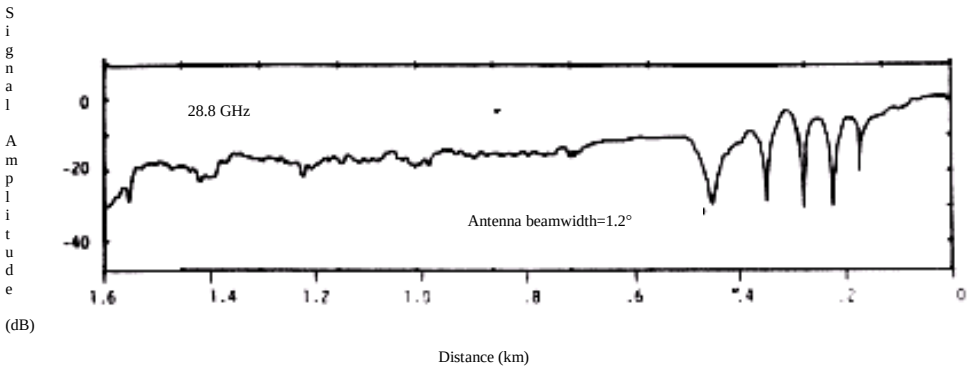

Figure 5.13 Signal Amplitude as a Function of Range [25]

Within the first few hundred meters multipath occurs, but after that the signal becomes stable around approximately –20dB. To look at the other principal reflecting surface a radio link range scan was set up in the middle of a street in downtown Denver, CO. As the scan is conducted the angle of incidence may be increased to a point where surfaces once seen as rough are now smooth (θ_i = 0°; H≤0.13cm; θ_i = 89°; H≤7.67cm). Figure 5.14 shows the signal amplitude as a function of range measured along 17th Street in downtown Denver, CO [25].

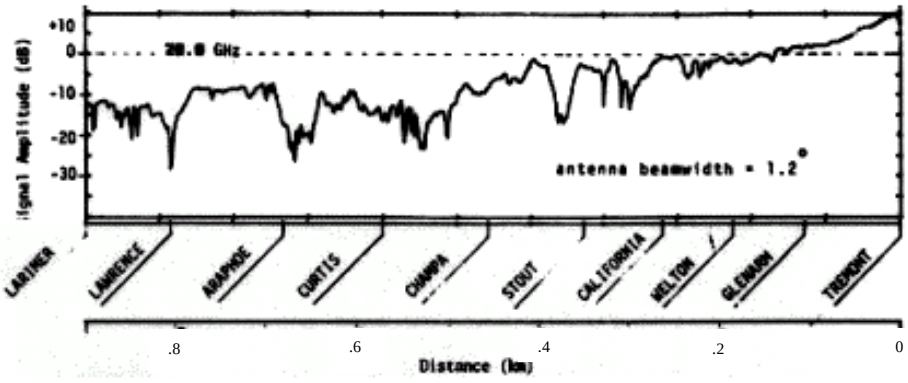

Figure 5.14 Signal Amplitude Measured along 17th St. in Downtown Denver, CO [25]

Note that the urban street range of Figure 5.14 shows fewer deep fades than the rural road scan of Figure 5.13. The reason for this is the presence of many more multipath components due to reflections from the building walls along the street; and these additional reflected signals reduce the probability of deep fades in the received signals. Where a deep fade occurs when the sum of all the multipath signals equals the amplitude of the direct path amplitude but is 180° out of phase with the direct path signal.

5.9 Siting and Path Profiles

The path profile integrates refractive effects, first Fresnel zone, and multipath fading. After reviewing a topographic map of the region of interest, a straight line needs to be drawn connecting the transmitter and receiver. Once this is complete a path profile needs to be done. A path profile confirms terrain clearance and determines required antenna heights. To do a path profile, elevation data on the topographic map needs to extracted relative to the path in question. Looking at the highest, lowest, and intermediate terrain contours between the transmitter and receiver does this. It is advisable to check the path by flying over it to check for obstructions on the path that may not be listed on the map (forest, houses, etc.). Once the elevations and obstructions are found they should then be plotted on K=4/3 paper (assuming K=4/3 is appropriate); this will allow for the appropriate choice of antenna heights. Figure 5.15 shows elevations and obstructions plotted on K=4/3 paper. This is followed by an example which shows the procedure for choosing antenna height [24].

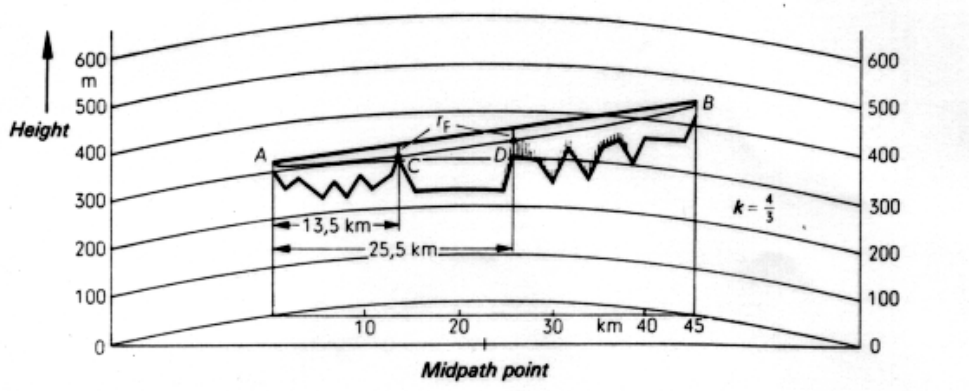

Figure 5.15 Path Profile Plotted on K=4/3 Paper [24]

1. Plot the path profile on K=4/3 paper.
2. Find antenna heights to overcome first Fresnel zone requirement:
    - Inspect path finding likely obstruction points then calculate the first Fresnel zone for those points.
    - The obstructions in this example are at points C (13.5km from point A) and at point D (25.5km from terminal A). Therefore at point C d_1=13.5km and d_2=31.5km. At point D d_1=25.5km and

d_2=19.5km. The first Fresnel zone values at points C and D for a radio link operating at 4 GHz using equation (5.37) are 26.6m and 28.8m.

3. Put these values on the path profile above the heights listed for points C and D.
4. Then choose antenna heights at points A and B so that a radio line of site passes through points C and D.
5. Determine the antenna heights from the path profile in this case h_A=20m and h_B=25m.
6. Draw in first the Fresnel zone below the line of site as a check.
7. The next step would be to check to see if the reflection point is in a place where it will not pose a problem. Using equation (5.45) the ratio of antenna heights n is found to be 0.8. Looking at Figure 5.12 K=grazing and K=∞ are found to be 0.48 and 0.44. Multiplying the path length by the K values found gives a reflection point range between 19.8km and 21.6km. This range falls around mid path for this example. In looking at the path profile the reflection point shouldn't pose a problem since there are mountains and trees on either side of the reflection point range.

What was just shown was the reasoning and procedure for doing a path profile on paper. Recently with the advent of Geographical Information Systems (GIS), siting and digital elevation mapping (DEM) can be done. The rest could be done by writing computer programs that upgrade the existing GIS package. These would take refractive effects, first Fresnel zone, and multipath fading into account; this was decided upon in consultation with our on site GIS personnel.

Now that all the preliminary geographical siting is done, the planner has to check the model with the identified site. The most important criteria to check is that the line of sight criteria is met. After the line of sight criteria is met a site survey should be conducted. The following is a general listing of information needed for a site survey [14].

- Precise location of the sites done by a surveyor.
- Site layout plan showing where structures will be planned to be located relative to the survey.
- Describe the site by taking photos. Attempt to have the photos show the type of soil, vegetation, existing structures, etc.
- Describe any potential obstructions on the path or anything that is lacking in existing mapping information.
- Determine the availability of power and fuel.
- Locate local building materials and contractors.
- Review local zoning regulations.
- Geologic and seismic data .
- Weather pattern information.
- Electromagnetic Interference (EMI) survey.

The combination of the path profile and site survey should provide the radio link designer with enough information to find the appropriate site and antenna tower height for a proposed radio link.

5.10 Rain Fading / Attenuation Calculation

The effects of rain can generally be neglected within the 1 – 10 GHz frequency range. However, it must be accounted for in frequencies above 10GHz. Excess path attenuation due to rainfall is the principal factor affecting path loss at these frequencies. The performance metric of the radio link relative to rain attenuation is exceedance. A radiolink must be designed to overcome rain attenuation, therefore meeting a specified exceedance metric. An exceedance of 0.01% characterizes the link being unavailable for 0.01% of the time and available for 99.99% of the time. To convert this to actual minutes see Table 5.8 below:

Table 5.8 Minutes/Year Attenuation is Exceeded

Percentage of Time Unavailable	Minutes/Year Radiolink Unavailable
1%	5256 min. (87.6 hrs.)
0.1%	525.6 min. (8.76 hrs.)
0.01%	52.56 min. (0.876 hrs.)
0.001%	5.256 min. (0.0876 hrs.)

Rainfall is typically measured in mm/hr with long periods of light rain affecting the radiolink availability much less than severe rainfall lasting 10-20 minutes. Light rainfall is typically characterized as stratiform rain. It encompasses areas of hundreds of kilometers, lasts for periods exceeding one hour, and is characterized by rain rates of less than 25mm/hr distributed uniformly over the region [26]. Severe "thunderstorm like" rainfall is typically characterized as convective rain. It tends to move in clusters with intercellular separations on the order of 5-6 km [27] and encompasses areas that are 2-6 km across [15]. The lifetime of such an individual convective raincell is often 10-20 minutes, and is characterized by heavy downpour rain. These rains are the most common source of high rain rates in the U.S. and Canada [26].

The coverage area for low rainfall rates, as previously mentioned, is large; therefore the path average rainfall rate equals the local rainfall rate. But the typical coverage area for high rainfall rates is small, typically 2-6 km across as previously mentioned. This means that the path average rainfall rate equals the local rain rate for short links, but for longer paths a path averaging factor has to be included. This accounts for the limited radius of the high rainfall rate cell.

The procedural steps [28] for calculating excess path attenuation due to rain will now be shown.

Step1: Calculate the "specific attenuation" equation (5.46)

$$A_{dB/km} = aR^{b} \tag{5.46}$$

The values for a, b, and R (rain rate) are found in [29, 30]. The appropriate frequency and antenna polarization need to be selected when finding the values for a and b. The rain rate (R) needs to be chosen for the appropriate exceedance, in this case we start with 0.01%, and geographical region.

Step2: Determine the path averaging factor equation (5.47)

$$r = \frac{1}{1 + d/d_0} \tag{5.47}$$

Determine the path length of the radio link (d) and enter it into equation (5.47). Then find d_0 via equation (5.48-5.49).

$$d_0 = 35e^{-0.015R_{0.01}}; R_{0.01} \leq 100mm/hr \tag{5.48}$$

$$d_0 = 35e^{-0.015\times 100}; R_{0.01} \geq 100mm/hr \tag{5.49}$$

With this data the path averaging factor (r) can be found.

Step3: Now find the attenuation for a 0.01% exceedance (equation (5.50)).

$$A_{0.01} = A_{dB/km} \times d \times r \tag{5.50}$$

Step4: Attenuation for other exceedance percentages can be calculated by using equation (5.51).

$$A_p / A_{0.01} = 0.12 \times p^{-(0.546+0.043\log_{10} p)} \tag{5.51}$$

To reinforce this procedure an example calculation for Virginia Tech ITU-R region K will now be included.

Step1: Select a and b for a frequency of 28GHz and a vertical antenna polarization. In this case a=0.1534 and b=1.012. Select R for an exceedance of 0.01% within ITU-R region K. In this case R=42mm/hr.

Find the specific attenuation (A_{dB})

$$A_{dB/km} = (0.1534)(42^{1.012}) = 6.74dB/km$$

Step2: Determine d, d_0, and r; in this case d=5km, d_0 and r are calculated below.

$$d_0 = 35e^{(-0.015)(42)} = 18.64$$

$$r = \frac{1}{1 + 5/18.64} = 0.7885$$

Step3: Find the attenuation for 0.01% exceedance.

$$A_{0.01} = 6.74 \times 5 \times 0.7885 = 26.57dB$$

This tells us that a 99.99% availability on a 5km path requires a 26.6 dB margin included in the link budget. To find the attenuation for 1%, 0.1%, and 0.001% exceedances factors need to be generated for these exceedances via equation (5.51). These factors (relative to the above exceedances) are 0.12, 0.39, and 2.14. The attenuation for these exceedances are now calculated below.

$$A_1 = (0.12)(26.57) = 3.19dB$$

$$A_{0.1} = (0.39)(26.57) = 10.36dB$$

$$A_{0.001} = (2.14)(26.57) = 56.86dB$$

As can be seen from these calculations, less margin has to be designed into the radio link for lower availability requirements. The opposite is true for higher availability requirements. This becomes even more evident when reviewing Figures 5.16-5.18, which show exceedance vs. attenuation over various path lengths for ITU-R regions K,D, and N.

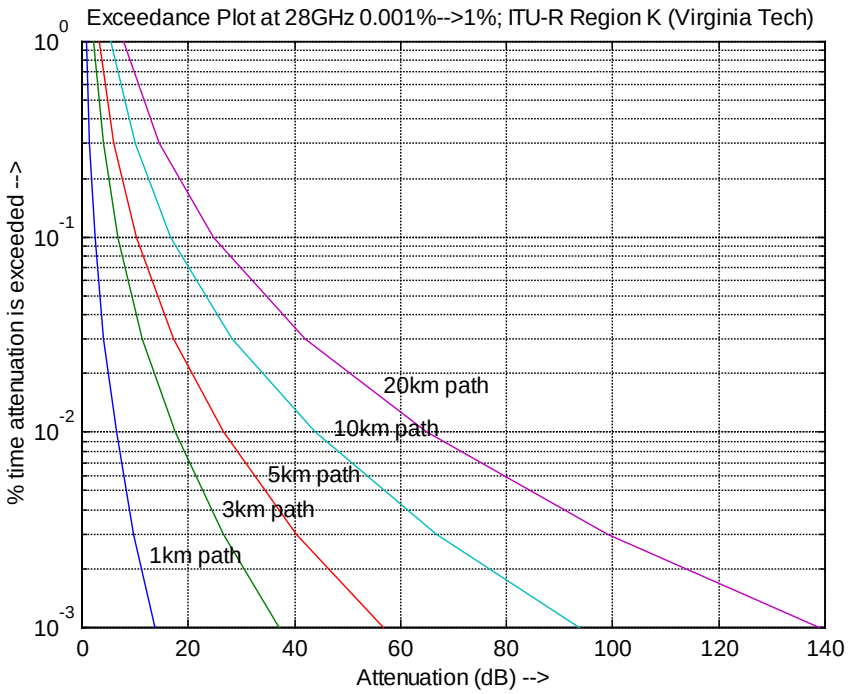

Figure 5.16 Exceedance vs. Attenuation Curves for 28GHz Line of Sight Path; ITU-R Region K (Virginia Tech)

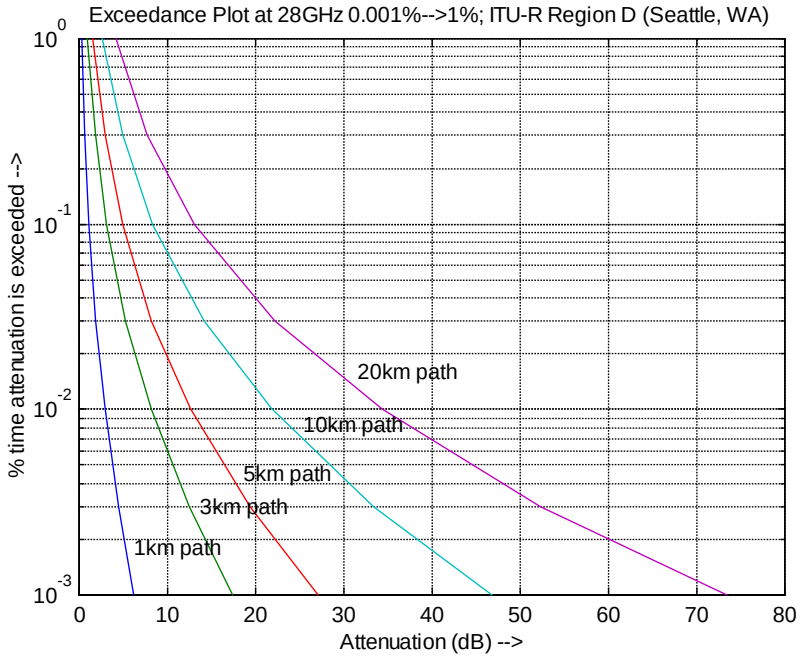

Figure 5.17 Exceedance vs. Attenuation Curves for 28GHz Line of Sight Path; ITU-R Region D (Seattle, WA)

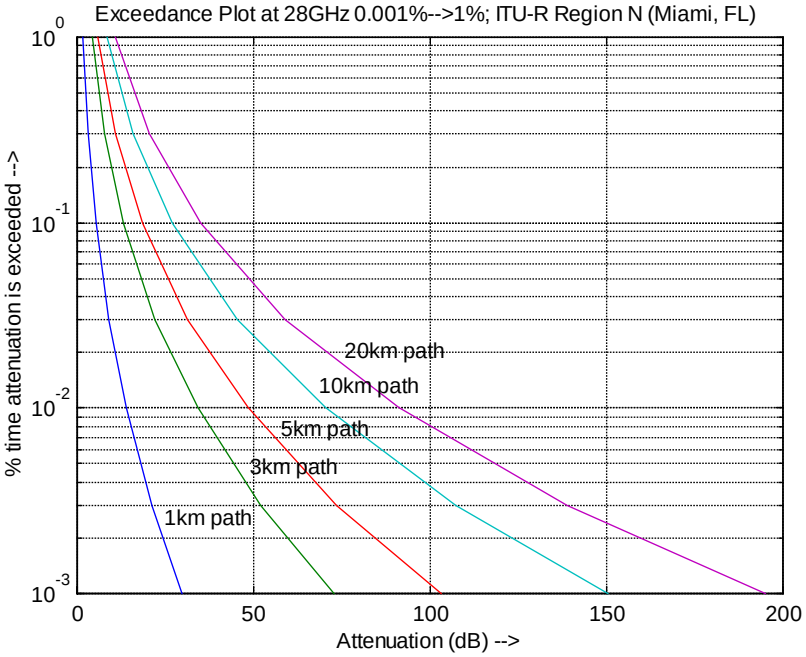

Figure 5.18 Exceedance vs. Attenuation Curves for 28GHz Line of Sight Path; ITU-R Region N (Miami, FL)

5.11 Vegetative Fading

For a point to point radiolink, attenuation due to vegetation becomes an important factor at frequencies approaching millimeter wavelengths. As an example, Figures 5.19-5.20 show the vegetative loss of a 28.8GHz radio path through a pecan orchard in Texas [31]. This excess attenuation is due to scattering and absorption of the transmitted wave as it propagates through areas of vegetation. Extensive experimental investigations have revealed that these transmission losses are influenced by parameters such as the dielectric constant, density, physical size, and shape of the vegetation [32].

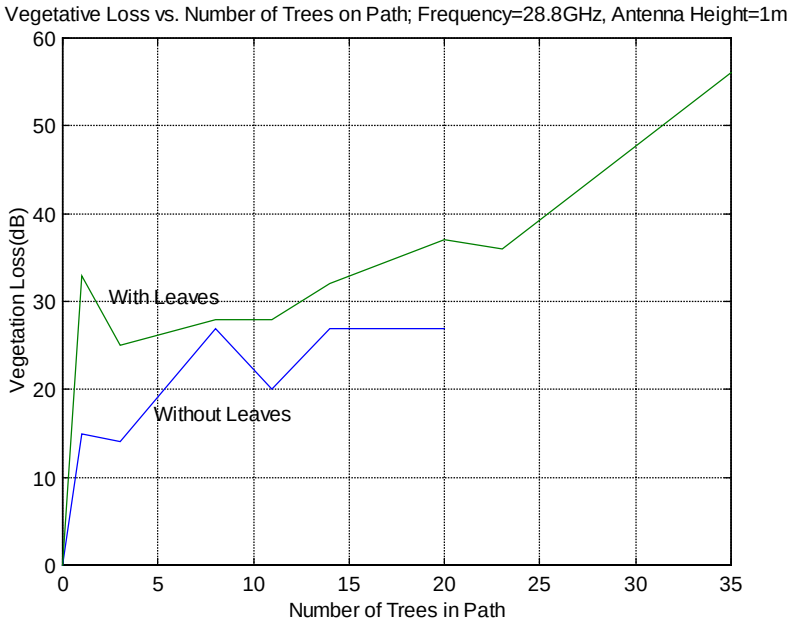

Figure 5.19 Vegetative Loss vs. Number of Trees on Path; Antenna Height=1m [31]

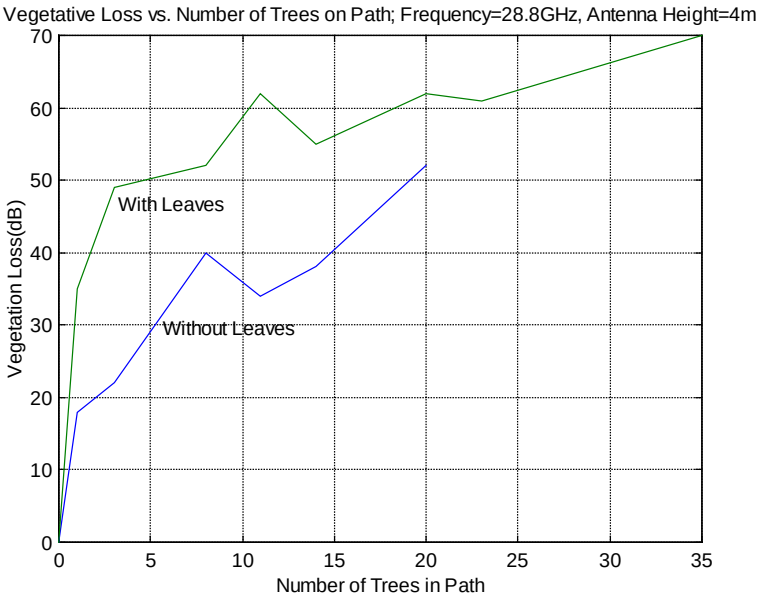

Figure 5.20 Vegetative Loss vs. Number of Trees on Path; Antenna Height=4m

In reviewing Figures 5.19 and 5.20 [31] an initially high rate of attenuation occurs at a short depth of vegetation, but as one goes deeper into the vegetation this attenuation rate becomes smaller. Experiment [31] concluded that this is caused by the degradation of the dominant coherent propagation mode. As the vegetation depth increases the received wave changes from one predominantly influenced by the coherent component to one which consists mostly of the incoherent component due to the forward scatter caused by leaves and branches [33]. We do not agree with this conclusion, arguments to the contrary will be presented in chapter 6.

In reviewing the literature there are a number of models that characterize attenuation vs. vegetation depth; the review has not shown a truly exact model. This is not a fault of the developers of the model, but the problem lies in the difficulty of trying to accurately model a media with random structure.

The attenuation models reviewed here relative to vegetation are the ITU-R [34], Fitted ITU-R (FITU-R) [33], and the Improved ITU-R (IITU-R) [34] model.

The ITU-R model was developed from measurements carried out mainly at UHF where the transmit and receive terminals are placed such that the majority of the radio path falls within the vegetation medium, assumed to have a maximum depth of 400 meters. The model expressed below in equation (5.52) is stated to be applicable in the frequency range 200MHz to 95GHz [33].

$$A = 0.2 f^{0.3} d^{0.6} (dB) \qquad (5.52)$$

Where: A = attenuation (dB)

f = frequency (MHz)

d = distance (meters)

The FITU-R model attempts to optimize the ITU-R model. It provides a characterization of vegetative attenuation for both the in leaf and out of leaf state; these expressions are shown in equations (5.53-5.54)

$$A = 0.39 f^{0.39} d^{0.25} (dB) \quad \text{in-leaf state} \tag{5.53}$$

$$A = 0.37 f^{0.18} d^{0.59} (dB) \quad \text{out of leaf state} \tag{5.54}$$

These equations were generated using a least squared error fit for a data set at the frequencies of 11.2 GHz and 20 GHz in an in leaf and out of leaf state; where the performance metric for this was the RMS error in dB (Table 5.9). The authors in [33] recommended that this model is applicable in the frequency range of 10-40 GHz.

Table 5.9 RMS Error (dB) for Sites Fermi, Mound, and Ridgeway in Study [33]

	Model	Model
	ITU-R	FITU-R
Site	RMS Error (dB)	RMS Error (dB)
Fermi	12.70	10.85
Mound	20.73	19.80
Ridgeway	16.85	9.38
All out-of-leaf	15.36	8.98
All in-leaf	9.85	9.42

The IITU-R model also attempts to optimize the ITU-R model. This was also done using a least squared error fit, but with a more extensive data set from various studies. Actually parts if not all of the data from the 11.2 GHz –20 GHz data set are included in this model. Table 5.9 shows the type of vegetation and frequencies of the data set used to generate this model.

Table 5.10 Vegetative and Frequency Data Set Parameters for the IITU-R Model [34]

Sycamore/ Lime Tree	Line of Horse Chestnuts	Pecan Forest	Apple Orchard
Frequency (GHz)	Frequency (GHz)	Frequency (GHz)	Frequency (GHz)
11.2	11.2	9.6	11.2
20	20	28.8	
37.5	37.5	57.6	

The equations that characterize the IITU-R model are

$$A = 15.6 f^{-0.009} d^{0.026} (dB) \text{ in-leaf state} \quad (5.55)$$

$$A = 26.6 f^{-0.2} d^{0.5} (dB) \text{ out-of-leaf state} \quad (5.56)$$

The performance of this model was measured using the standard deviation (σ) relative to the measured data. In the case of the ITU-R model a σ = 26.6dB for the in-leaf case and a σ = 22.1 dB was found [34]. The σ of the IITU-R model is 10.8dB for an in-leaf state and 10.4dB for an out-of-leaf state.

Which model provides the best characterization is to be seen in later investigation, but it seems that the FITU-R and IITU-R model will perform better than the ITU-R model.

The experimental and investigative portion of the thesis, which are reported in the following chapter, will focus on the effects of vegetation on the LMDS channel. Specifically we will be measuring how vegetation impacts magnitude, phase, and error vector magnitude (EVM).

5.12 Frequency Planning and Reuse

The topics discussed so far in this chapter are focused on point-to-point radio system architectures. The topic that is now going to be discussed is frequency reuse; this is more applicable to a point to multipoint radio system architecture. The topics that were discussed prior to this topic are still applicable in a point to multipoint radio system architecture. The only difference is an increased level of complexity. This is due to many more radio links running simultaneously as opposed to one radio link running in a point to point radio system architecture.

Frequency reuse is what makes a cellular fixed or mobile system work. Within a certain region cellular systems rely on the reuse of allocated regional radio channels. Each hub site within this cellular architecture covers a geographical area called a cell. Typically in an LMDS system architecture, this “cell” is split up into four 90° sectors and the allocated regional radio channels are parsed up amongst the sectors within the cell. By limiting the coverage area to within the boundaries of the cell, the same group of channels may be arranged or “frequency planned” in a way that they can be used to cover different cells that are separated from one another by distances large enough to keep interference levels within tolerable limits [21]. Proposed frequency plans for LMDS are shown in Figures 5.21 and 5.22 [35].

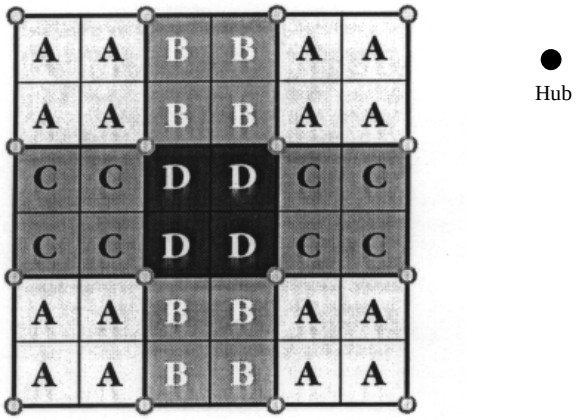

Figure 5.21 LMDS Frequency Plan for Maximum Coverage [35]

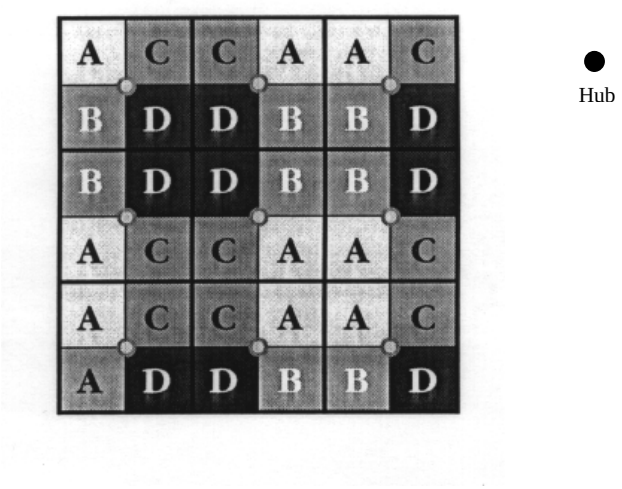

Figure 5.22 LMDS Frequency Plan for Minimum Number of Hubs [35]

Figure 5.21 shows a layout for maximum coverage where sixteen hub sites are used to cover a service area. In this scenario a user can access one of four of the hub sites. Figure 5.22 shows a layout for minimum hub site usage where nine hub sites are used to cover a service area. In this scenario users in the corners are only serviced by one hub site and two hub sites can only service users on the edges [36].

Each of the sectors in Figures 5.21 and 5.22 are assigned different frequencies with the frequency assignments being labeled A, B, C, and D. By alternating frequency assignments the result is an overall area coverage and a reduced potential for co-channel interference. As an example, five cell radii separate the closest potential co-channel interferer in Figure 5.21 [37].

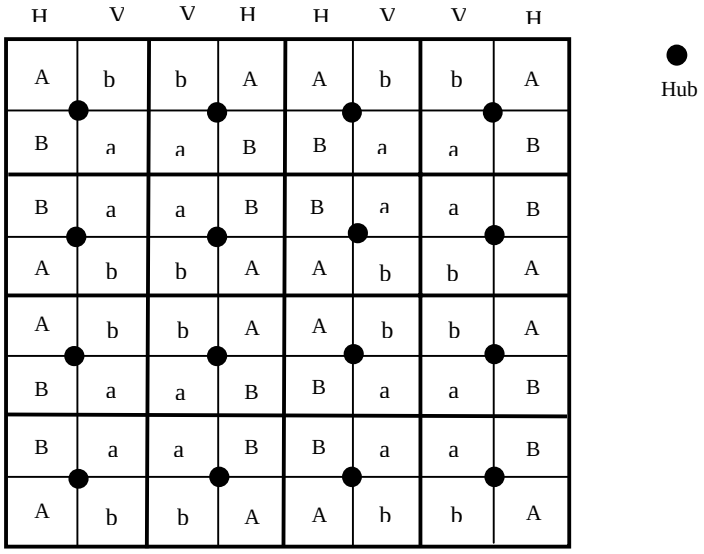

Figure 5.23 LMDS Frequency Plan with Frequency Reuse of Two

The frequency reuse in Figures 5.21 and 5.22 is one. Figure 5.23 shows a frequency plan arrangement that provides a frequency reuse of two, which means that two channels support a four-sectored cell. This is possible through the use of frequency diversity and polarization discrimination; this is the alternation of the antenna polarization's between horizontal and vertical.

Frequency reuse of four has also been investigated; this is achieved by strictly using polarization diversity. In this investigation depolarization effects were found. Therefore four-frequency reuse is only practical in selected environments [38].

It can be seen that by using frequency and polarization diversity a reasonable level of frequency reuse can be implemented thereby optimizing the use of the radio channels allocated to a region.

5.13 Co-channel and Adjacent Channel Interference

Co-channel interference occurs when the desired received signal from the closest hub station is degraded due to interference from other hub stations. These interfering hub stations operate at a certain separation distance from the desired hub station and at the same frequency. Figure 5.24 shows a typical LMDS frequency plan with identified first tier co-channel interferers separated by five radii. The separation between the desired hub station and interfering hub stations is determined when a signal to interference ratio (S/I) is specified.

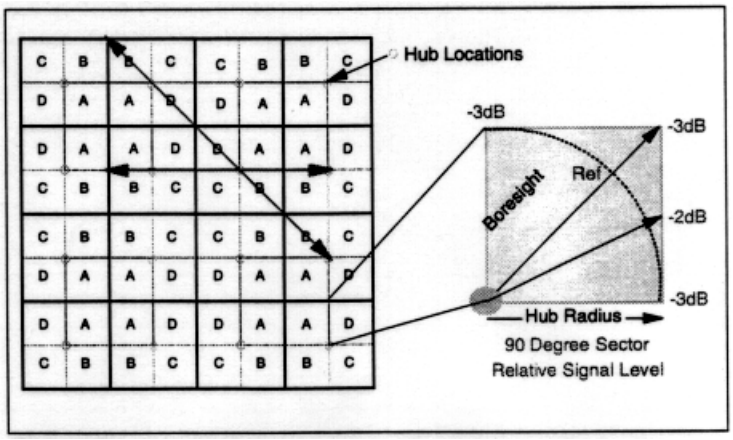

Figure 5.24 LMDS Frequency Plan for Maximum Coverage; First Tier Co-channel Interferers Separated by Five Radii [35].

S/I is expressed by:

$$\frac{S}{I} = \frac{S}{\sum_{i=1}^{i_o} I_i} \tag{5.57}$$

Where S = the received signal from the desired hub station.

I_I = the interfering received signal from the i^{th} interfering hub station.

If the radius of all the cells in the frequency plan, the transmitted power of each hub station, and the path loss exponent (n) are the same over the coverage area then equation (5.57) can be express by:

$$\frac{S}{I} = \frac{R^{-n}}{\sum_{i=1}^{i_0} D^{-n}} \tag{5.58}$$

Where R = the distance from the desired hub station to the user.

n = path loss exponent.

D = the distance from the i^{th} interferer to the user.

Therefore the level of co-channel interference or S/I can be determined by knowing the radius of the desired cell and the distance from the desired cell to the i^{th} interferer.

Adjacent channel interference occurs when an adjacent frequency channel interferes with a receiver. There are a number of reasons why this occurs. Two are insufficient filtering of adjacent frequency channels at the victim receiver and improper power control of the adjacent channel. The adjacent may not be of the same service (e.g. ham radio interfering with a television receiver). By carefully specifying filter performance parameters, the frequency plan (keeping adjacent channels separated), and keeping track of the transmitted power of adjacent channels of different services, this bleed over condition can be greatly eliminated [21].

Chapter 6.0 Experimental Study of Vegetation Effects

The motivation for this experiment comes from the review of a number of papers and people simply asking "what will happen to LMDS signals in vegetation?" Figure 6.1 shows the amount of attenuation that can be expected for deciduous trees with leaves at 28.8GHz [31].

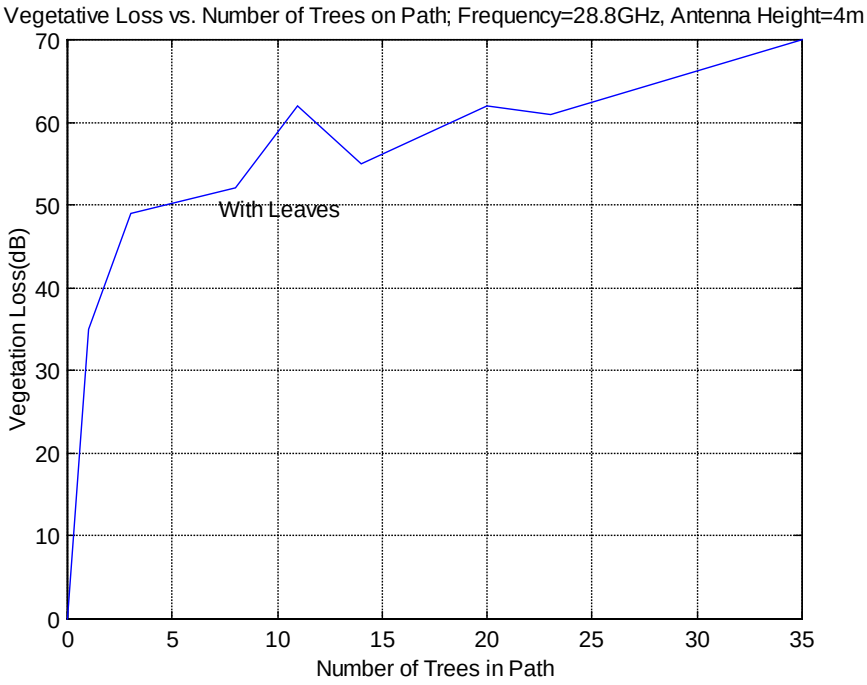

Figure 6.1 Attenuation due to Deciduous Vegetation at 28.8GHz [31]

The figure indicates that a dramatic attenuation occurs for the first few trees, after which the attenuation increase becomes more gradual. The study from which the data from Figure 6.1 was taken [31] shows that at the point where the attenuation changed, substantial beam broadening occurred (Figure 6.2).

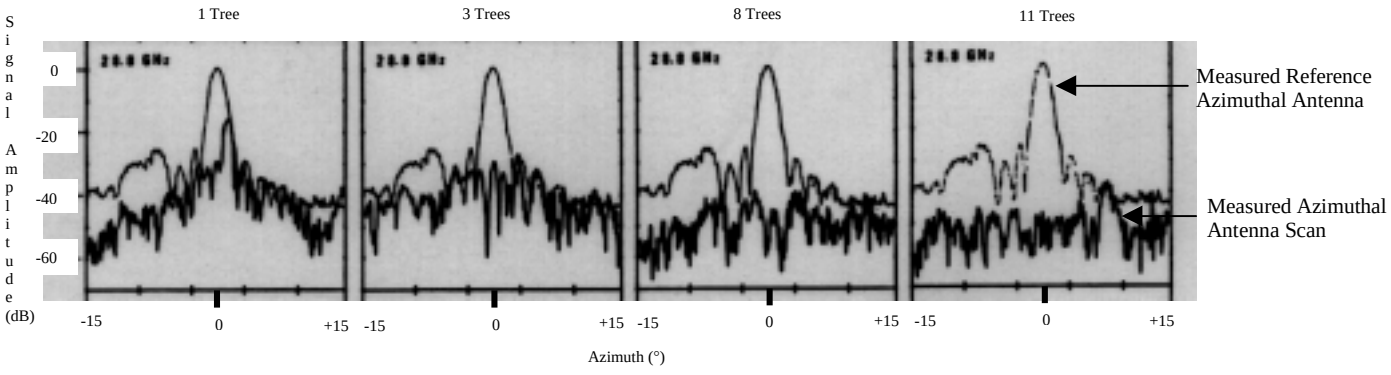

Figure 6.2 Received Power vs. Scan Angle for Azimuthal Antenna Scans at Height of 4m; Trees without Leaves [31]

This was interpreted as a changeover from a dominant direct path propagation mode (coherent propagation mode) to a multiple scattering propagation mode (incoherent propagation mode). If the propagation is truly incoherent, a phase modulated signal might be of no use, since the phase information would be corrupted.

While incoherent propagation offers one potential explanation for the abrupt change of the slope of the curve in Figure 6.1, there are several other alternatives. One [42] is that multipath signals 50-60dB down from the direct path signal are reaching the receiving antenna. After the direct path attenuation passes 50dB, the multipath components dominate. If the multipath components are scattered from objects well away from the line-of-sight path, they may pass through only a few trees near the receiving antenna and thus are relatively insensitive to the total number of trees in the line-of-sight path. Another mechanism is depolarization. This could also produce the antenna pattern degradations of figure 6.2. We will discuss depolarization in more detail below.

A study [39] eight years after the original study ([31]) was done on the same test range; this had two goals. First, it made sure that the attenuation vs. vegetation was reproducible within reason, considering natural change of the range over eight years. Secondly, it measured the BER of a 30.3GHz 500Mbps BPSK waveform with pseudo random characteristics. If vegetative attenuation is incoherent, we would expect to see an increase in BER from phase errors over and above the BER calculated from E_b/N_o.
A review of the results of [39] showed that propagation through vegetation seems to be incoherent. Thus, the phase front falls apart causing the receiving antenna to show gain degradation. Therefore the phase of the received signal becomes incoherent. This means that BER is not uniquely related to C/N or E_b/N_o. This is apparent in Figures 6.2 - 6.5 (reference data on left plot and actual data on right plot) and Table 6.1.

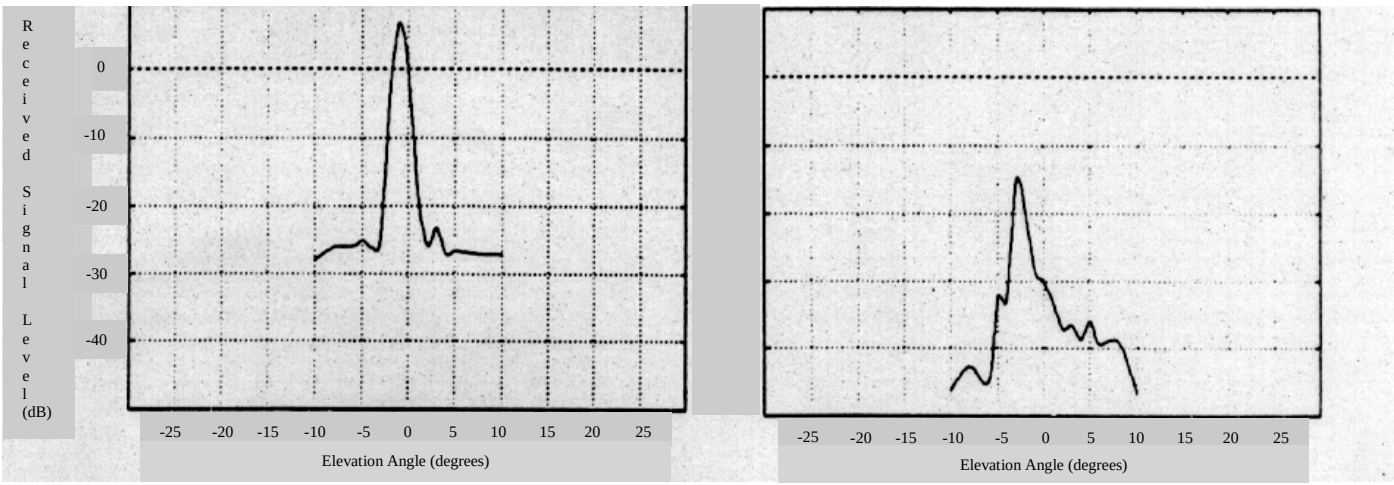

Figure 6.3 Amplitude Data (1m Transmitter Height) at 30.3GHz as a Function of Elevation Angle (No Leaves) [39]

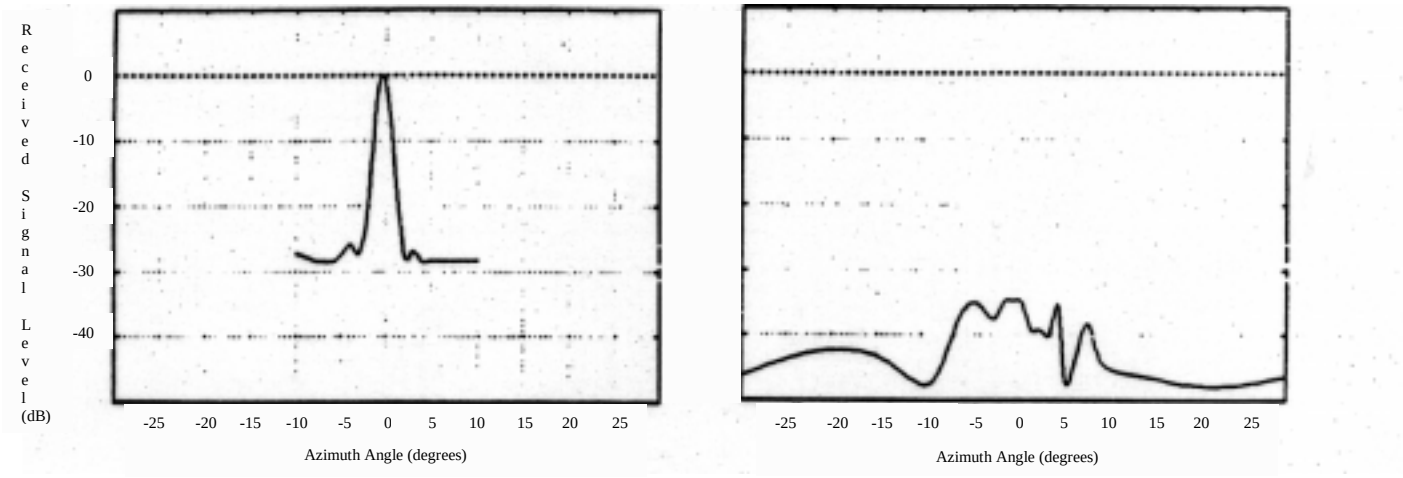

Figure 6.4 Amplitude Data (1m Transmitter Height) at 30.3GHz as a Function of Elevation Angle (with Leaves) [39]

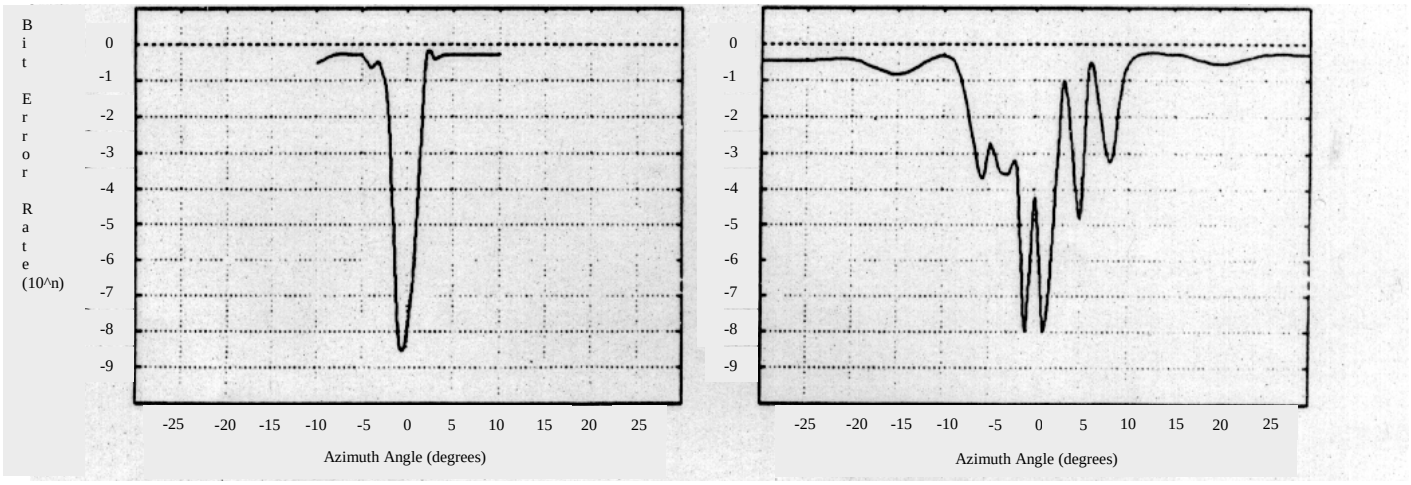

Figure 6.5 Bit Error Rate (1m Transmitter Height) at 30.3GHz as a Function of Elevation Angle (with Leaves) [39]

Table 6.1 Received Signal Level vs. Bit Error Rate for a Given Azimuth Angle

Approximate Received Signal Level (dB)	Bit Error Rate (10^n)	Azimuth Angle (Degrees)
-37.0	n = -8	2
-35.0	n = -8	-1
-35.0	n = -4	0

From this we determined that a good experiment to do in support of the others would be to measure how the phase and magnitude of a phase shift keyed waveform are affected by vegetation. This we believed would give us better insight into the relationship between C/N and BER.

6.1 The Experiment

The experiment was designed to investigate the effects of vegetation on the magnitude, phase, and error vector magnitude (EVM) on a transmitted waveform in a LMDS channel. In it we transmitted a quadrature phase shift keyed (QPSK) waveform. Therefore the magnitude of the transmitted waveform is constant and the phase contains the information.

6.2 Experimental Procedure

Through this investigation we determined whether errors in the demodulated magnitude and phase due to vegetation fading could be overcome by increasing transmitter power. This gave us insight into whether vegetative scattering is an incoherent process and whether the harmful effects of vegetation fading could be overcome by allowing a suitable fade margin as is done for rain fading. The experiment was conducted in the following fashion:

- The transmitter – receiver group was calibrated during a clear line of site transmission.
- A coniferous (white pine) tree mounted on a Christmas tree stand was first moved into the path of the receiver. The spectrum of the received waveform was then measured on a spectrum analyzer. The magnitude and phase error, the error vector magnitude, and the burst symbol error rate relative to the transmitted waveform were measured on a vector signal analyzer (VSA). The transmitter power was then increased to achieve the clear air calibration signal level (if possible) at the receiver. The measurements discussed previously were redone.
- The same measurements were performed with 2, 3, and 4 trees in the path.

6.3 Equipment Used in the Experiment

Two companies lent the majority of the equipment used for this experiment:

Hewlett-Packard Company
Test and Measurement Organization
5301 Stevens Creek Blvd.
Bldg. 51L-SC
Santa Clara, CA 95052-8059
1-800-452-4844

HP E4433B	RF Signal Generator
HP 89441A	Vector Signal Analyzer

mm-Tech, Inc.
20 Meridian Rd.
Eatontown, NJ 07724
732-935-7150

TRLA003	1st IF / 100MHz Reference / DC Voltage Module
TRSS001	Solid State LMDS Transmitter
AN36UVH2R5P	12” Parabolic Antenna
AN30NVH4E4	6” x 6.5” Flat Panel Antenna
RVSS001	Ka-Band Low Noise Receiver
LUCA007	100MHz Reference / DC Voltage Module

We also used the following items belonging to Virginia Tech:

Hewlett Packard (HP8594E)	Spectrum Analyzer
----------	WR-34 to WR-28 Waveguide Transitions
----------	WR-34 Waveguide Attenuator
Alpha Industries Inc.	Precision WR-28 Waveguide Attenuator
Airtron, Inc.	WR-28 Flexible Waveguide
----------	Coaxial Cabling with BNC, N-type, and SMA interfaces
----------	Connectors and Transitions

Below are short descriptions of the major components of the experimental system. Following this Figures 6.8 –6.9 will show a diagram of how this equipment was integrated.

- The HP E4433B RF signal generator can provide an array of signaling for both analog and digital measure. The E4433B signal generator is capable of supplying a carrier up to 4GHz. The architecture of this signal generator allows for the creation of digitally modulated signals, the modification of existing digital protocols, and simulated transmissions as specified by existing communications standards [40]. In our case we were concerned with creating a digitally modulated signal. The aspects of that signal will be covered in the following section. This signal generator provides the following building blocks for creating a digitally modulated signal: modulations, symbol rates, data types, burst shaping, filtering, flexible frames/timeslots, and frame triggering /delay.

- The HP89441A (DC – 2.65GHz) Vector Signal Analyzer (VSA) with option AYA is a high performance RF signal analyzer useful for measuring the performance of digitally modulated waveforms. The modulation formats it can accommodate are: 2FSK, 4FSK, BPSK, 8PSK, QPSK,

OQPSK, DQPSK, π/4 DQPSK, 16QAM and 32QAM. The difference between a conventional signal analyzer and a vector signal analyzer is shown in Figure 6.6.

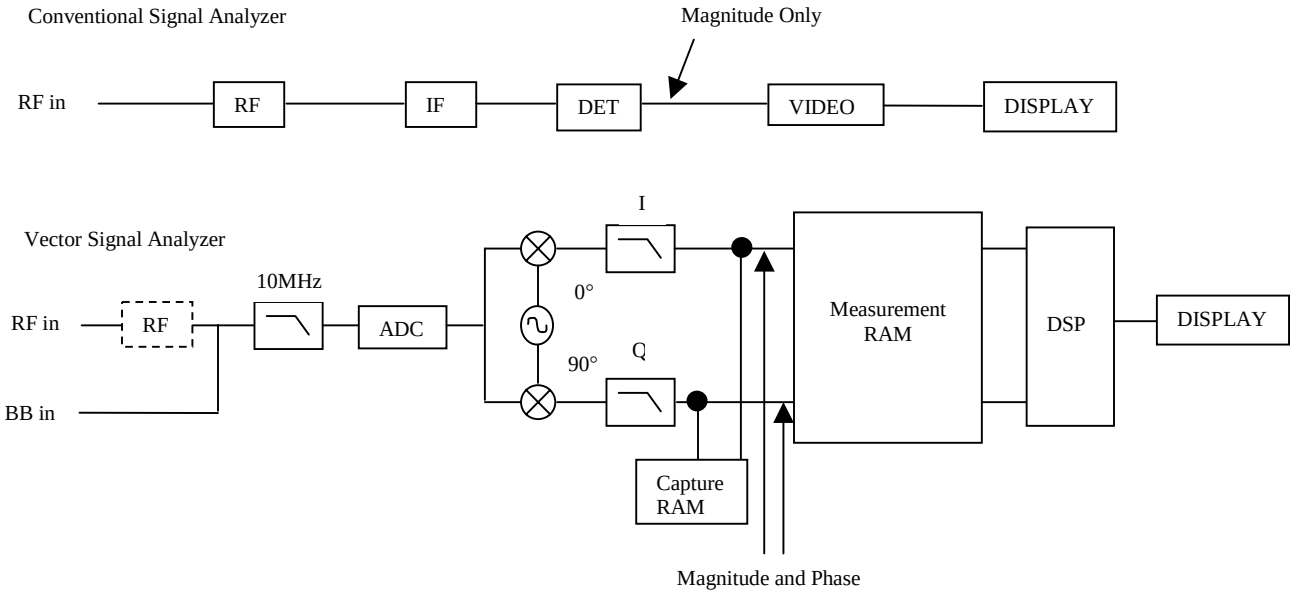

Figure 6.6 Block Diagram Comparison of Conventional Signal Analyzer and Vector Signal Analyzer [41]

A VSA can represent the recovered waveform in the time or frequency domain. It can also do vector modulation analysis (with the AYA option); this gives both visual and numerical insights into system performance. For example a few types of visual and numerical analysis performed by the VSA are constellation analysis, magnitude analysis, phase analysis, and I/Q analysis. Comparing the recovered waveform with a reference waveform that the user specifies does vector modulation measurement comparisons.

- The TRLA003 module provides a 100MHz reference and power to the TRSS001 solid state transmitter. It also provides a second IF conversion (2.100 – 2.137GHz); this is also fed into the transmitter.
- The TRSS001 solid state transmitter translates the second IF supplied by the TRLA003 to an RF signal (27.500 – 27.537GHz). The transmitter supplied to us also provides 30dB of gain.
- The AN36UVH2R5P 12” parabolic antenna was used on the transmit side of the radio link. It has a gain of approximately 36dBi and was set up for horizontal polarization.
- The AN30NVH4E4 6” x 6.5” flat panel antenna was used on the receive side of the radio link. It has a gain of approximately 31dBi and was set up for horizontal polarization.
- The RVSS001 Ka-band low noise receiver translates a Ka-band RF signal to an IF in the 710 – 747MHz range. It provides 6dB of gain.

- The LUCA007 provides a 100MHz reference and power to the RVSS001.
- The HP8594E spectrum analyzer is capable of frequency spectrum magnitude analysis in the 9kHz to 2.9GHz range.
- The Alpha Industries Inc. Precision Waveguide Attenuator has an average power rating of 500mW and provides measurable attenuation up to 50dB.

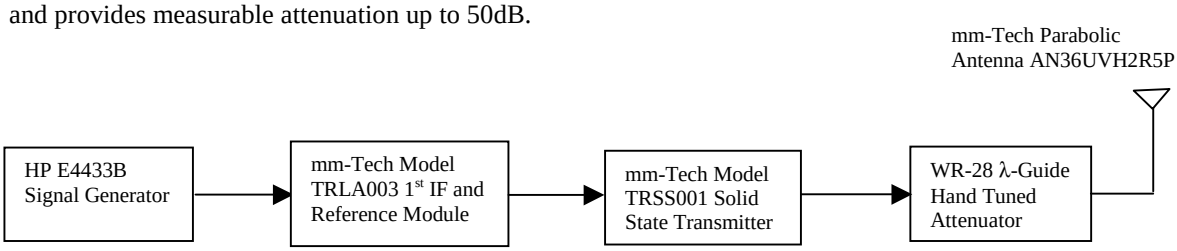

Figure 6.7 LMDS Transmitter Section Block Diagram

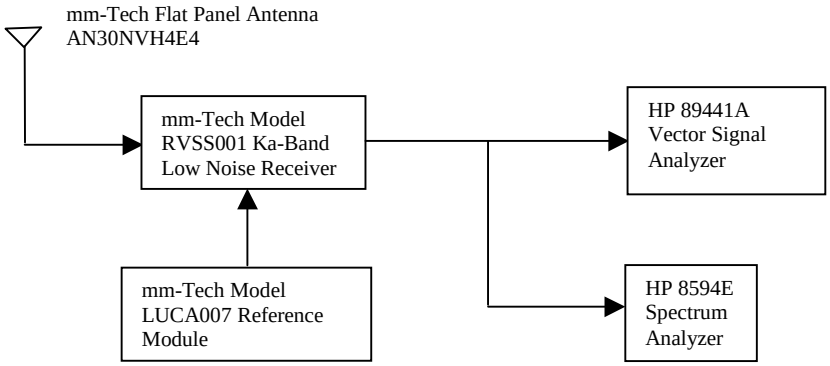

Figure 6.8 LMDS Receiver Section Block Diagram

Pictures of the major components of the system are shown in Figures 6.9 – 6.11

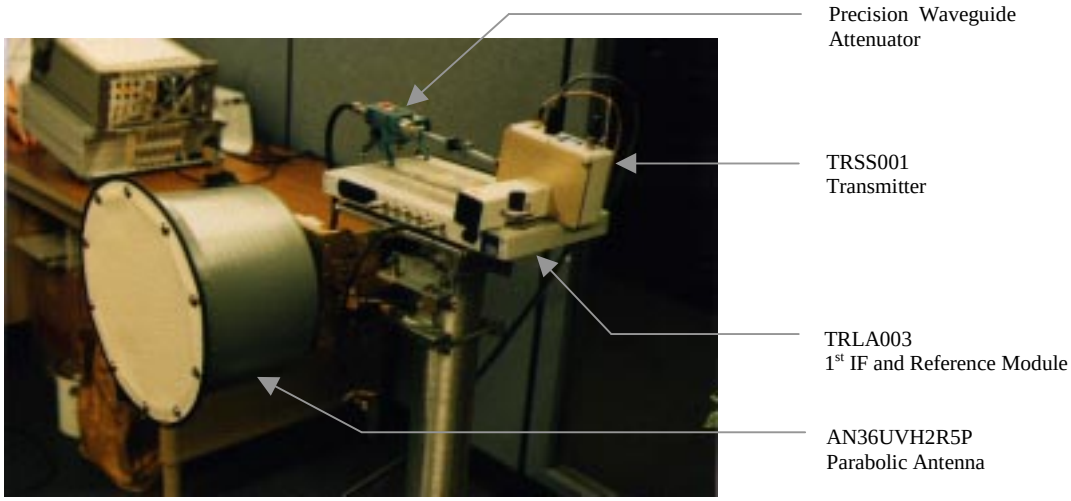

Figure 6.9 LMDS Transmitter Section

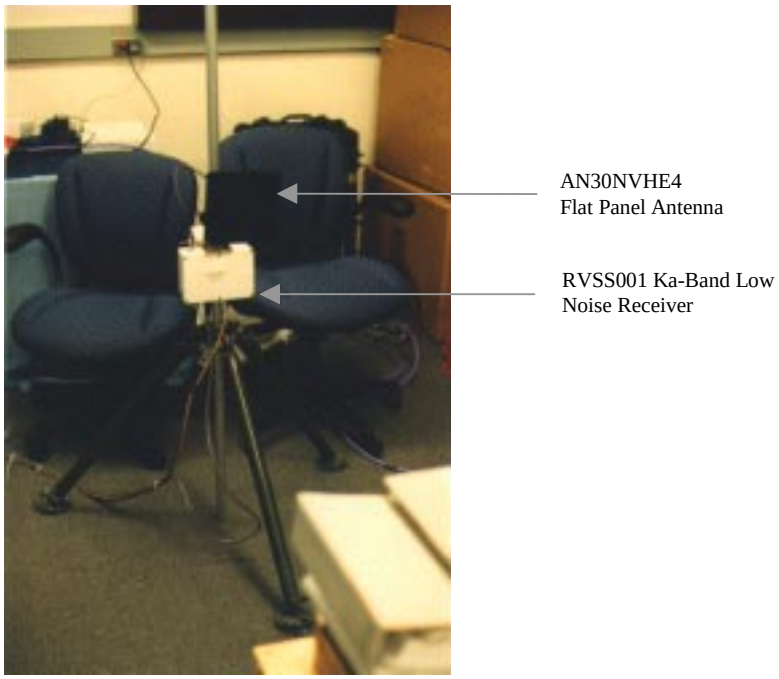

Figure 6.10 LMDS Receiver Section

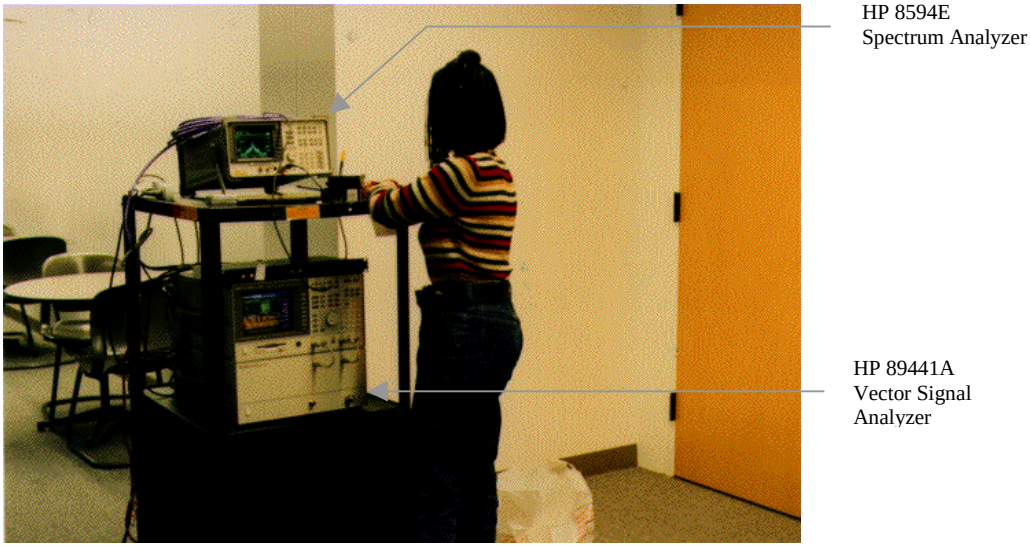

Figure 6.11 Test Equipment Used for Evaluation (operated by Katina Reece)

6.4 Integration and Testing in the Lab

Once the equipment arrived from Hewlett Packard and mm-Tech it was integrated in our laboratory and an over the air test transmission was done. A representation of this integration is found in Figures 6.12 - 6.13.

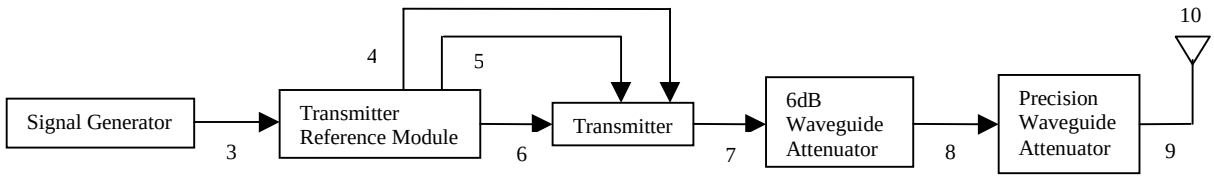

Figure 6.12. LMDS Test System Integration Transmit Side

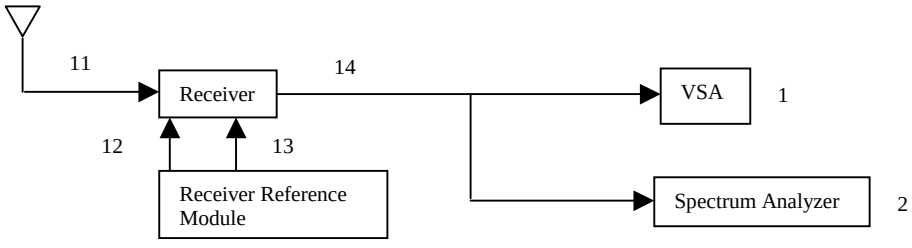

Figure 6.13. LMDS Test System Integration Receive Side

The system described in Figures 6.12 and 6.13 has numbers placed throughout the block diagram. These numbers represent signal flow, references, and measurements critical to system operation.

The following discussion will cover each of these points; this will describe the signal levels at each point and explain the equipment set up and other parameters at that point.

At signaling point 1 the VSA demodulates an IF from the mm-Tech receiver. Following demodulation, the VSA represented the result in one of the following manners specified by the user: constellation diagram; measured magnitude, phase, or I/Q; reference magnitude, phase, or I/Q; magnitude, phase, or I/Q error. It also stored a symbol error table which shows magnitude error, phase error, frequency error, error vector magnitude (EVM) and received symbol burst error.

The VSA was set up to measure the system at various signal flow points; therefore the VSA parameter that is changing at different points is the center frequency with all other parameters being the same. The VSA was set up in the following manner for the test transmission done in the CWT laboratory.

- Demodulation format = QPSK
- Symbol rate = 2.5Msps
- Measurement filter = Rectangular
- Reference filter = Rectangular, since errors are measured by comparing measured data with reference data the transmission and reception filters need to be equivalent for correct measure.
- Center frequency = 75MHz, 2.125GHz, and 725MHz
- Span = 6MHz. Equation (6.1) was presented in Hewlett Packard product note HP 89400-8; this was used to determine the span range requirement.

$$\frac{20\times(R_s)}{1.28} > FrequencySpan > (1+r)(R_s) \qquad (6.1)$$

Where R_s = the symbol rate

r = the pulse shaping filter roll off factor (rectangular filter; r=1)

Using rectangular filters, the frequency span in which the VSA needs to be operated must be between 39.06MHz and 5MHz.

- Channel 1 range = -20dBm. If the VSA is not set up for the correct signal acquisition range then vector signal analysis cannot be accurately done.
- Trigger = free run. Carrier and symbol locking are automatic with the 89441A; therefore no external inputs are necessary.

At signaling point 2 the spectrum analyzer was used to measure the magnitude of the received waveform in the frequency domain. In this case it measured waveforms at signal flow points in the system and was set up in the following manner:

- Center frequency = 75MHz, 2.125GHz, and 725MHz
- Span = 50MHz
- Marker placement done by Peak Search option

The signal generator at signaling point 3 supplied both the signal and carrier. The result of this was a modulated QPSK waveform. QPSK in this case is represented in the magnitude/phase form by equation (6.2).

$$s(t) = A_c \cos\left[\omega_c t + \left(\frac{\pi m(t)}{2} + \frac{\pi}{4}\right)\right] \qquad (6.2)$$

Where: A_c is the magnitude of the waveform, which is held constant.

ω_c is the angular frequency of the carrier.

m(t) is the level of the message signal. For QPSK this is either a 0, 1, 2, or 3.

Typically a QPSK waveform is plotted on a constellation diagram; this is represented in Figure 6.14.

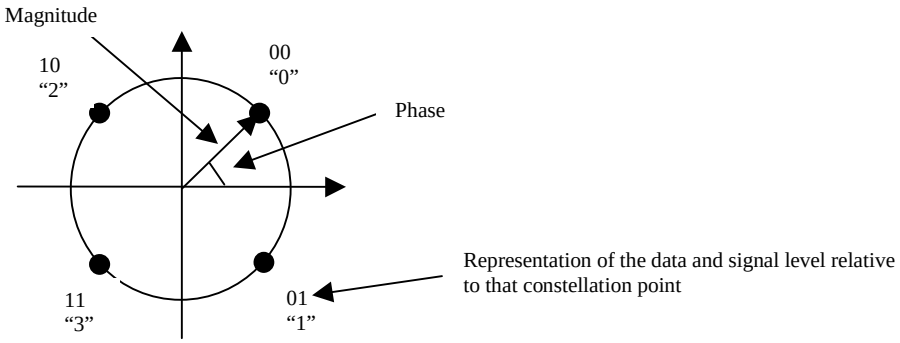

Figure 6.14 QPSK Constellation Diagram

If this were presented in quadrature form then the constellation points would be referred to in terms of the in phase (I) and quadrature (Q) components.

In the test transmission done in the CWT laboratory the signal generator was set up with the following parameters:

- 1st IF center frequency = 75MHz
- Amplitude = -20dBm
- Modulation = QPSK
- Bits / Symbol = 2
- Symbol rate = 2.5Msps
- Filter = Rectangular
- Data Format = four 1's and four 0's. The data format of four 1's and four 0's was chosen since it would allow us to know what was transmitted. This made the analysis of the data at the receiver possible.

The measured spectrum and signal constellation for signal flow point 3 appears in Figures 6.15 and 6.16. In reviewing Figure 6.16 the magnitude was measured to be –24.61dBm when –20.00dBm was input from

the signal generator. This 4.61dB loss difference was later traced to a bad connector. In looking at the signal constellation plot in Figure 6.16 a "cal?" is evident in the upper right hand corner of the plot. This implies that the VSA was out of calibration. When we contacted Hewlett Packard Help Line representatives, they had us conduct a test to see how much it was out of calibration. The test measurement swept the frequency range of the instrument showing how much it deviated from a known reference. We found that this calibration error was negligible; at the low and high end (frequency) of the instrument, the deviation was no more than 1dB, and at midband the deviation was significantly less than 1dB. Thus, the instrument was accurate even though "cal?" was on.

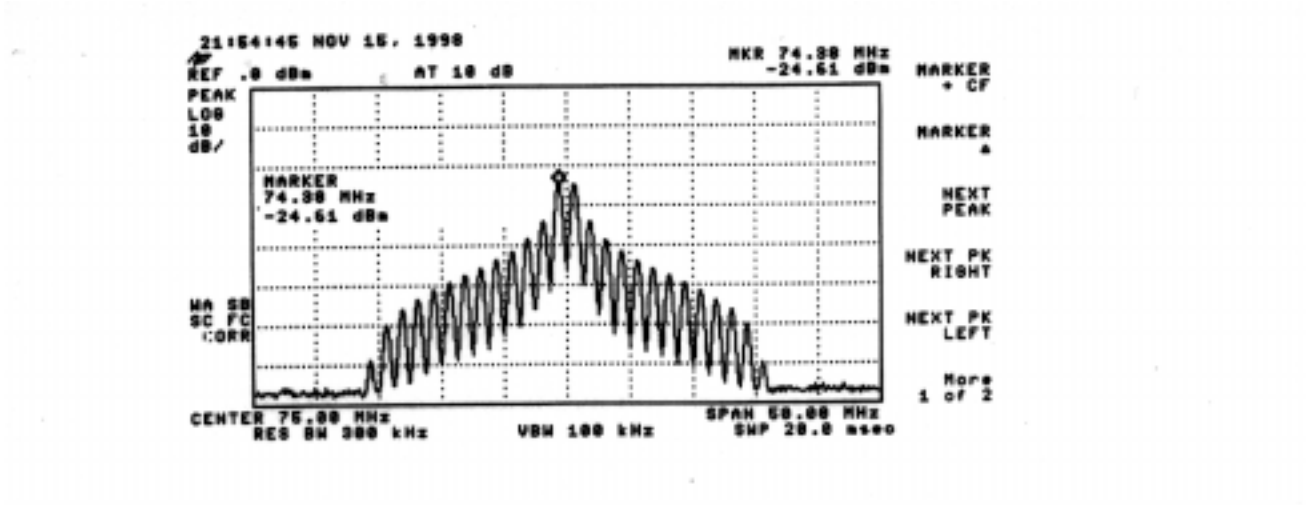

Figure 6.15 Measured Spectrum at Signal Point 3

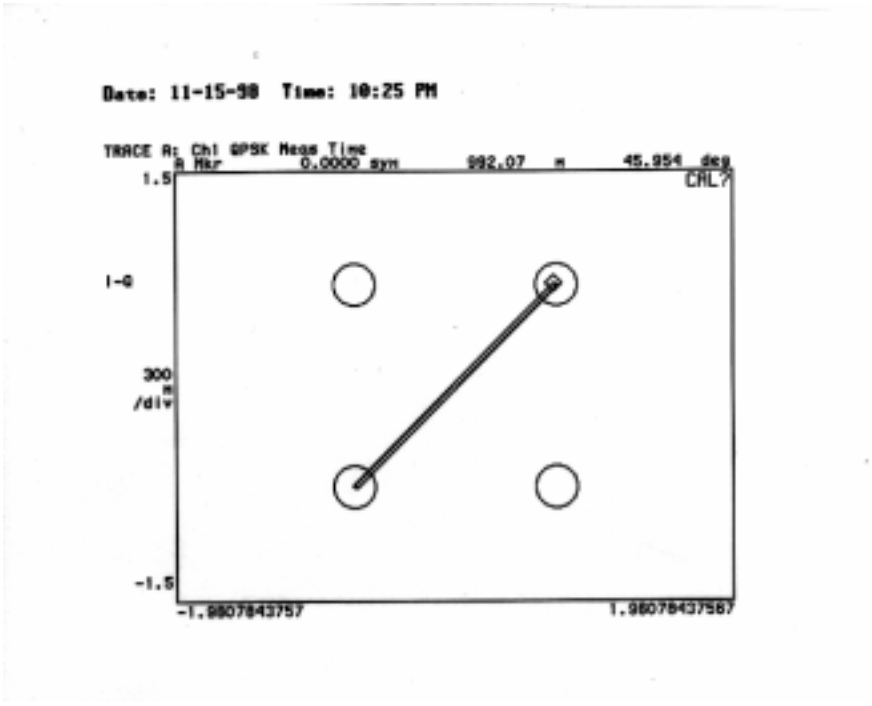

Figure 6.16 Measured Signal Constellation at Signal Point 3

The TRLA003 at points 4 and 5 provides power and a 100MHz reference for synchronization to the TRSS001 transmitter. It also provides (point 6) a 2.125GHz IF to the TRSS001. This is the 2nd IF in the system. The measured spectrum and signal constellation can be viewed in Figures 6.17 and 6.18.

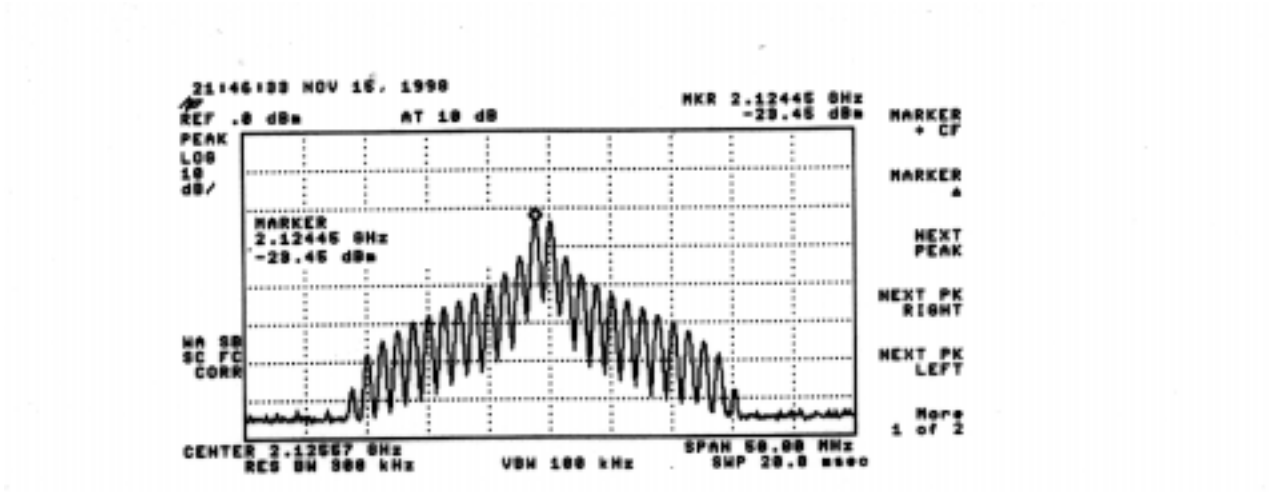

Figure 6.17 Measured Spectrum at Signal Point 6

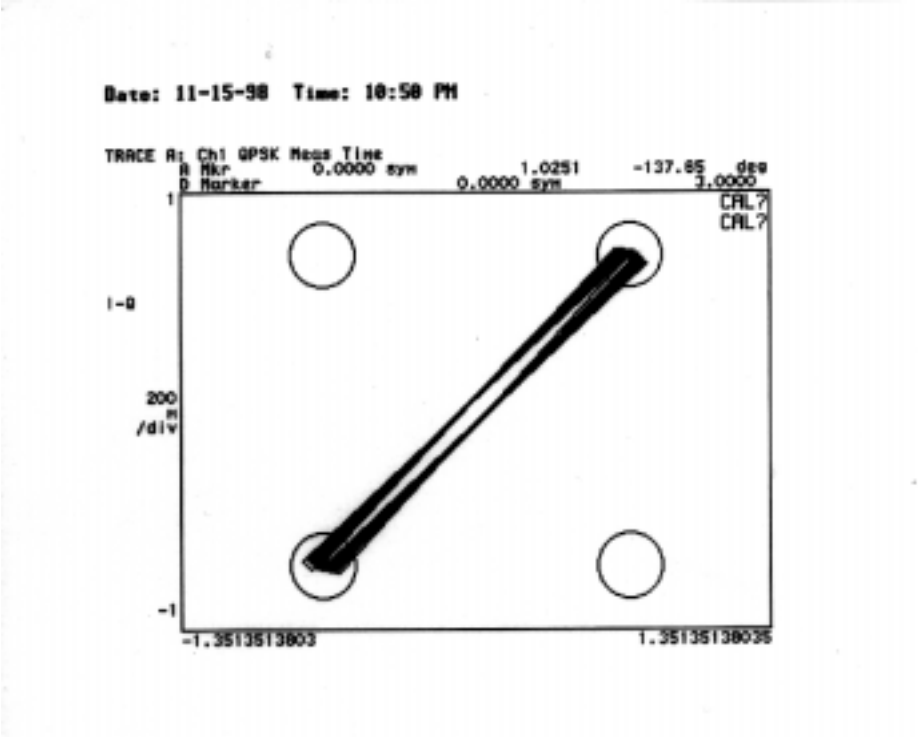

Figure 6.18 Measured Signal Constellation at Signal Point 6

In comparing the spectra between points 3 and 6 there is approximately unity gain via the TRLA003. In comparing the constellation plots at these points there is not much of a difference other than the scaling of the I/Q. In the plot for point 3 it was at 300m/div and for point 6 it was at 200m/div.

The RF output frequency of the TRSS001 transmitter was 27.525GHz. A power or spectral measurement was not done because of the risk of damaging equipment. The transmitter was designed to supply 30dB of gain; therefore a 1mW (0dBm) input becomes a 1000mW (30dBm) output.

A waveguide attenuator that was calibrated to attenuate by 6dB attenuated the output of the TRSS001 (point 8); this calibration was done by a power meter. The procedure used to do this follows:

1. Set the attenuator for maximum attenuation. Then connect the power meter to make sure that the attenuator is providing an attenuation (Figure 6.19).

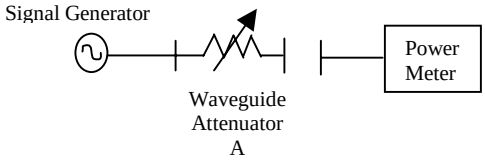

Figure 6.19 Procedure 1 for Calibrating Waveguide Attenuator

2. Reduce attenuation until P_0 = 10mW or 10dBm (Figure 6.20)

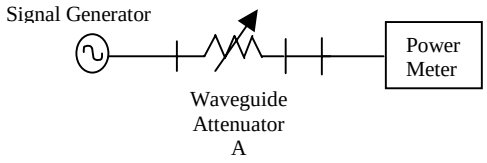

Figure 6.20 Procedure 2 for Calibrating Waveguide Attenuator

3. Adjust attenuator B for 6dB attenuation (Figure 6.21).

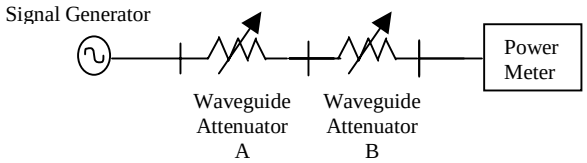

Figure 6.21 Procedure 3 for Calibrating Waveguide Attenuator

Attenuator A was first put in line to limit the power to the power meter since it was rated at a maximum of 300mW. Once this was done the waveguide attenuator could be calibrated to 6dB for application between the TRSS001 and the precision waveguide attenuator. This 6dB attenuation was put in line to limit the input to the precision waveguide attenuator to 250mW, since it has a maximum rating of 500mW.

This signal flow point (point 9) represents a place where signals can be adjusted over a 50dB range by the precision waveguide attenuator. This attenuator in essence provides 50dB of dynamic range; this does not include the additional signal variability at the signal generator. The signal level at point 9 was measured with a power meter with the signal generator set at –20dBm; this can be viewed in Table 6.2.

Table 6.2 Power Measurement Out of Precision Waveguide Attenuator

Attenuation (dB)	Measured output power of precision waveguide attenuator (dBm)
0	4.95
10	-5.03
20	-15.05
30	-25.80
40	-36.40

A flexible waveguide was attached to the output of the precision attenuator so that it would be easier to connect to the transmitting antenna. The signal levels at the output of the flexible waveguide can be viewed in Table 6.3.

Table 6.3 Power Measurement Out of Flexible Waveguide

Attenuation (dB)	Measured output power of flexible waveguide (dBm)
0	4.16
10	-5.92
20	-15.90
30	-25.44
40	-32.75

These measurements are within 1dB of the measured output of the precision waveguide attenuator. The only exception is the last measurement at 40dB of attenuation. This is attributable to the minimum measuring capability of the power meter, which is in the –30 to –40dBm range.

Point 10 is the output of the transmitting antenna with no measurement being done here. This point can also be considered the beginning of the transmission channel. The transmitter – receiver separation in the lab was 2.54m (8’ 4”); this equates to a path loss of 69.23 dB

Point 11 is the output of the receiving antenna. A measure of the output of the receive antenna was not done.

The LUCA007 provides the power and a 100MHz reference to the RVSS001. This is for signaling points 12 and 13.

The waveform at point 14 is a 725MHz IF coming out of the RVSS001. The RVSS001 translated the 27.525GHz waveforms to the above mentioned IF. It should be noted that the RVSS001 provides a 6dB gain. The measured spectrum and signal constellation can be viewed in Figures 6.22 and 6.23.

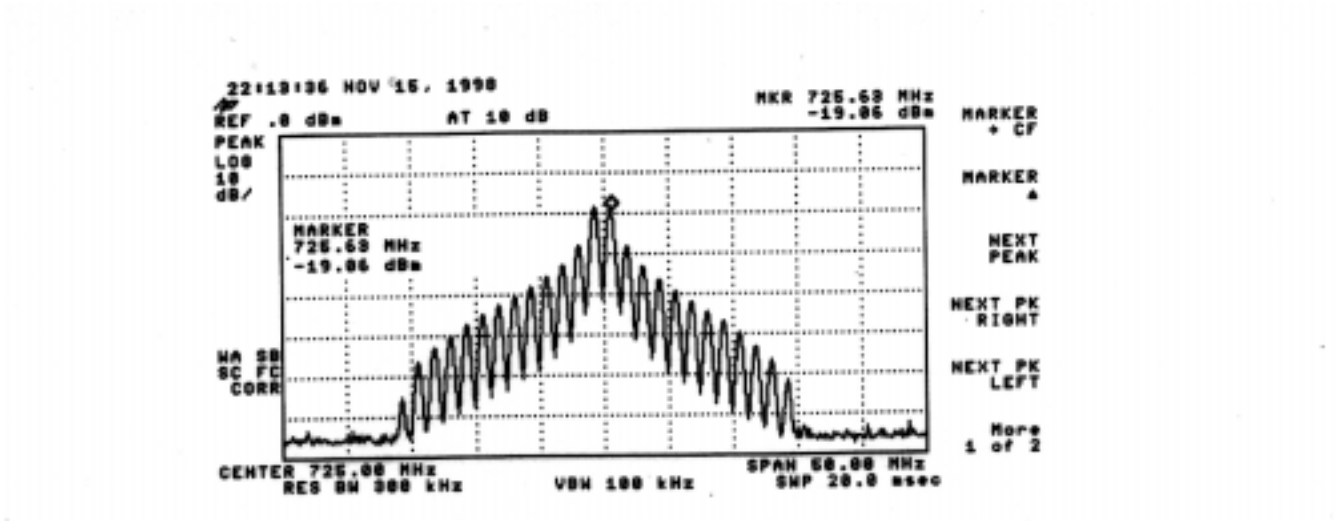

Figure 6.22 Measured Spectrum at Signal Point 14

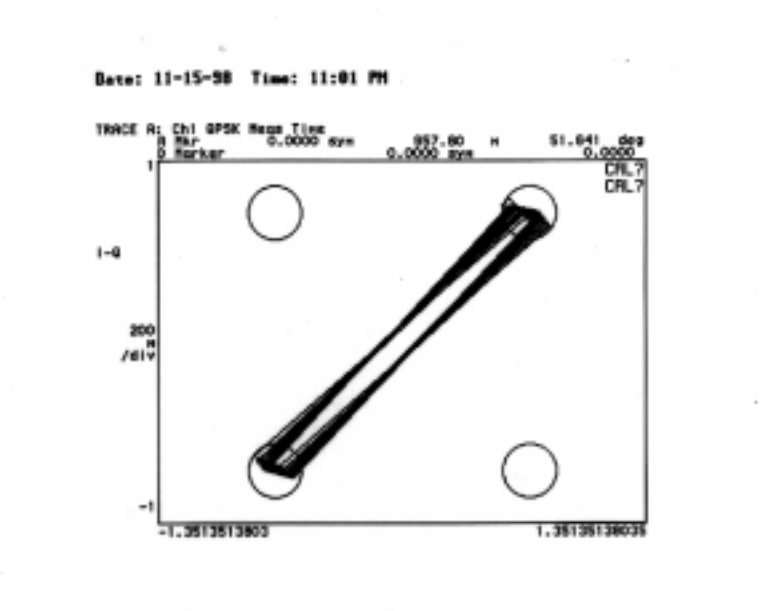

Figure 6.23 Measured Signal Constellation at Signal Point 14

The received signal level was measured to be –19.06dBm. We can check this for consistency with the calculated power budget.

$$P_r = P_t + G_t + G_r + Gain - PL - Losses$$

Where P_t = -20dBm

G_t = 36dBi

Gr = 31dBi

Gain = 6dB

PL = 69.32dB

Losses = 4.61dB

$$P_r = -20 + 36 + 31 + 6 - 69.32 - 4.61 = -20.93 dBm$$

$$P_{rmeasure} - P_{rcalculated} = -19.06 + 20.93 = 1.87dB$$

The difference between the measured and calculated power budget is 1.87dB; this is quite acceptable. The signal constellation shows a small increase in error for all parameters; this should be expected considering all the signal processing that takes place.

To prove that the link would be able to measure and overcome a fade, the following procedure was carried out. First a clear plastic gallon jug of water was introduced at midpath. We used water as an attenuator, since it is well characterized at 27.5GHz. The received signal level was measured to be –10dBm. Next we took the jug of water out of the path and measured the received signal to be 14.77dBm. From this we were able to determine that the attenuation introduced by the jug of water was 24.77dB. We then set the precision waveguide attenuator to this 24.77dB value to see if we could get back the previously measured received signal level of –10dBm. Once this was done we did achieve a received signal level of –9.98dBm; this is considered an acceptable result. The jug of water was then re-inserted into the system and the received signal was then re-measured to be –35dBm; this was a second measure for added confidence.

6.5 Roof Top Experiment

We conducted measurements using an antenna range located on the roof of Whittemore Hall on the Blacksburg Campus of Virginia Tech. The physical layout appears in Figure 6.24.

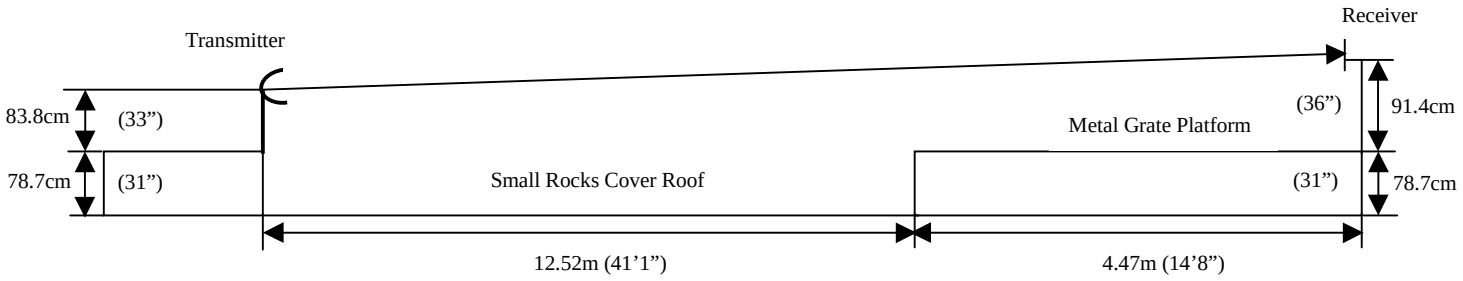

Figure 6.24 Rooftop Clear Air Transmission Physical Layout

Once the equipment was set up and the antennas were aligned, measurements began. The measurement was carried out in the following manner:

1. Make a clear air measurement with the precision attenuator set to a level which was determined on range. Measure the received spectrum and signal constellation at this point.
2. Move a tree onto the receive side platform as close as possible to the receiving antenna. Decrease level of attenuation until the received signal magnitude is at the same level as in clear air. Measure the received spectrum, signal constellation, and attenuation.

3. Repeat step 2 for tree depths of 2, 3, and 4 trees. If it is not possible restore the clear air signal level using the precision attenuator, then increase the input power from the signal generator. If the signal generator cannot be varied any more, then the precision attenuator and 6dB attenuator will be taken out. By doing this a dynamic range of 51dB (25 dB at the signal generator, 20 dB at the precision attenuator, and 6dB at the fixed attenuator) can be achieved at the transmit side. At the receive side the –45 dBm mark is the point at which the VSA measurement is questionable; considering we started with a clear air received signal strength of –26 dBm we have a receiver dynamic range of 19dB. This gives a system dynamic range of 70dB, which was suitable for our investigation.

The trees used for this investigation were coniferous. They were acquired from a Christmas tree farm and cut a few hours before the investigation. The trees were then put on Christmas tree stands so they could be put in the path in a stable manner. The trees had an average height of 2.20m (7’ 2.75”) and an average thickness at the base of 1.12m (3’ 8”). Figure 6.25 shows the radio link with four trees in the path.

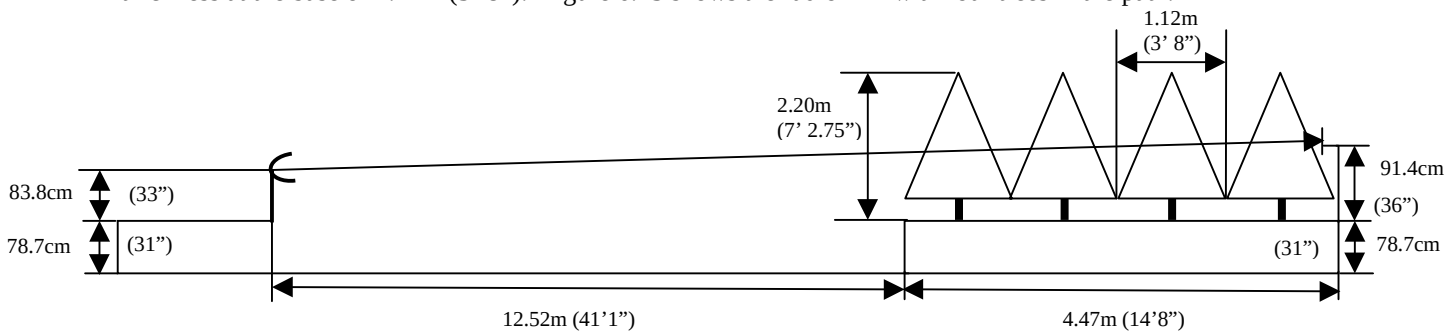

Figure 6.25 Rooftop Radio Link Transmission Physical Layout with Four Trees in Path

The measured spectrum and constellation for each stage in the measurements will now be reviewed. Also changes in the set up of the radio link will be reviewed. It should also be noted that the two days during which the measurements were taken the weather was clear but windy.

The first measurement was in clear air. The signal generator was set to –20dBm and the precision attenuator was set to 20dB. The received spectrum and signal constellation can be reviewed in Figures 6.26 – 6.27.

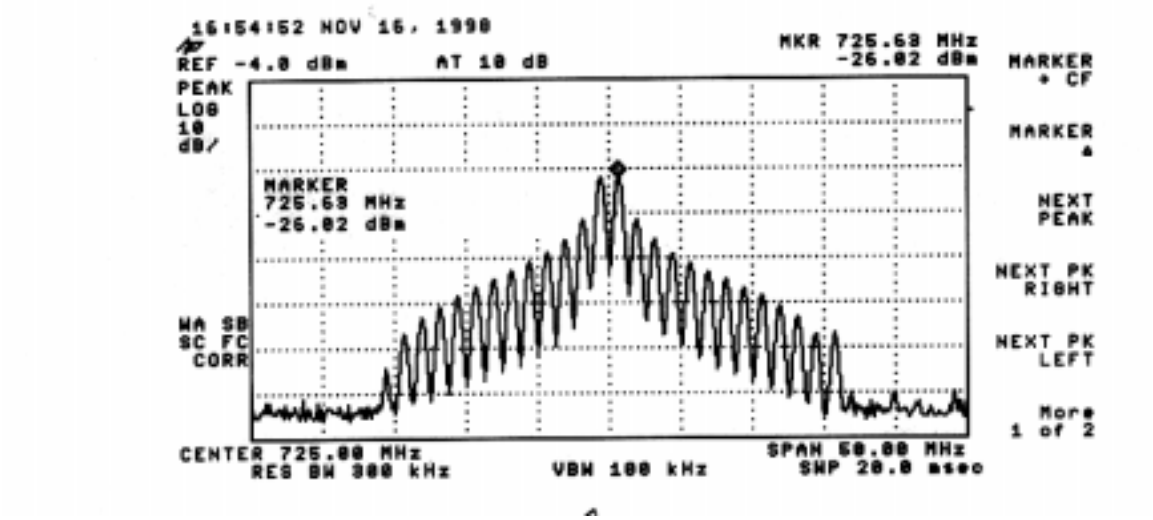

Figure 6.26 Measured Received Spectrum: Clear Air Path

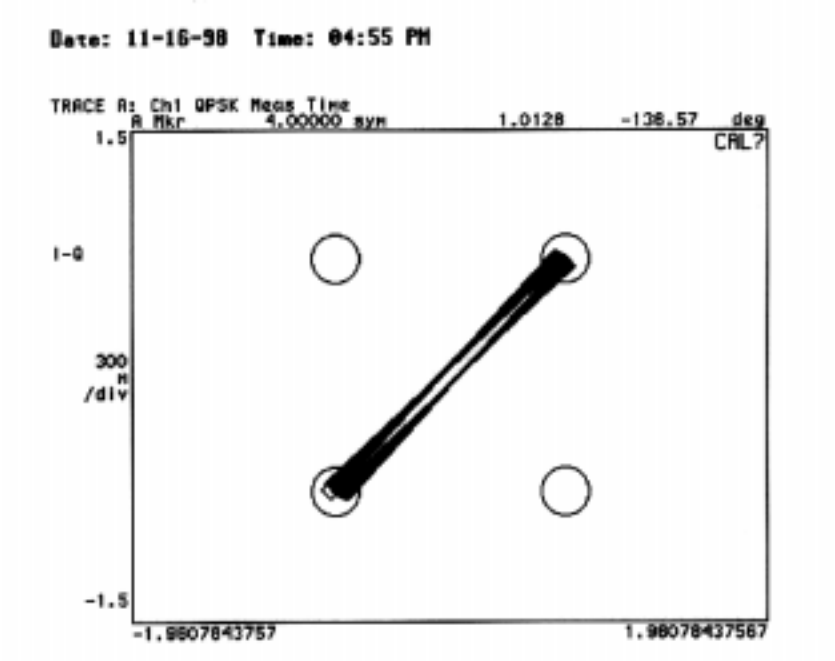

Figure 6.27 Measured Signal Constellation: Clear Air Path

At this point it would seem logical to prove that the measured spectrum is reasonably close to the calculated power budget. The measured receive power was –26.02dBm. The calculated power budget is as follows:

$$P_r = P_t + G_t + G_r + Gain - PL = -15.90 + 36 + 31 + 6 - 86 = \underline{-28.90dBm}$$

The difference between the measured and calculated power budgets is 2.88dB. This difference could be attributed to at least one issue if not more. It was expected that –14dBm would be fed to the transmit antenna instead of –15.90dBm (Table 6.3), which was measured at the output of the flex waveguide. This difference could either be attributed to the accuracy of the power measurement and / or the calibrating of

the 6dB attenuator. If this is the case then the measured and calculated power budgets would be within 1dB, which is quite acceptable.

The second measurement was done with one tree in the path. The signal generator was set at –20dBm and the precision attenuator was set at 3dB. The received signal spectrum and signal constellation can be viewed in Figures 6.28 – 6.29.

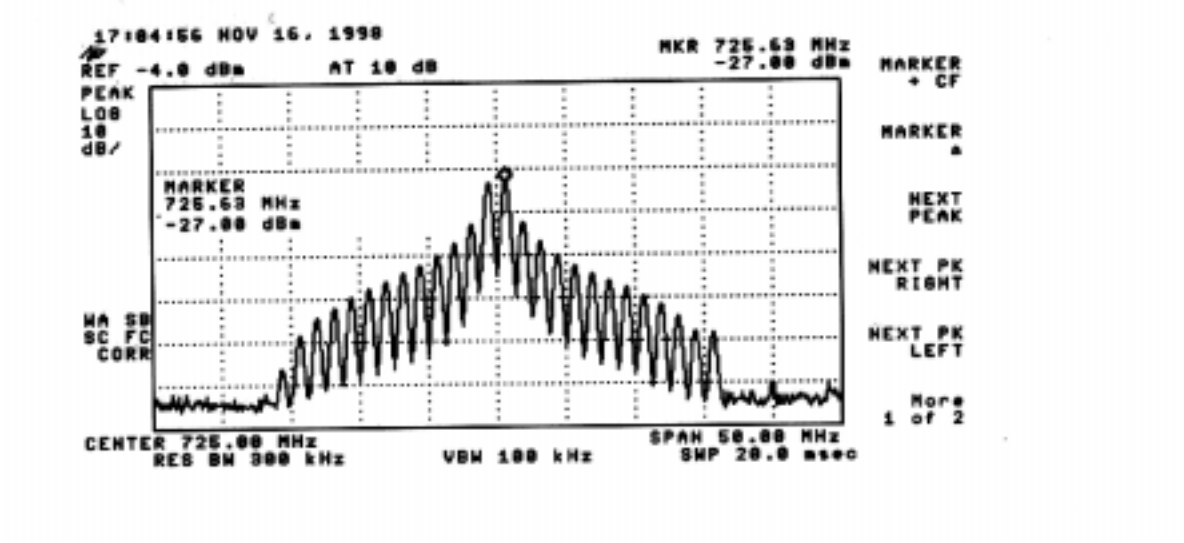

Figure 6.28 Measured Received Spectrum: One Tree in Path

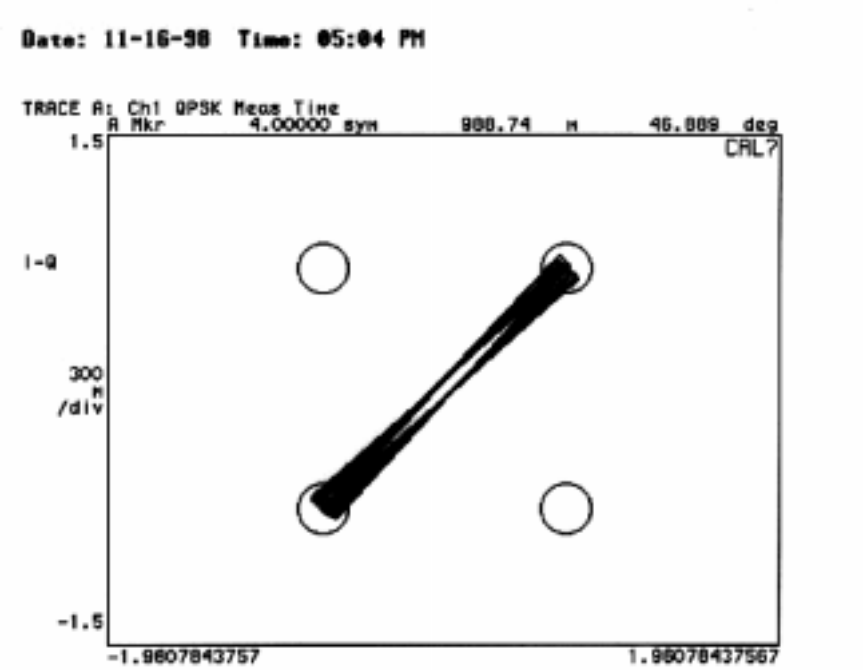

Figure 6.29 Measured Signal Constellation: One Tree in Path

From this it can be seen that it was possible to get back to the same level that was measured in clear air. Considering this an attenuation of 17dB was found for one tree in the path.

We then moved on to putting two trees in the path. The signal generator was set for –5dBm and the precision attenuator was set for 1dB. The received signal spectrum and signal constellation can be reviewed in Figures 6.30 – 6.31.

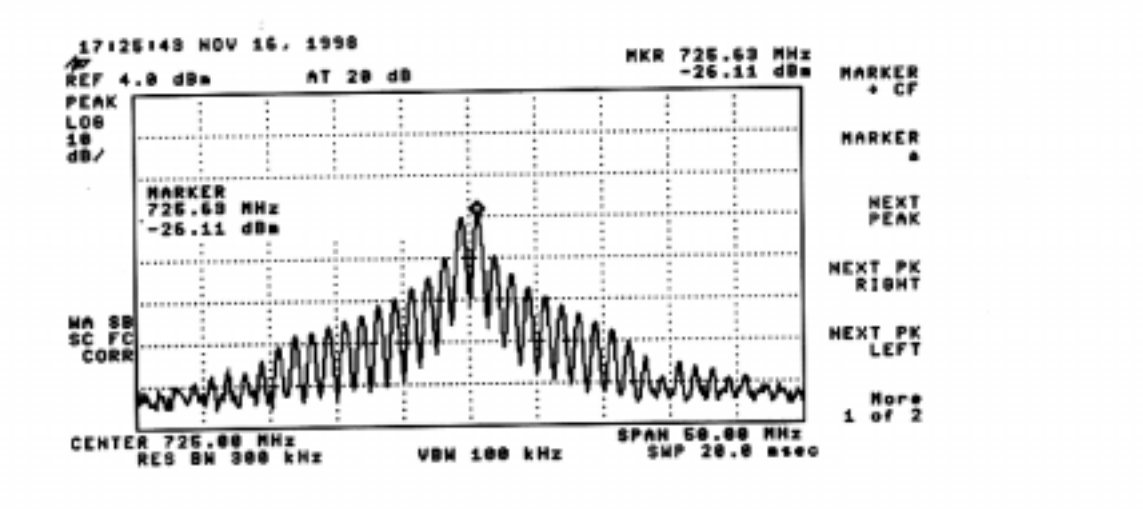

Figure 6.30 Measured Received Spectrum: Two Trees in Path

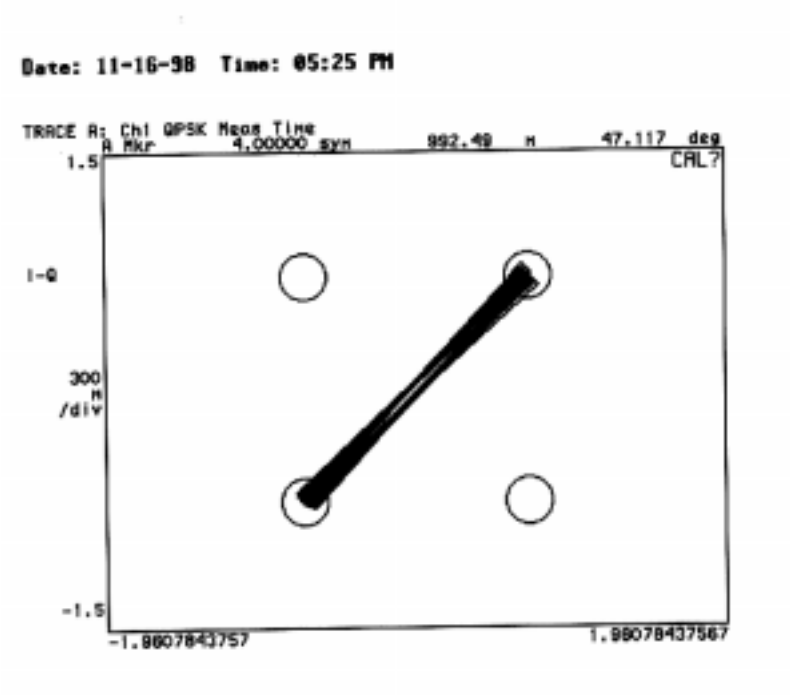

Figure 6.31 Measured Signal Constellation: Two Trees in Path

We were able to attain the same level that was measured in clear air. Considering this an attenuation of 34dB was found for two trees in the path.

The fourth measurement taken was with three trees in the path. The signal generator was set for 5dBm and the precision attenuator was set to 0dB. The received signal spectrum and signal constellation can be viewed in Figures 6.32 – 6.33.

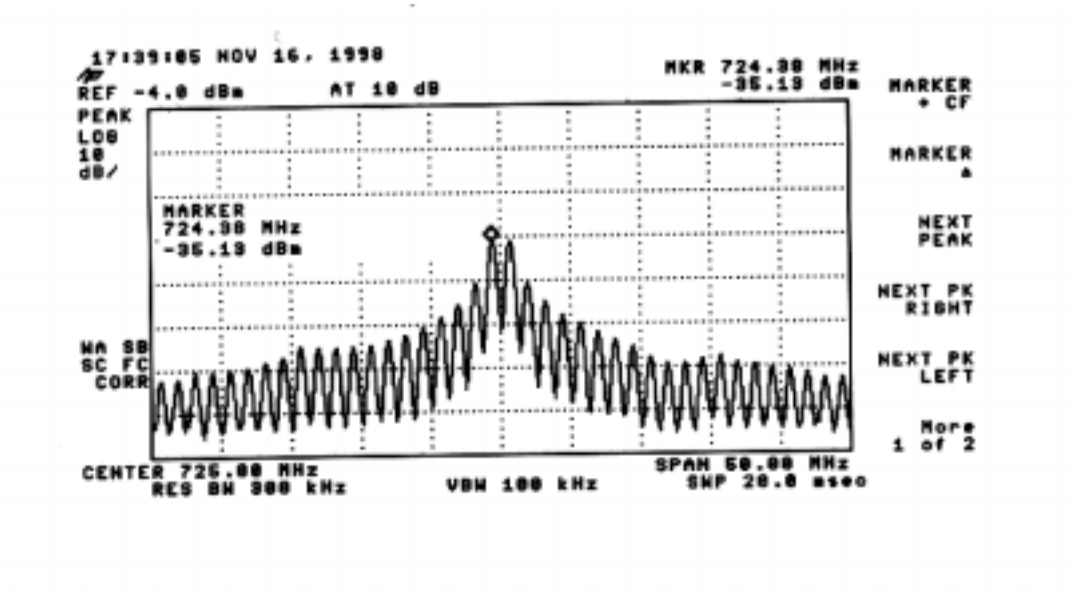

Figure 6.32 Measured Received Spectrum: Three Trees in Path

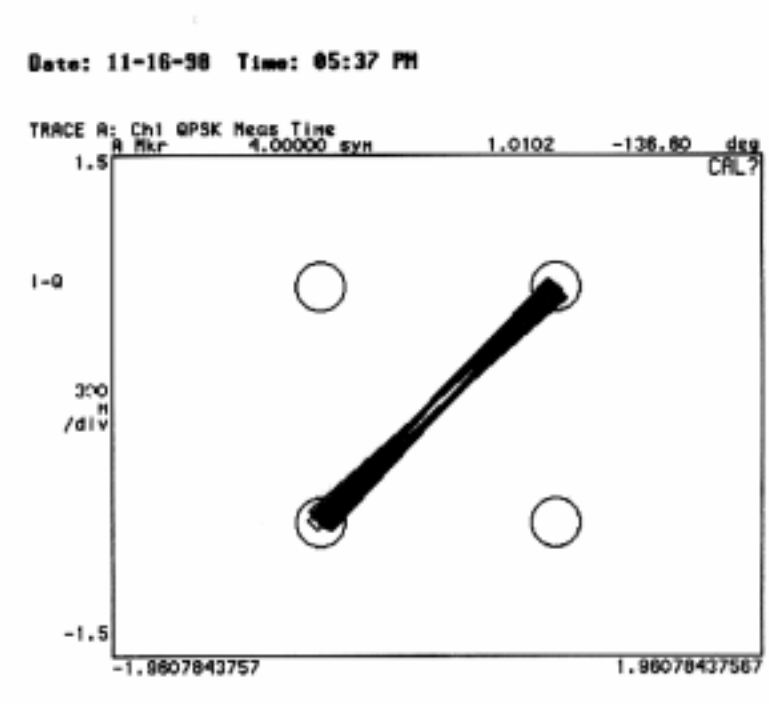

Figure 6.33 Measured Signal Constellation: Three Trees in Path

In this case we were not able to attain the same level that was measured in clear air. Considering this an attenuation of 55dB was found for three trees in the path.

The measurements on 11/16/98 were concluded with three trees in the path because of nightfall. We resumed measurements on 11/17/98 in mid-morning. The first step was to put three trees in the radio link path and re-create the three-tree measurement that was done on 11/16/98. This was done and the spectral and vector results can be reviewed in Figures 6.34 – 6.35.

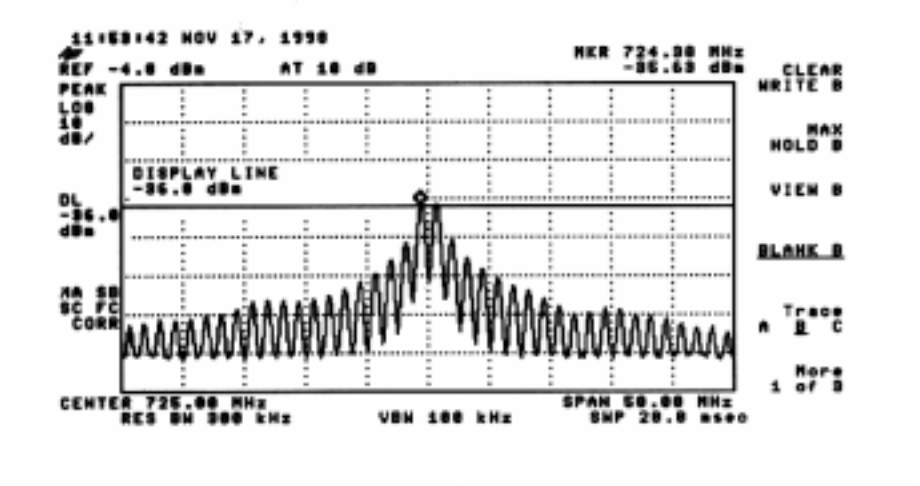

Figure 6.34 Measured Received Spectrum: Three Trees in Path

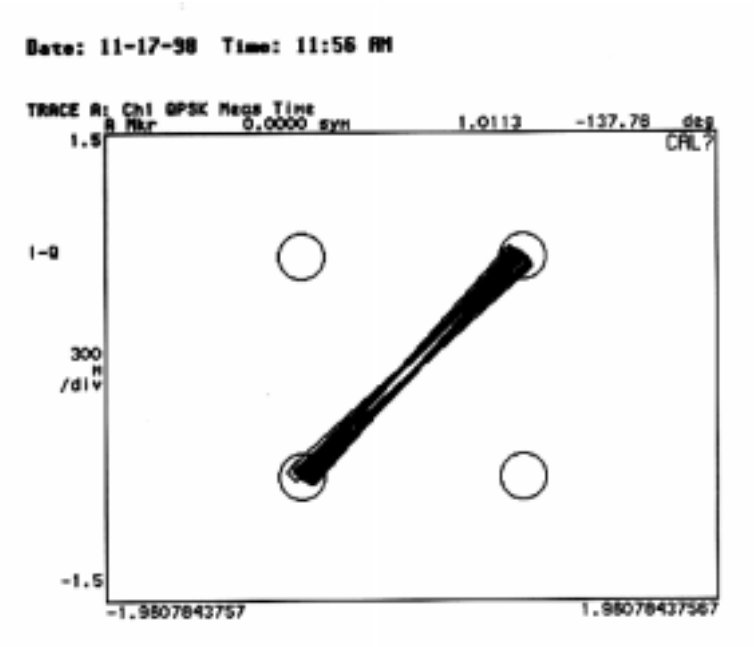

Figure 6.35 Measured Signal Constellation: Three Trees in Path

We then put four trees in the path. There were two measures done for this number of trees. Both measurements had the signal generator set at 5dBm, but one had the 6dB attenuator in line and the

precision attenuator set equal to zero and the other had both the fixed and variable attenuation taken out of the network. The spectral and vector measurements for the first measurement can be seen in Figures 6.36 – 6.37 and the second set of measurements are shown in Figures 6.38 – 6.39.

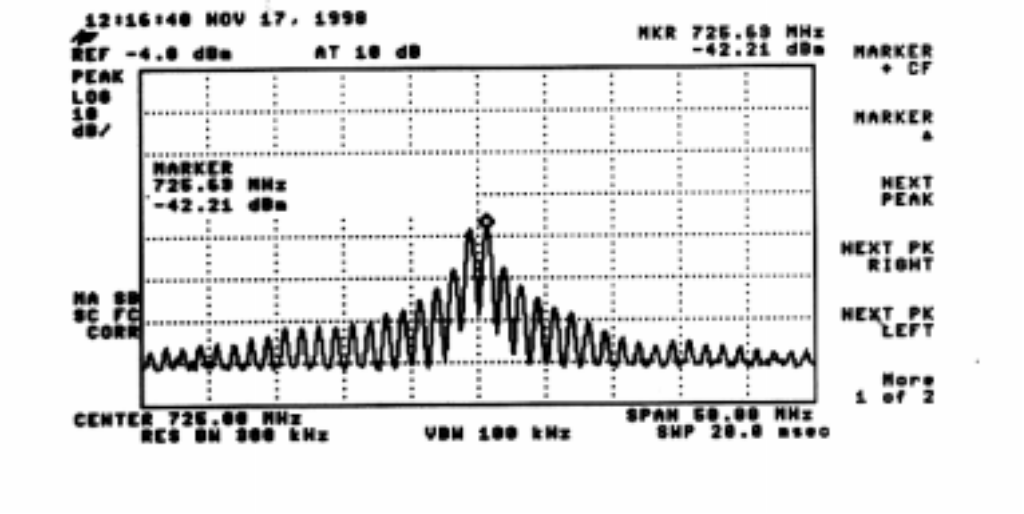

Figure 6.36 Measured Received Spectrum: Four Trees in Path

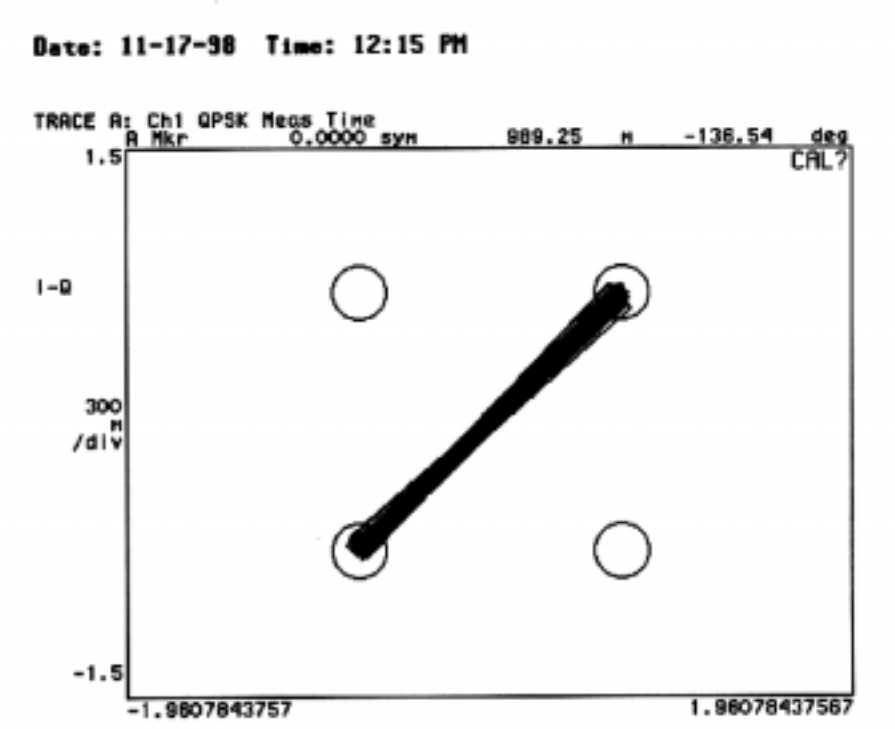

Figure 6.37 Measured Signal Constellation: Four Trees in Path

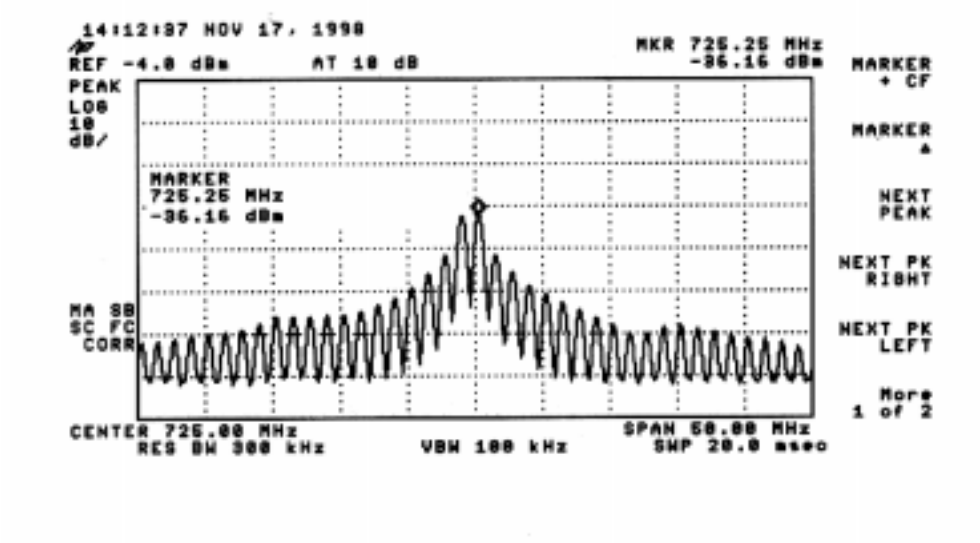

Figure 6.38 Measured Received Spectrum: Four Trees in Path (No Attenuation)

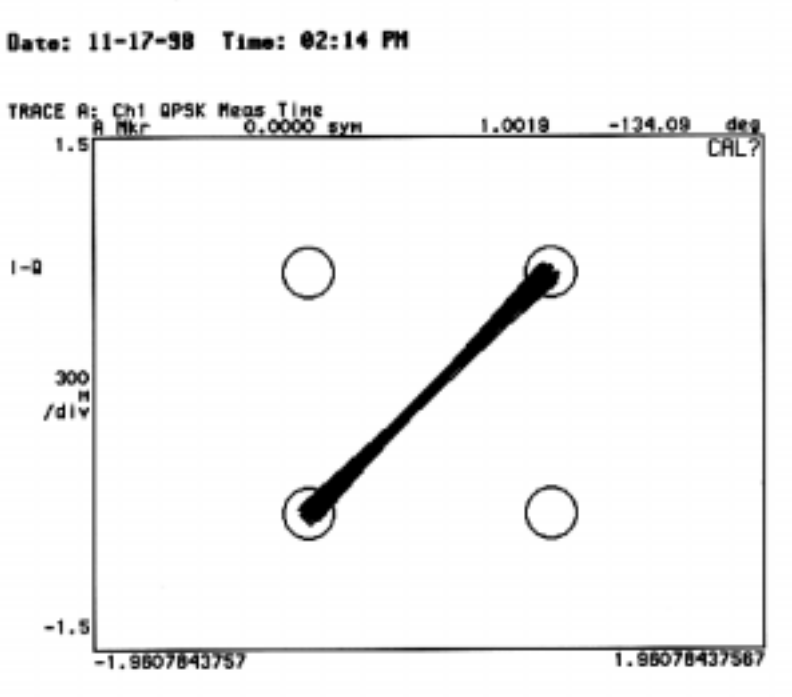

Figure 6.39 Measured Signal Constellation: Four Trees in Path (No Attenuation)

From this it can be seen that we were not able to achieve the same level that was measured in clear air. Considering this a 61dB attenuation was found for this number of trees in the path. Another good performance measure can be viewed by comparing Figure 6.34 and 6.38; here a 6dB change at the transmitter showed a 6dB change at the receiver.

Once this part of the experiment was completed the receiving antenna was set up for co-polarization (horizontal polarization) and cross polarization (vertical polarization) measurements with 4, 3, 2, and 1 trees in the path. For this the signal generator was set at 5dBm and all attenuation was taken out of the system. The spectral results for this measurement can be viewed in Appendix A Figures A.1 – A.10. The results of these measurements and the others previously reviewed in this subsection will be discussed further in section 8.

6.6 Types of Measurement Data Captured

The intent of this section is to discuss what types of data were captured during the vegetation measurements. The measurements that were captured and printed on paper are the frequency spectrum, signal constellation, and symbol error table measurements. These measurements were presented in previous portions of section 6. The only measurement that was not shown is the symbol error table; this is shown in Figure 6.40.

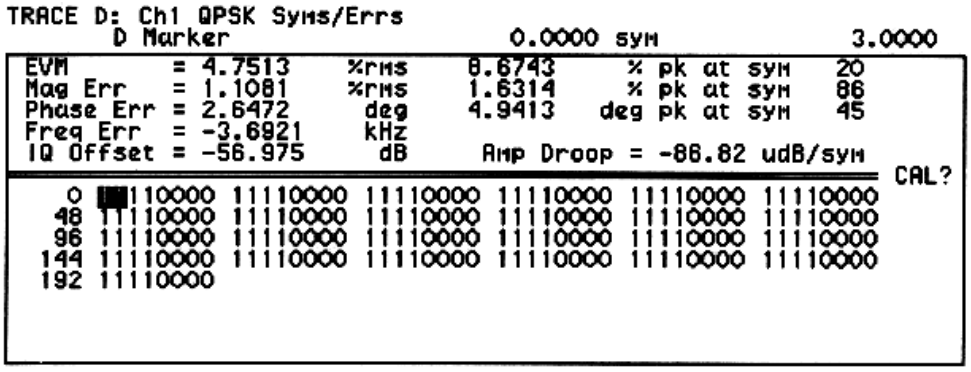

Figure 6.40 Symbol Error Table (No Trees in Path)

The symbol error table shows the following measures:

- Error Vector Magnitude (EVM)
- Magnitude Error
- Phase Error
- Frequency Error
- IQ Offset
- Symbol Error Table

Data were also captured and stored on a floppy disk. For each data point the symbol error table, measured magnitude, and reference magnitude was taken for a 100-symbol burst. This data was processed using Hewlett Packard DOS utilities. These were the Standard Data Format (SDF) and Viewdata utilities. The SDF utility allowed the data to be converted to ASCII via the SDFTOACS command. This data could then be pasted into a spread sheet. The Viewdata utility provided a graphical representation of captured data.

The basis of the measurements described so far will now be discussed:

- The spectrum analyzer displays the total power in the analyzer bandwidth. The measure is in watts/Hz but is typically represented in dBm, which is a decibel referenced to 1mW.
- The VSA: measured and reference magnitude, phase, and symbol measurements:

- All of these measurements are referenced to the time at which a symbol has occurred. Here each time point occurs at 400ns which is equivalent to a symbol rate of 2.5Msps which was the transmitted symbol rate.
- Magnitude measure for a PSK waveform is a voltage normalized to one volt. For the measured magnitude signal there is deviation from the reference voltage point and the reference magnitude signal is equal to the reference voltage point. The difference between the two for a given symbol is the magnitude error.
- Phase measured for the PSK waveform in our case varied between 45° and -135°; this is due to the 11110000-bit sequence that was transmitted over the channel. For the measured signal case there is a deviation from these values, and the reference signal is equal to these values. The difference between the measured and reference phases is called the phase error.

It is presumed that if the magnitude and phase information is detected then the I and Q information is found in the following manner (equations (6.3 – 6.6)).

To transform from magnitude/phase form to I/Q [17]:

$$I(t) = R(t)\cos\theta(t) \tag{6.3}$$

$$Q(t) = R(t)\sin\theta(t) \tag{6.4}$$

To transform from I/Q to magnitude/phase [17]:

$$R(t) = \sqrt{I(t)^2 + Q(t)^2} \tag{6.5}$$

$$\theta(t) = \tan^{-1}\left[\frac{Q(t)}{I(t)}\right] \tag{6.6}$$

- I and Q measurements for the PSK waveform in our case varied between 0.7071 and –0.7071; this is due to the transmitted data sequence.
- The symbol measure shows the decimal representation of the detected received symbol. In this case either a 0 or 3 was received, again due to the transmitted data sequence. These decimal values represent the transmitted symbols “00” and “11”. If an error has occurred then either a 0 or a 3 occurs out of place or a 1 or 4 is registered.

A listing of measured and reference magnitude, phase, I, Q, and symbols is presented in Appendix B Tables B.1 – B.5. This data set is from the second day of roof measurements with three trees in the path.

6.7 Data Representation

The magnitude and phase information gathered over the two day trial was exported from the previously mentioned Hewlett Packard SDF utility to Microsoft Excel; this allowed for the data to be represented in tabular form. Microsoft Excel and Matlab by Mathworks was used to process all the data.

The reference magnitude data was compared to the measured magnitude data. This difference or error was listed in a column for each symbol measured. From that an error average and error standard deviation was calculated. The procedure was carried out for the magnitude, phase, and I/Q measurements done over the two-day period. The results of these calculations are listed below in Tables 6.4 – 6.7.

Table 6.4 LMDS Propagation Measurement in Vegetation Results: Magnitude

Number of Trees	Magnitude Error Average	Magnitude Error Standard Dev.
0	0.010845078	0.002288329
1	0.010276478	0.002630525
2	0.008236483	0.003976486
3	0.008645596	0.004620067
3	0.010677956	0.006067179
4	0.014736196	0.009874431

Table 6.5 LMDS Propagation Measurement in Vegetation Results: Phase

Number of Trees	Phase Error Average (degrees)	Phase Error Standard Dev. (degrees)
0	2.3027767	1.131231826
1	2.4767478	1.712219162
2	1.9475733	1.323131352
3	2.0950945	1.417884951
3	2.1918983	1.383218489
4	1.6011387	1.05886727

Table 6.6 LMDS Propagation Measurement in Vegetation Results: I (Real)

Number of Trees	I (Real) Error Average	I (Real) Error Standard Dev.
0	0.03592023	0.016372003
1	0.036147516	0.023050641
2	0.02823754	0.018385887
3	0.030526356	0.019002787
3	0.032505447	0.019417152
4	0.022413297	0.015243421

Table 6.7 LMDS Propagation Measurement in Vegetation Results: Q(Imaginary)

Number of Trees	Q (Imaginary) Error Average	Q (Imaginary) Error Standard Dev.
0	0.022155343	0.01459785
1	0.026171547	0.018671396
2	0.020663637	0.014284589
3	0.022436033	0.015768187
3	0.022623722	0.015809338
4	0.021767477	0.01504146

From Tables 6.6 and 6.7 the average error vector magnitude (EVM) for each measurement could be calculated from equation (6.7).

$$EVM = \sqrt{I_{errorave.}^2 + Q_{errorave.}^2} \tag{6.7}$$

The EVM is the magnitude of the phasor difference as a function of time between an ideal reference signal and the measured transmitted signal [41] (Figure 6.41). Table 6.8 shows the result of the EVM calculations.

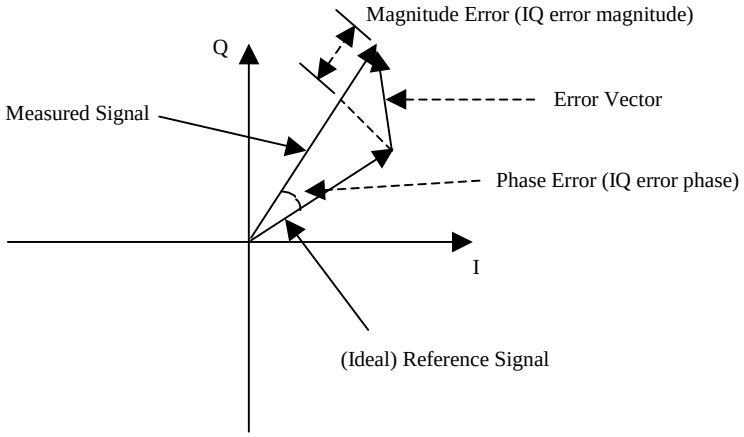

Figure 6.41 Error Vector Magnitude Concept [41]

Table 6.8 LMDS Propagation Measurement in Vegetation Results: Average Error Vector Magnitude

Number of Trees	Average Error Vector Magnitude	% Average Error Vector Magnitude
0	0.042203343	4.220334284
1	0.044627265	4.462726504
2	0.034990635	3.499063531
3	0.037884482	3.788448215
3	0.039603496	3.960349583
4	0.031243862	3.124386239

The signal to noise ratio (SNR or S/N) corresponding to the EVM measured at the receiver output is defined in equation (6.8) [42]. Table 6.9 shows the SNR calculated from the EVM data presented in Table 6.8.

$$\frac{S}{N} = -20\log(EVM) \tag{6.8}$$

Table 6.9 LMDS Propagation Measurement in Vegetation Results: Average Signal to Noise Ratio

Number of Trees	Average Signal to Noise Ratio (SNR) dB
0	27.49306296
1	27.00799456
2	29.12096344
3	28.4307729
3	28.04532954
4	30.10470567

Table 6.10 relates EVM and SNR to BER for a QPSK modulated waveform; this was found in review of documentation provided by Hewlett Packard.

Table 6.10 EVM and SNR Relation to BER for a QPSK Modulated Waveform

EVM→	1%	5%	10%	20%	30%
SNR					
5dB	$1x10^{-1}$				
10dB	$1.4x10^{-2}$	$1.9x10^{-2}$	$2.7x10^{-2}$	$5.5x10^{-2}$	
15dB	$4.8x10^{-5}$	$1.1x10^{-4}$	$3.2x10^{-4}$	$2.2x10^{-3}$	$1.1x10^{-2}$
20dB	$1.6x10^{-12}$	$2.5X10^{-11}$	$6.4X10^{-10}$	$2x10^{-7}$	$2.3x10^{-5}$

The next set of measurements that will be presented are for attenuation vs. number of trees (Table 6.11 and Figure 6.42).

Table 6.11 LMDS Propagation Measurement in Vegetation Results: Attenuation vs. Number of Trees

Number of Trees	Attenuation (dB)
0	0
1	17
2	34
3	55
4	61

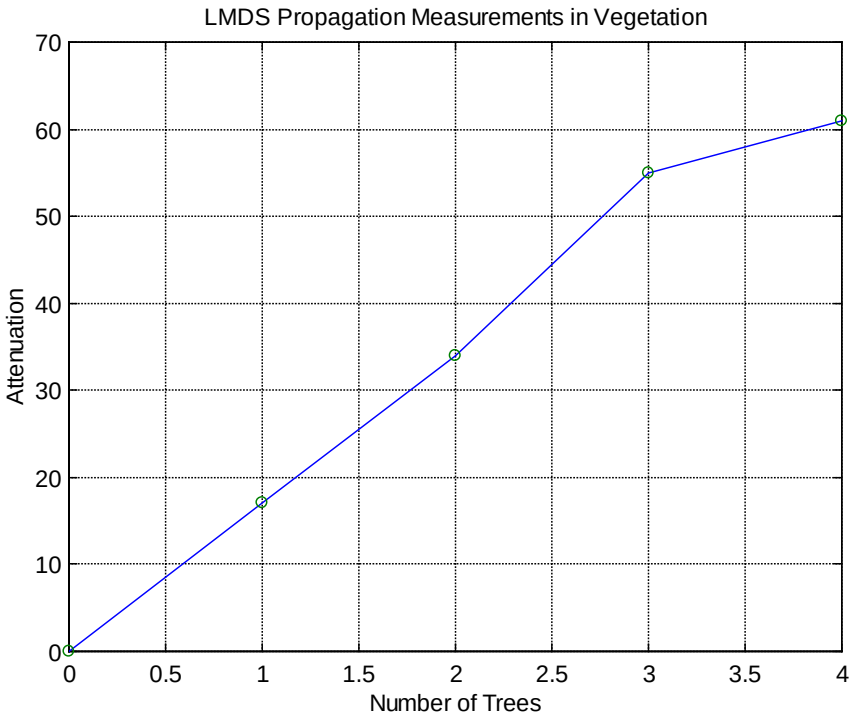

Figure 6.42 LMDS Propagation Measurement in Vegetation Results: Attenuation vs. Number of Trees

The co and cross polarization measurements will now be presented with the co-polarization measurement occurring when the receiving antenna is set at horizontal polarization and the cross polarization measurement occurring when the receiving antenna is set at vertical polarization (Table 6.12 and Figure 6.43).

Table 6.12 LMDS Propagation Measurement in Vegetation Results: Polarization Measurements

Number of Trees	Polarization (H/V)	Signal Level (dB)
0	V	-16.55
0	H	-4.79
1	V	-26.56
1	H	-19.56
2	V	-39.55
2	H	-32.41
3	V	-44.39
3	H	-37.62
4	V	-42.63
4	H	-41.5

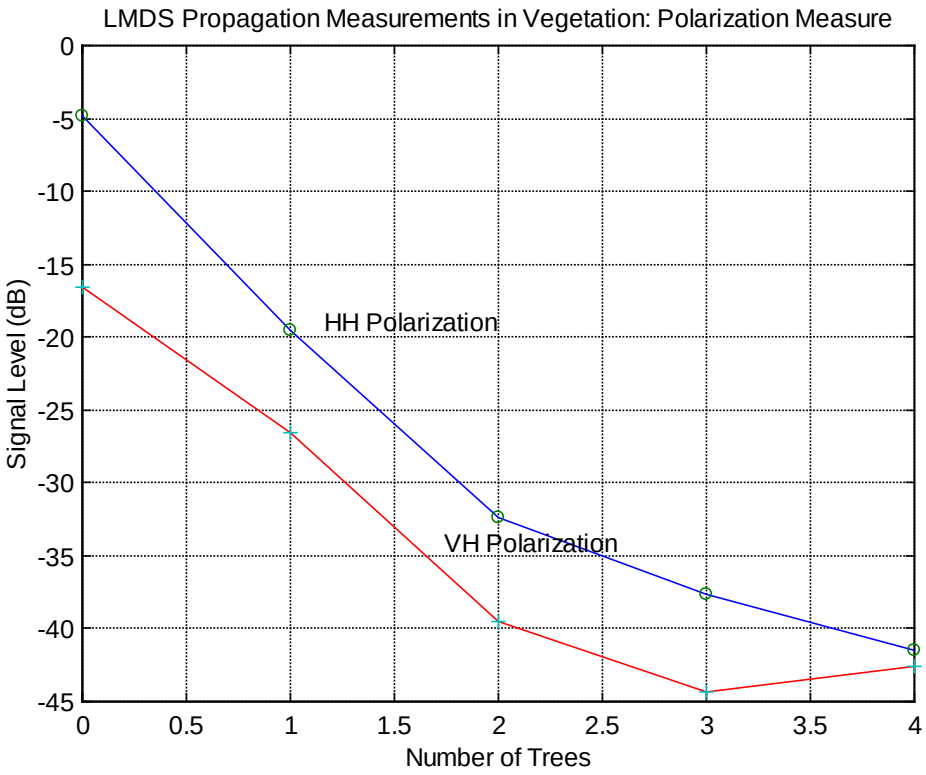

Figure 6.43 LMDS Propagation Measurement in Vegetation Results: Polarization Measurements

6.8 Results

The average magnitude, phase, and I/Q error for the measurements done (0 → 4 trees) shows that for all cases there is low error. If there is a low error measurement then one would expect a reasonably high SNR. This is the case when the SNR is related to the EVM (0 → 4 trees) with a maximum SNR being 30.1dB with four trees in path and a minimum being 27.01dB with one tree in path. Also Table 6.9 shows that the BER associated with this SNR is low, which would be expected.

The polarization measurements initially show that there is an approximate 12dB cross polarization discrimination (XPD) with no trees in the path. This drops to about 7dB of XPD for the 1-3 tree measurement and at four trees the two polarization measures are converging on each other.

The attenuation vs. number of trees measurement result is what was expected; this being an initial high attenuation and then becoming more gradual after a few trees. We believe that the signal is attenuated as it travels through these trees, but also as the signal passes through several trees it becomes randomly polarized explaining the gradual transition in attenuation. So, phase does not vary randomly with time; therefore it is coherent. This is supported by the measurements showing a low level of phase error. Although we offer the above conclusion to the gradual transition in attenuation, it is not possible absolutely to eliminate the possibility of multipath components 50dB (or more) below the line of site signal as stated in section 6.0. Nevertheless, in our opinion, three things argue against a multipath mechanism.

- If multipath were present, the antenna patterns of Figure 6.2 should show an angular shift of the main lobe. They do not. The lobe structure of the antenna patterns simply disappears.
- If multipath were present, we would expect a significant increase in BER at high attenuation due to frequency-selective fading. This was not observed.
- The observations that the slope of the attenuation curve changes at approximately 50dB attenuation were made on two quite-different test ranges using entirely different equipment.

The most important result from these measurements is that vegetative attenuation introduces no significant incoherent phase effects. Like rain, vegetation in an LMDS path simply reduces the received signal level. We can compensate either kind of fading by increasing the transmitter output power (or, presumably, the transmitting antenna gain). So far as LMDS is concerned, this is the key contribution of our experiment.

Chapter 7.0 Conclusion

The thesis reviewed LMDS and discussed its competitive advantages. We reviewed link budgets and radio link design as it pertained to the mm-wave frequency region where LMDS presides. As the thesis progressed through the previously mentioned review, topics related to LMDS system engineering were also discussed. Specific results from chapter 5 are listed below.

- Refractive effects can typically be neglected because in most cases LMDS radio links range between 3-5km.
- Diffraction effects need to be accounted for by having proper first Fresnel zone (F_1) clearance (typically 0.6 F_1 is sufficient). First Fresnel zone clearances for a 1-5km LMDS radio path range from 1.63 – 3.66m.
- Multipath fading should be rare at LMDS frequencies considering the following
  - Man made and natural surfaces appear rough.
  - High gain antennas are used, which exclude multipath.
- Rain fading must be accounted for when working above 10GHz. As an example: The fade margin that would be needed for ITU-R region K at a frequency of 28GHz, a path length of 3km, and an exceedance of 0.001% is approximately 37dB.

In reviewing these radio link design topics we identified vegetation as a problem; this being fading and suspect incoherent effects. This required further investigation through experimentation specifically we wanted to determine whether errors in the demodulated magnitude and phase due to vegetation fading could be overcome by increasing transmitter EIRP.

The investigation showed that the observed effects are almost certainly not due to incoherent propagation. It also showed that vegetative fading can be alleviated by increasing transmitter EIRP.

Appendix A: Spectral Results for Co and Cross Polarization Measurements

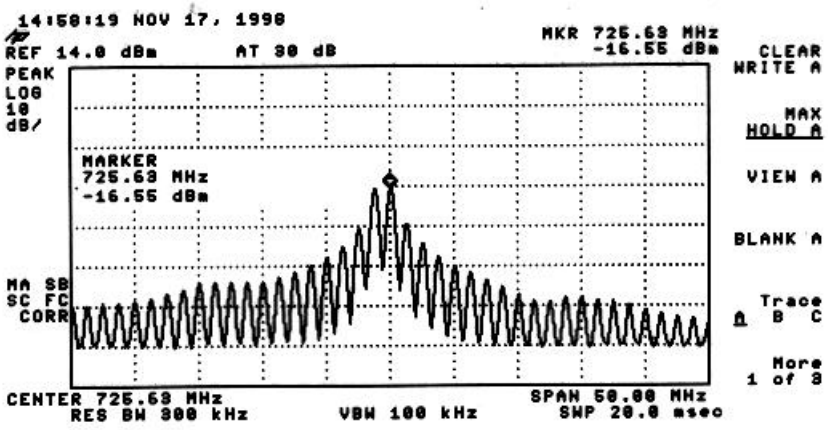

Figure A.1 Cross (Vertical) Polarization Measure with No Trees in Path

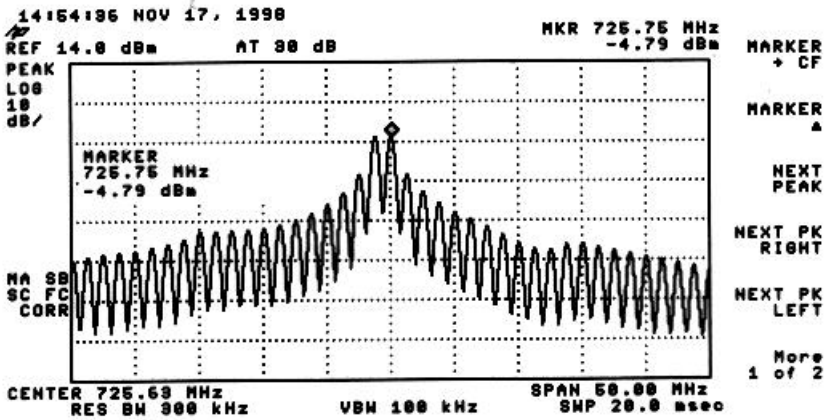

Figure A.2 Co (Horizontal) Polarization Measure with No Trees in Path

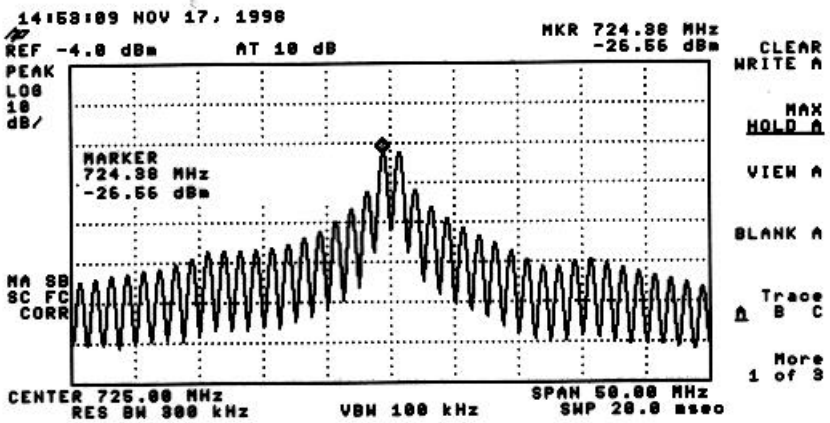

Figure A.3 Cross (Vertical) Polarization Measure with 1 Tree in Path

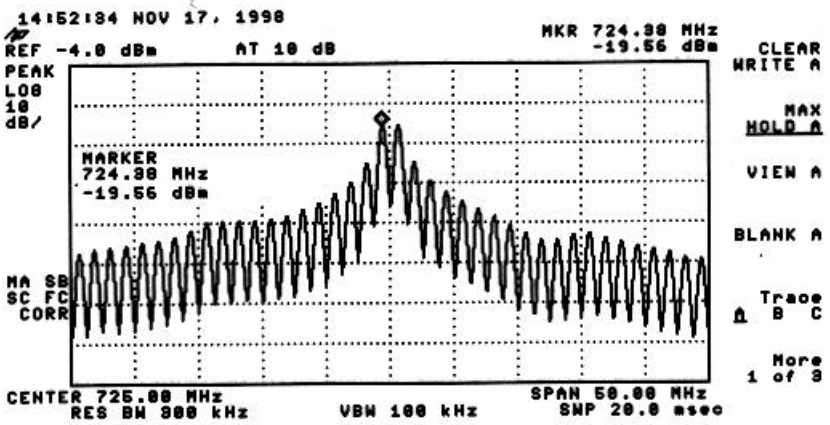

Figure A.4 Co (Horizontal) Polarization Measure with 1 Tree in Path

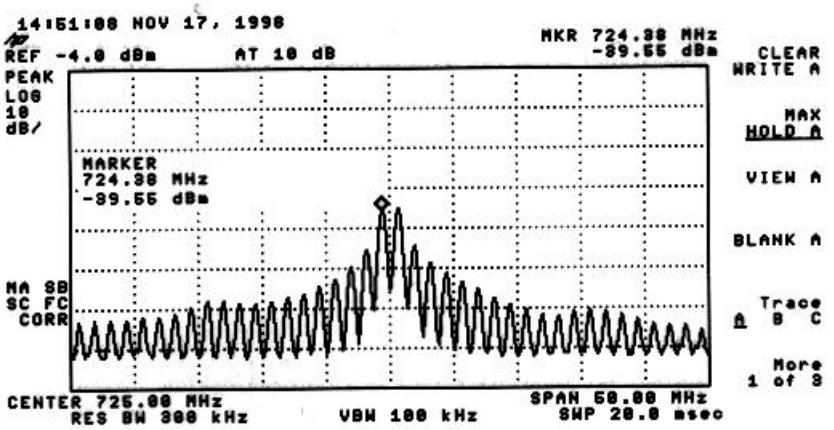

Figure A.5 Cross (Vertical) Polarization Measure with 2 Trees in Path

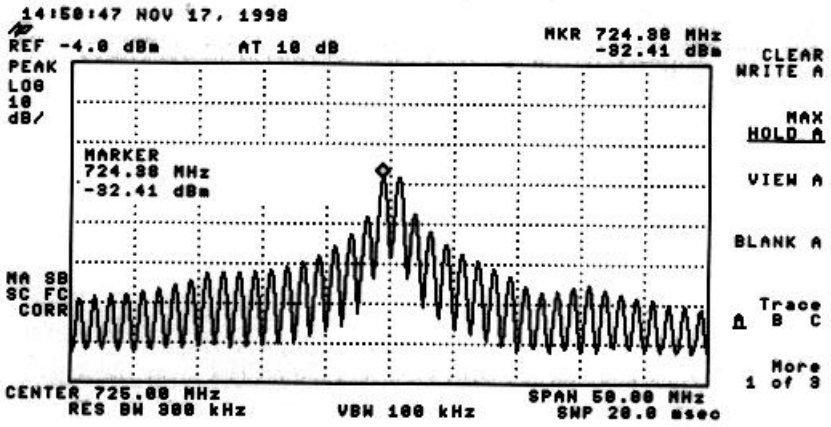

Figure A.6 Co (Horizontal) Polarization Measure with 2 Trees in Path

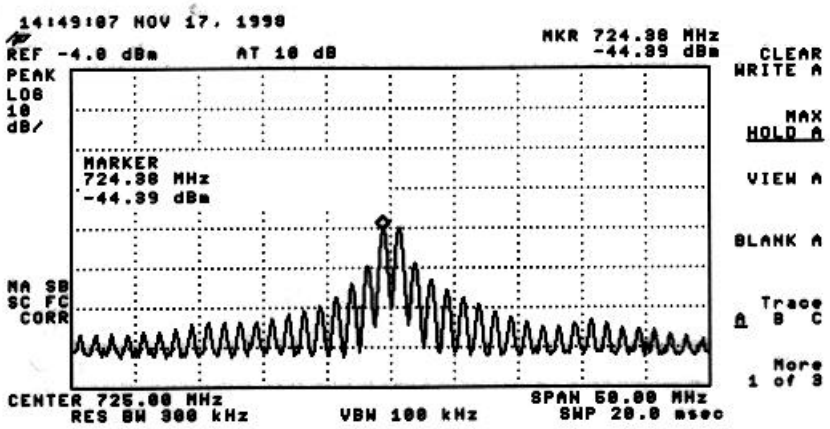

Figure A.7 Cross (Vertical) Polarization Measure with 3 Trees in Path

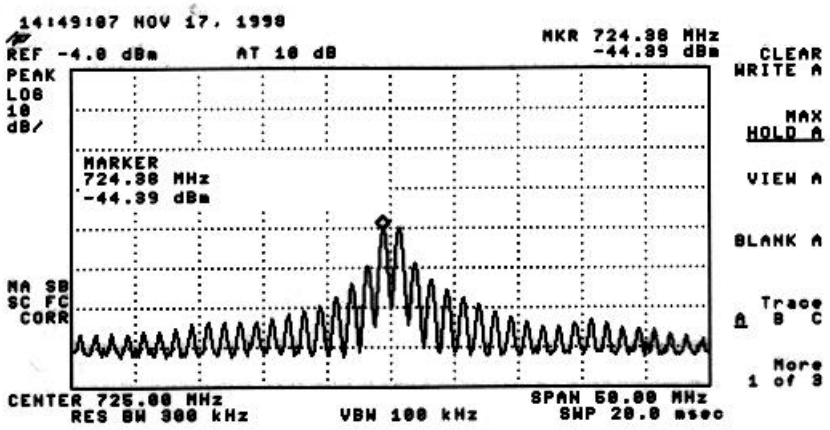

Figure A.8 Co (Horizontal) Polarization Measure with 3 Trees in Path

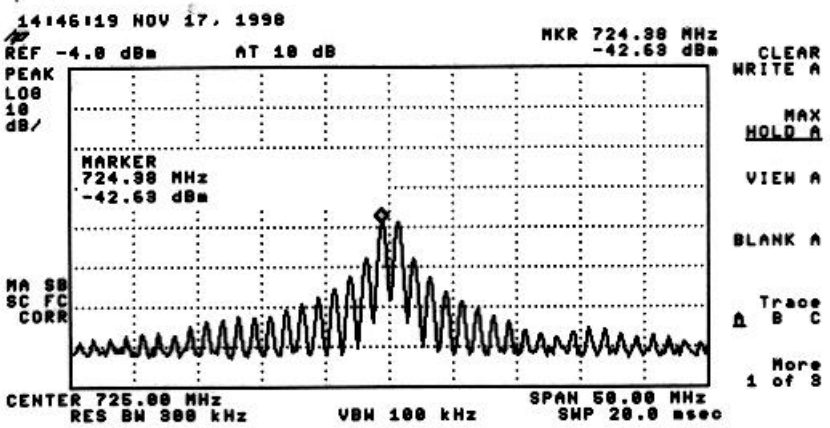

Figure A.9 Cross (Vertical) Polarization Measure with 4 Trees in Path

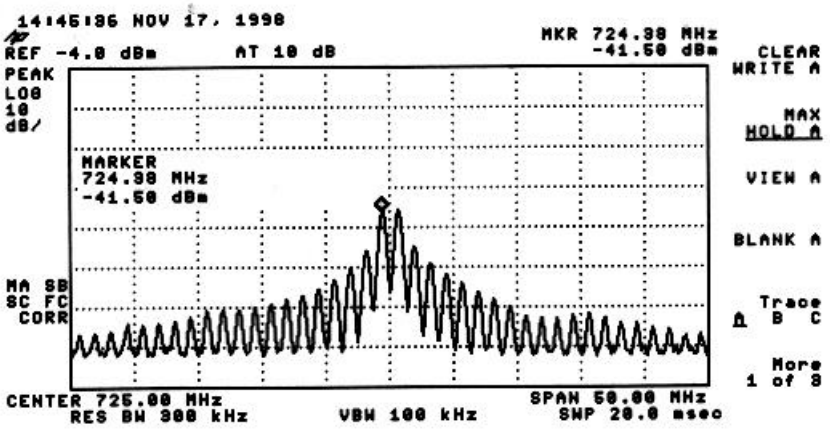

Figure A.10 Co (Horizontal) Polarization Measure with 4 Trees in Path

Appendix B: Measured and Reference Data

Table B.1 Measured Magnitude and Phase with 3 Trees in Path

Measurements taken on roof of Whittemore Hall at Virginia Tech University 11/17/98
Number of trees in path = 3; Signal generator = 5dBm; Attenuator = 0dB

Measured Symbol Time Point	Measured Magnitude	Measured Phase
0.0000E+00	1.0113E+00	-1.3776E+02
4.0000E-07	9.9363E-01	-1.3365E+02
8.0000E-07	1.0157E+00	4.2732E+01
1.2000E-06	9.8351E-01	4.6253E+01
1.6000E-06	9.9659E-01	-1.3645E+02
2.0000E-06	9.9134E-01	-1.3175E+02
2.4000E-06	1.0111E+00	4.4279E+01
2.8000E-06	9.9321E-01	4.8533E+01
3.2000E-06	9.9800E-01	-1.3500E+02
3.6000E-06	9.8541E-01	-1.3064E+02
4.0000E-06	1.0078E+00	4.6432E+01
4.4000E-06	9.9186E-01	5.1191E+01
4.8000E-06	1.0139E+00	-1.3416E+02
5.2000E-06	9.8769E-01	-1.3134E+02
5.6000E-06	1.0076E+00	4.3670E+01
6.0000E-06	1.0019E+00	4.7308E+01
6.4000E-06	1.0119E+00	-1.3659E+02
6.8000E-06	1.0020E+00	-1.3358E+02
7.2000E-06	1.0151E+00	4.1981E+01
7.6000E-06	9.9748E-01	4.6167E+01
8.0000E-06	1.0058E+00	-1.3798E+02
8.4000E-06	9.9583E-01	-1.3379E+02
8.8000E-06	1.0083E+00	4.2476E+01
9.2000E-06	9.9827E-01	4.7405E+01
9.6000E-06	1.0072E+00	-1.3676E+02
1.0000E-05	9.9672E-01	-1.3304E+02
1.0400E-05	1.0215E+00	4.3346E+01
1.0800E-05	1.0026E+00	4.6357E+01
1.1200E-05	9.9532E-01	-1.3792E+02
1.1600E-05	9.9066E-01	-1.3393E+02
1.2000E-05	1.0157E+00	4.1809E+01
1.2400E-05	9.8664E-01	4.5316E+01
1.2800E-05	1.0095E+00	-1.3868E+02
1.3200E-05	9.8538E-01	-1.3512E+02
1.3600E-05	1.0023E+00	3.9740E+01
1.4000E-05	9.8814E-01	4.4262E+01
1.4400E-05	1.0026E+00	-1.4076E+02
1.4800E-05	9.9014E-01	-1.3640E+02
1.5200E-05	1.0155E+00	4.0441E+01
1.5600E-05	9.8668E-01	4.4694E+01

1.6000E-05	9.9662E-01	-1.3906E+02
1.6400E-05	9.8889E-01	-1.3463E+02
1.6800E-05	9.9289E-01	4.1050E+01
1.7200E-05	9.9818E-01	4.5147E+01
1.7600E-05	1.0160E+00	-1.3819E+02
1.8000E-05	9.9558E-01	-1.3443E+02
1.8400E-05	1.0113E+00	4.2177E+01
1.8800E-05	9.7548E-01	4.6554E+01
1.9200E-05	1.0257E+00	-1.3861E+02
1.9600E-05	9.9515E-01	-1.3484E+02
2.0000E-05	9.9990E-01	4.1955E+01
2.0400E-05	9.8841E-01	4.6236E+01
2.0800E-05	1.0124E+00	-1.3732E+02
2.1200E-05	9.9386E-01	-1.3274E+02
2.1600E-05	1.0235E+00	4.3495E+01
2.2000E-05	9.8016E-01	4.8273E+01
2.2400E-05	1.0042E+00	-1.3698E+02
2.2800E-05	9.8527E-01	-1.3308E+02
2.3200E-05	9.9604E-01	4.3812E+01
2.3600E-05	9.9168E-01	4.7308E+01
2.4000E-05	1.0161E+00	-1.3686E+02
2.4400E-05	9.8434E-01	-1.3276E+02
2.4800E-05	1.0059E+00	4.3859E+01
2.5200E-05	9.9038E-01	4.8438E+01
2.5600E-05	1.0077E+00	-1.3517E+02
2.6000E-05	9.9533E-01	-1.3074E+02
2.6400E-05	1.0042E+00	4.5988E+01
2.6800E-05	9.9028E-01	4.9247E+01
2.7200E-05	1.0137E+00	-1.3441E+02
2.7600E-05	9.8314E-01	-1.2968E+02
2.8000E-05	1.0157E+00	4.6037E+01
2.8400E-05	9.8161E-01	4.9929E+01
2.8800E-05	1.0089E+00	-1.3380E+02
2.9200E-05	9.9262E-01	-1.3063E+02
2.9600E-05	1.0134E+00	4.5577E+01
3.0000E-05	1.0057E+00	4.8900E+01
3.0400E-05	1.0138E+00	-1.3605E+02
3.0800E-05	9.8992E-01	-1.3224E+02
3.1200E-05	1.0167E+00	4.2562E+01
3.1600E-05	9.8562E-01	4.6814E+01
3.2000E-05	1.0103E+00	-1.3819E+02
3.2400E-05	9.8386E-01	-1.3284E+02
3.2800E-05	1.0019E+00	4.2506E+01
3.3200E-05	9.8610E-01	4.7128E+01
3.3600E-05	1.0156E+00	-1.3757E+02
3.4000E-05	9.8406E-01	-1.3319E+02
3.4400E-05	1.0107E+00	4.2169E+01
3.4800E-05	9.7039E-01	4.6369E+01
3.5200E-05	1.0067E+00	-1.3670E+02

3.5600E-05	9.9813E-01	-1.3291E+02
3.6000E-05	1.0150E+00	4.4048E+01
3.6400E-05	9.8431E-01	4.7153E+01
3.6800E-05	1.0167E+00	-1.3662E+02
3.7200E-05	1.0059E+00	-1.3315E+02
3.7600E-05	1.0180E+00	4.2395E+01
3.8000E-05	9.8658E-01	4.5421E+01
3.8400E-05	1.0146E+00	-1.3879E+02
3.8800E-05	9.8058E-01	-1.3437E+02
3.9200E-05	1.0161E+00	4.1397E+01
3.9600E-05	9.9022E-01	4.4654E+01

Table B.2 Measured I and Q with 3 Trees in Path

Measurements taken on roof of Whittemore Hall at Virginia Tech University 11/17/98
Number of trees in path = 3; Signal generator = 5dBm; Attenuator = 0dB

Measured Symbol Time Point	Meausured I (Real)	Measured Q (Imaginary)
0.0000E+00	-7.4878E-01	-6.7981E-01
4.0000E-07	-6.8580E-01	-7.1901E-01
8.0000E-07	7.4606E-01	6.8923E-01
1.2000E-06	6.8007E-01	7.1049E-01
1.6000E-06	-7.2224E-01	-6.8670E-01
2.0000E-06	-6.6014E-01	-7.3957E-01
2.4000E-06	7.2392E-01	7.0592E-01
2.8000E-06	6.5768E-01	7.4425E-01
3.2000E-06	-7.0568E-01	-7.0570E-01
3.6000E-06	-6.4177E-01	-7.4778E-01
4.0000E-06	6.9460E-01	7.3021E-01
4.4000E-06	6.2163E-01	7.7289E-01
4.8000E-06	-7.0632E-01	-7.2745E-01
5.2000E-06	-6.5242E-01	-7.4153E-01
5.6000E-06	7.2886E-01	6.9578E-01
6.0000E-06	6.7938E-01	7.3643E-01
6.4000E-06	-7.3512E-01	-6.9544E-01
6.8000E-06	-6.9070E-01	-7.2584E-01
7.2000E-06	7.5462E-01	6.7901E-01
7.6000E-06	6.9081E-01	7.1955E-01
8.0000E-06	-7.4723E-01	-6.7331E-01
8.4000E-06	-6.8915E-01	-7.1885E-01
8.8000E-06	7.4369E-01	6.8089E-01
9.2000E-06	6.7564E-01	7.3488E-01
9.6000E-06	-7.3375E-01	-6.8991E-01
1.0000E-05	-6.8031E-01	-7.2844E-01
1.0400E-05	7.4288E-01	7.0118E-01
1.0800E-05	6.9195E-01	7.2553E-01
1.1200E-05	-7.3871E-01	-6.6706E-01
1.1600E-05	-6.8729E-01	-7.1346E-01

1.2000E-05	7.5710E-01	6.7715E-01
1.2400E-05	6.9380E-01	7.0150E-01
1.2800E-05	-7.5818E-01	-6.6646E-01
1.3200E-05	-6.9827E-01	-6.9527E-01
1.3600E-05	7.7071E-01	6.4077E-01
1.4000E-05	7.0766E-01	6.8966E-01
1.4400E-05	-7.7644E-01	-6.3424E-01
1.4800E-05	-7.1706E-01	-6.8280E-01
1.5200E-05	7.7286E-01	6.5871E-01
1.5600E-05	7.0140E-01	6.9395E-01
1.6000E-05	-7.5287E-01	-6.5302E-01
1.6400E-05	-6.9471E-01	-7.0377E-01
1.6800E-05	7.4877E-01	6.5205E-01
1.7200E-05	7.0401E-01	7.0763E-01
1.7600E-05	-7.5734E-01	-6.7729E-01
1.8000E-05	-6.9692E-01	-7.1097E-01
1.8400E-05	7.4944E-01	6.7899E-01
1.8800E-05	6.7081E-01	7.0822E-01
1.9200E-05	-7.6952E-01	-6.7812E-01
1.9600E-05	-7.0169E-01	-7.0566E-01
2.0000E-05	7.4360E-01	6.6847E-01
2.0400E-05	6.8368E-01	7.1383E-01
2.0800E-05	-7.4426E-01	-6.8629E-01
2.1200E-05	-6.7449E-01	-7.2994E-01
2.1600E-05	7.4251E-01	7.0448E-01
2.2000E-05	6.5238E-01	7.3151E-01
2.2400E-05	-7.3411E-01	-6.8517E-01
2.2800E-05	-6.7291E-01	-7.1968E-01
2.3200E-05	7.1876E-01	6.8955E-01
2.3600E-05	6.7242E-01	7.2889E-01
2.4000E-05	-7.4148E-01	-6.9477E-01
2.4400E-05	-6.6836E-01	-7.2265E-01
2.4800E-05	7.2532E-01	6.9699E-01
2.5200E-05	6.5705E-01	7.4104E-01
2.5600E-05	-7.1466E-01	-7.1046E-01
2.6000E-05	-6.4957E-01	-7.5415E-01
2.6400E-05	6.9775E-01	7.2225E-01
2.6800E-05	6.4645E-01	7.5017E-01
2.7200E-05	-7.0939E-01	-7.2407E-01
2.7600E-05	-6.2777E-01	-7.5662E-01
2.8000E-05	7.0508E-01	7.3107E-01
2.8400E-05	6.3189E-01	7.5118E-01
2.8800E-05	-6.9837E-01	-7.2813E-01
2.9200E-05	-6.4642E-01	-7.5328E-01
2.9600E-05	7.0935E-01	7.2379E-01
3.0000E-05	6.6112E-01	7.5786E-01
3.0400E-05	-7.2991E-01	-7.0357E-01
3.0800E-05	-6.6542E-01	-7.3291E-01
3.1200E-05	7.4882E-01	6.8765E-01

3.1600E-05	6.7453E-01	7.1865E-01
3.2000E-05	-7.5308E-01	-6.7350E-01
3.2400E-05	-6.6901E-01	-7.2139E-01
3.2800E-05	7.3863E-01	6.7697E-01
3.3200E-05	6.7090E-01	7.2269E-01
3.3600E-05	-7.4956E-01	-6.8527E-01
3.4000E-05	-6.7347E-01	-7.1751E-01
3.4400E-05	7.4908E-01	6.7848E-01
3.4800E-05	6.6958E-01	7.0236E-01
3.5200E-05	-7.3259E-01	-6.9042E-01
3.5600E-05	-6.7953E-01	-7.3110E-01
3.6000E-05	7.2957E-01	7.0572E-01
3.6400E-05	6.6937E-01	7.2167E-01
3.6800E-05	-7.3900E-01	-6.9827E-01
3.7200E-05	-6.8796E-01	-7.3379E-01
3.7600E-05	7.5179E-01	6.8635E-01
3.8000E-05	6.9248E-01	7.0272E-01
3.8400E-05	-7.6332E-01	-6.6843E-01
3.8800E-05	-6.8577E-01	-7.0090E-01
3.9200E-05	7.6221E-01	6.7190E-01
3.9600E-05	7.0441E-01	6.9595E-01

Table B.3 Measured Symbol Binary Value with 3 Trees in Path
Note: This table will be used to show reference symbol binary values, since the reference and measured symbol binary value are the same.

Measurements taken on roof of Whittemore Hall at Virginia Tech University 11/17/98
Number of trees in path = 3; Signal generator = 5dBm; Attenuator = 0dB
Binary 11 = 3.000E+00; Binary 00 = 0.0000E+00

Measured Symbol Time Point	Symbol Binary Value
0.0000E+00	3.0000E+00
4.0000E-07	3.0000E+00
8.0000E-07	0.0000E+00
1.2000E-06	0.0000E+00
1.6000E-06	3.0000E+00
2.0000E-06	3.0000E+00
2.4000E-06	0.0000E+00
2.8000E-06	0.0000E+00
3.2000E-06	3.0000E+00
3.6000E-06	3.0000E+00
4.0000E-06	0.0000E+00
4.4000E-06	0.0000E+00
4.8000E-06	3.0000E+00
5.2000E-06	3.0000E+00
5.6000E-06	0.0000E+00
6.0000E-06	0.0000E+00
6.4000E-06	3.0000E+00
6.8000E-06	3.0000E+00
7.2000E-06	0.0000E+00

7.6000E-06	0.0000E+00
8.0000E-06	3.0000E+00
8.4000E-06	3.0000E+00
8.8000E-06	0.0000E+00
9.2000E-06	0.0000E+00
9.6000E-06	3.0000E+00
1.0000E-05	3.0000E+00
1.0400E-05	0.0000E+00
1.0800E-05	0.0000E+00
1.1200E-05	3.0000E+00
1.1600E-05	3.0000E+00
1.2000E-05	0.0000E+00
1.2400E-05	0.0000E+00
1.2800E-05	3.0000E+00
1.3200E-05	3.0000E+00
1.3600E-05	0.0000E+00
1.4000E-05	0.0000E+00
1.4400E-05	3.0000E+00
1.4800E-05	3.0000E+00
1.5200E-05	0.0000E+00
1.5600E-05	0.0000E+00
1.6000E-05	3.0000E+00
1.6400E-05	3.0000E+00
1.6800E-05	0.0000E+00
1.7200E-05	0.0000E+00
1.7600E-05	3.0000E+00
1.8000E-05	3.0000E+00
1.8400E-05	0.0000E+00
1.8800E-05	0.0000E+00
1.9200E-05	3.0000E+00
1.9600E-05	3.0000E+00
2.0000E-05	0.0000E+00
2.0400E-05	0.0000E+00
2.0800E-05	3.0000E+00
2.1200E-05	3.0000E+00
2.1600E-05	0.0000E+00
2.2000E-05	0.0000E+00
2.2400E-05	3.0000E+00
2.2800E-05	3.0000E+00
2.3200E-05	0.0000E+00
2.3600E-05	0.0000E+00
2.4000E-05	3.0000E+00
2.4400E-05	3.0000E+00
2.4800E-05	0.0000E+00
2.5200E-05	0.0000E+00
2.5600E-05	3.0000E+00
2.6000E-05	3.0000E+00
2.6400E-05	0.0000E+00
2.6800E-05	0.0000E+00

2.7200E-05	3.0000E+00
2.7600E-05	3.0000E+00
2.8000E-05	0.0000E+00
2.8400E-05	0.0000E+00
2.8800E-05	3.0000E+00
2.9200E-05	3.0000E+00
2.9600E-05	0.0000E+00
3.0000E-05	0.0000E+00
3.0400E-05	3.0000E+00
3.0800E-05	3.0000E+00
3.1200E-05	0.0000E+00
3.1600E-05	0.0000E+00
3.2000E-05	3.0000E+00
3.2400E-05	3.0000E+00
3.2800E-05	0.0000E+00
3.3200E-05	0.0000E+00
3.3600E-05	3.0000E+00
3.4000E-05	3.0000E+00
3.4400E-05	0.0000E+00
3.4800E-05	0.0000E+00
3.5200E-05	3.0000E+00
3.5600E-05	3.0000E+00
3.6000E-05	0.0000E+00
3.6400E-05	0.0000E+00
3.6800E-05	3.0000E+00
3.7200E-05	3.0000E+00
3.7600E-05	0.0000E+00
3.8000E-05	0.0000E+00
3.8400E-05	3.0000E+00
3.8800E-05	3.0000E+00
3.9200E-05	0.0000E+00
3.9600E-05	0.0000E+00

Table B.4 Reference Magnitude and Phase with 3 Trees in Path

Measurements taken on roof of Whittemore Hall at Virginia Tech University 11/17/98
Number of trees in path = 3; Signal generator = 5dBm; Attenuator = 0dB

Reference Symbol Time Point	Reference Magnitude	Reference Phase
0.0000E+00	1.0000E+00	-1.3500E+02
4.0000E-07	1.0000E+00	-1.3500E+02
8.0000E-07	1.0000E+00	4.5000E+01
1.2000E-06	1.0000E+00	4.5000E+01
1.6000E-06	1.0000E+00	-1.3500E+02
2.0000E-06	1.0000E+00	-1.3500E+02
2.4000E-06	1.0000E+00	4.5000E+01
2.8000E-06	1.0000E+00	4.5000E+01
3.2000E-06	1.0000E+00	-1.3500E+02

3.6000E-06	1.0000E+00	-1.3500E+02
4.0000E-06	1.0000E+00	4.5000E+01
4.4000E-06	1.0000E+00	4.5000E+01
4.8000E-06	1.0000E+00	-1.3500E+02
5.2000E-06	1.0000E+00	-1.3500E+02
5.6000E-06	1.0000E+00	4.5000E+01
6.0000E-06	1.0000E+00	4.5000E+01
6.4000E-06	1.0000E+00	-1.3500E+02
6.8000E-06	1.0000E+00	-1.3500E+02
7.2000E-06	1.0000E+00	4.5000E+01
7.6000E-06	1.0000E+00	4.5000E+01
8.0000E-06	1.0000E+00	-1.3500E+02
8.4000E-06	1.0000E+00	-1.3500E+02
8.8000E-06	1.0000E+00	4.5000E+01
9.2000E-06	1.0000E+00	4.5000E+01
9.6000E-06	1.0000E+00	-1.3500E+02
1.0000E-05	1.0000E+00	-1.3500E+02
1.0400E-05	1.0000E+00	4.5000E+01
1.0800E-05	1.0000E+00	4.5000E+01
1.1200E-05	1.0000E+00	-1.3500E+02
1.1600E-05	1.0000E+00	-1.3500E+02
1.2000E-05	1.0000E+00	4.5000E+01
1.2400E-05	1.0000E+00	4.5000E+01
1.2800E-05	1.0000E+00	-1.3500E+02
1.3200E-05	1.0000E+00	-1.3500E+02
1.3600E-05	1.0000E+00	4.5000E+01
1.4000E-05	1.0000E+00	4.5000E+01
1.4400E-05	1.0000E+00	-1.3500E+02
1.4800E-05	1.0000E+00	-1.3500E+02
1.5200E-05	1.0000E+00	4.5000E+01
1.5600E-05	1.0000E+00	4.5000E+01
1.6000E-05	1.0000E+00	-1.3500E+02
1.6400E-05	1.0000E+00	-1.3500E+02
1.6800E-05	1.0000E+00	4.5000E+01
1.7200E-05	1.0000E+00	4.5000E+01
1.7600E-05	1.0000E+00	-1.3500E+02
1.8000E-05	1.0000E+00	-1.3500E+02
1.8400E-05	1.0000E+00	4.5000E+01
1.8800E-05	1.0000E+00	4.5000E+01
1.9200E-05	1.0000E+00	-1.3500E+02
1.9600E-05	1.0000E+00	-1.3500E+02
2.0000E-05	1.0000E+00	4.5000E+01
2.0400E-05	1.0000E+00	4.5000E+01
2.0800E-05	1.0000E+00	-1.3500E+02
2.1200E-05	1.0000E+00	-1.3500E+02
2.1600E-05	1.0000E+00	4.5000E+01
2.2000E-05	1.0000E+00	4.5000E+01
2.2400E-05	1.0000E+00	-1.3500E+02
2.2800E-05	1.0000E+00	-1.3500E+02

2.3200E-05	1.0000E+00	4.5000E+01
2.3600E-05	1.0000E+00	4.5000E+01
2.4000E-05	1.0000E+00	-1.3500E+02
2.4400E-05	1.0000E+00	-1.3500E+02
2.4800E-05	1.0000E+00	4.5000E+01
2.5200E-05	1.0000E+00	4.5000E+01
2.5600E-05	1.0000E+00	-1.3500E+02
2.6000E-05	1.0000E+00	-1.3500E+02
2.6400E-05	1.0000E+00	4.5000E+01
2.6800E-05	1.0000E+00	4.5000E+01
2.7200E-05	1.0000E+00	-1.3500E+02
2.7600E-05	1.0000E+00	-1.3500E+02
2.8000E-05	1.0000E+00	4.5000E+01
2.8400E-05	1.0000E+00	4.5000E+01
2.8800E-05	1.0000E+00	-1.3500E+02
2.9200E-05	1.0000E+00	-1.3500E+02
2.9600E-05	1.0000E+00	4.5000E+01
3.0000E-05	1.0000E+00	4.5000E+01
3.0400E-05	1.0000E+00	-1.3500E+02
3.0800E-05	1.0000E+00	-1.3500E+02
3.1200E-05	1.0000E+00	4.5000E+01
3.1600E-05	1.0000E+00	4.5000E+01
3.2000E-05	1.0000E+00	-1.3500E+02
3.2400E-05	1.0000E+00	-1.3500E+02
3.2800E-05	1.0000E+00	4.5000E+01
3.3200E-05	1.0000E+00	4.5000E+01
3.3600E-05	1.0000E+00	-1.3500E+02
3.4000E-05	1.0000E+00	-1.3500E+02
3.4400E-05	1.0000E+00	4.5000E+01
3.4800E-05	1.0000E+00	4.5000E+01
3.5200E-05	1.0000E+00	-1.3500E+02
3.5600E-05	1.0000E+00	-1.3500E+02
3.6000E-05	1.0000E+00	4.5000E+01
3.6400E-05	1.0000E+00	4.5000E+01
3.6800E-05	1.0000E+00	-1.3500E+02
3.7200E-05	1.0000E+00	-1.3500E+02
3.7600E-05	1.0000E+00	4.5000E+01
3.8000E-05	1.0000E+00	4.5000E+01
3.8400E-05	1.0000E+00	-1.3500E+02
3.8800E-05	1.0000E+00	-1.3500E+02
3.9200E-05	1.0000E+00	4.5000E+01
3.9600E-05	1.0000E+00	4.5000E+01

Table B.5 Reference I and Q with 3 Trees in Path

Measurements taken on roof of Whittemore Hall at Virginia Tech University 11/17/98
Number of trees in path = 3; Signal generator = 5dBm; Attenuator = 0dB

Reference Symbol Time Point	Reference I (Real)	Reference Q (Imaginary)
0.0000E+00	-7.0711E-01	-7.0711E-01
4.0000E-07	-7.0711E-01	-7.0711E-01
8.0000E-07	7.0711E-01	7.0711E-01
1.2000E-06	7.0711E-01	7.0711E-01
1.6000E-06	-7.0711E-01	-7.0711E-01
2.0000E-06	-7.0711E-01	-7.0711E-01
2.4000E-06	7.0711E-01	7.0711E-01
2.8000E-06	7.0711E-01	7.0711E-01
3.2000E-06	-7.0711E-01	-7.0711E-01
3.6000E-06	-7.0711E-01	-7.0711E-01
4.0000E-06	7.0711E-01	7.0711E-01
4.4000E-06	7.0711E-01	7.0711E-01
4.8000E-06	-7.0711E-01	-7.0711E-01
5.2000E-06	-7.0711E-01	-7.0711E-01
5.6000E-06	7.0711E-01	7.0711E-01
6.0000E-06	7.0711E-01	7.0711E-01
6.4000E-06	-7.0711E-01	-7.0711E-01
6.8000E-06	-7.0711E-01	-7.0711E-01
7.2000E-06	7.0711E-01	7.0711E-01
7.6000E-06	7.0711E-01	7.0711E-01
8.0000E-06	-7.0711E-01	-7.0711E-01
8.4000E-06	-7.0711E-01	-7.0711E-01
8.8000E-06	7.0711E-01	7.0711E-01
9.2000E-06	7.0711E-01	7.0711E-01
9.6000E-06	-7.0711E-01	-7.0711E-01
1.0000E-05	-7.0711E-01	-7.0711E-01
1.0400E-05	7.0711E-01	7.0711E-01
1.0800E-05	7.0711E-01	7.0711E-01
1.1200E-05	-7.0711E-01	-7.0711E-01
1.1600E-05	-7.0711E-01	-7.0711E-01
1.2000E-05	7.0711E-01	7.0711E-01
1.2400E-05	7.0711E-01	7.0711E-01
1.2800E-05	-7.0711E-01	-7.0711E-01
1.3200E-05	-7.0711E-01	-7.0711E-01
1.3600E-05	7.0711E-01	7.0711E-01
1.4000E-05	7.0711E-01	7.0711E-01
1.4400E-05	-7.0711E-01	-7.0711E-01
1.4800E-05	-7.0711E-01	-7.0711E-01
1.5200E-05	7.0711E-01	7.0711E-01
1.5600E-05	7.0711E-01	7.0711E-01
1.6000E-05	-7.0711E-01	-7.0711E-01
1.6400E-05	-7.0711E-01	-7.0711E-01

1.6800E-05	7.0711E-01	7.0711E-01
1.7200E-05	7.0711E-01	7.0711E-01
1.7600E-05	-7.0711E-01	-7.0711E-01
1.8000E-05	-7.0711E-01	-7.0711E-01
1.8400E-05	7.0711E-01	7.0711E-01
1.8800E-05	7.0711E-01	7.0711E-01
1.9200E-05	-7.0711E-01	-7.0711E-01
1.9600E-05	-7.0711E-01	-7.0711E-01
2.0000E-05	7.0711E-01	7.0711E-01
2.0400E-05	7.0711E-01	7.0711E-01
2.0800E-05	-7.0711E-01	-7.0711E-01
2.1200E-05	-7.0711E-01	-7.0711E-01
2.1600E-05	7.0711E-01	7.0711E-01
2.2000E-05	7.0711E-01	7.0711E-01
2.2400E-05	-7.0711E-01	-7.0711E-01
2.2800E-05	-7.0711E-01	-7.0711E-01
2.3200E-05	7.0711E-01	7.0711E-01
2.3600E-05	7.0711E-01	7.0711E-01
2.4000E-05	-7.0711E-01	-7.0711E-01
2.4400E-05	-7.0711E-01	-7.0711E-01
2.4800E-05	7.0711E-01	7.0711E-01
2.5200E-05	7.0711E-01	7.0711E-01
2.5600E-05	-7.0711E-01	-7.0711E-01
2.6000E-05	-7.0711E-01	-7.0711E-01
2.6400E-05	7.0711E-01	7.0711E-01
2.6800E-05	7.0711E-01	7.0711E-01
2.7200E-05	-7.0711E-01	-7.0711E-01
2.7600E-05	-7.0711E-01	-7.0711E-01
2.8000E-05	7.0711E-01	7.0711E-01
2.8400E-05	7.0711E-01	7.0711E-01
2.8800E-05	-7.0711E-01	-7.0711E-01
2.9200E-05	-7.0711E-01	-7.0711E-01
2.9600E-05	7.0711E-01	7.0711E-01
3.0000E-05	7.0711E-01	7.0711E-01
3.0400E-05	-7.0711E-01	-7.0711E-01
3.0800E-05	-7.0711E-01	-7.0711E-01
3.1200E-05	7.0711E-01	7.0711E-01
3.1600E-05	7.0711E-01	7.0711E-01
3.2000E-05	-7.0711E-01	-7.0711E-01
3.2400E-05	-7.0711E-01	-7.0711E-01
3.2800E-05	7.0711E-01	7.0711E-01
3.3200E-05	7.0711E-01	7.0711E-01
3.3600E-05	-7.0711E-01	-7.0711E-01
3.4000E-05	-7.0711E-01	-7.0711E-01
3.4400E-05	7.0711E-01	7.0711E-01
3.4800E-05	7.0711E-01	7.0711E-01
3.5200E-05	-7.0711E-01	-7.0711E-01
3.5600E-05	-7.0711E-01	-7.0711E-01
3.6000E-05	7.0711E-01	7.0711E-01

3.6400E-05	7.0711E-01	7.0711E-01
3.6800E-05	-7.0711E-01	-7.0711E-01
3.7200E-05	-7.0711E-01	-7.0711E-01
3.7600E-05	7.0711E-01	7.0711E-01
3.8000E-05	7.0711E-01	7.0711E-01
3.8400E-05	-7.0711E-01	-7.0711E-01
3.8800E-05	-7.0711E-01	-7.0711E-01
3.9200E-05	7.0711E-01	7.0711E-01
3.9600E-05	7.0711E-01	7.0711E-01

References:

1 "BWA LMDS Tutorial." < http://www.bni.ca/lmds.html > (31 October 1998).

2 "Dudley Lab's list of Frequency Allocations." < http://www.dudleylab.com/freqaloc.html > (31 October 1998)

3 McCabe, Tom, "What Lies Ahead for LMDS." *America's Network*, July 1998, S-8 – S-13.

4 Nakonecznyj, Ihor, "Marketplace Demand for Bandwidth Here and Now Gives LMDS Edge.", *America's Network*, July 1998, S-14 – S-16.

5 Sukow, Randy, "LMDS", *Wireless Business and Technolog*, August 1998, 18-34.

6 "How do Cable Modems Work ???." <http://www.cablemodems.com/work.html> (31 October 1998).

7 "Cable Networks." <http://videotron.ab.ca/Technology/netpt1.html > (31 October 1998).

8 "Digital Subscriber Line, The Future of Remote Access." < http://www.ascend.com> (31 October 1998) Check home machine for verification.

9 "How Does ADSL Work." <http://www.orckit.com/how_does_ads_works.html> (31 October 1998)

10 "General Introduction to Copper Access Technologies." <http://www.adsl.com/general_tutorial.html > (31 October 1998)

11 "ADSL Tutorial, Twisted Pair Access to the Information Highway." <http://indy.net/adsl/tutorial.html > (31 October 1998)

12 "Federal Communications Commission, FCC98-231, MM Docket No. 97-217, File No. RM-906." <http://www.fcc.gov/Bureaus/Mass_Media/Orders/1998/fcc98231.pdf> (31 October 1998)

13 Champy, Ed, "Press Release, Spike Technologies PRIZM BDS Captures two of twelve SuperQuest Awards at Supercomm 98 in Atlanta. ", June 1998.

14 Freeman, Roger L., *Radio Systems Design Telecommunications*, John Wiley & Sons, Inc., New York, NY, 1997.

15 Freeman, Roger L., *Telecommunications Transmission Handbook 2nd Edition*, John Wiley & Sons, Inc., New York, NY, 1981.

16 Woerner, Brian D., "Class Notes EE5984 Digital Communications Spring Semester 1998. ", January 1998.

17 Woerner, Brian D., "Class Notes EE4634 Analog and Digital Communications Fall Semester 1997.", August 1997.

18 Bostian, Charles and Pratt, Timothy, *Satellite Communications*, John Wiley & Sons, Inc., New York, NY, 1986.

19 Couch, Leon W., *Digital and Analog Communication Systems 5th Edition*, Prentice-Hall, Inc., Upper Saddle River, NJ, 1997.

20 Sklar, Bernard, *Digital Communications Fundamentals and Applications*, Prentice-Hall, Inc., Upper Saddle River, NJ, 1988.

21 Rappaport, Theodore S., *Wireless Communications Principles & Practices*, Prentice-Hall, Inc., Upper Saddle River, NJ, 1996.

22 Bostian, Charles and Manning, Edward, "LMDS Propagation Workshop", Charlotte, NC, September 1998.

23 Allen, Arnold O., *Probability, Statistics, and Queuing Theory with Computer Science Applications, Second Edition*, Academic Press, Inc., San Diego, CA, 1990.

24 Brodhage, Helmut and Hormuth, Wilhelm, *Planning and Engineering of Radio Relay Links*, Heyden & Son Ltd., London, England, 1977.

25 Violette, Edmond; Espeland, Richard; DeBolt, Robert; and Schwering, Felix, "Millimeter-Wave Propagation at Street Level in and Urban Environment." *IEEE Transactions on Geoscience and Remote Sensing*, Vol. 26, No. 3, pp. 368-380, May 1988.

26 Ippolito, Louis J., *Propagation Effects Handbook for Satellite Systems Design, Fourth Edition*, NASA RP-1082 (04), Washington, DC, February 1989.

27 Allnutt, J.E., *Satellite to Ground Radiowave Propagation*, Peter Peregrinus Ltd., London, UK, 1989.

28 Rec. ITU-R P.530-7, "Propagation Data and Prediction Methods Required for the Design of Terrestrial Line-of-Sight Systems.", International Telecommunications Union, Radiocommunications Assembly, Geneva, Switzerland, 1997.

29 Rec. ITU-R P.838, "Specific Attenuation Model for Rain Use in Prediction Methods.", International Telecommunications Union, Radiocommunications Assembly, Geneva, Switzerland, 1997.

30 Rec. ITU-R PN.837, "Characteristics of Precipitation Modeling.", International Telecommunications Union, Radiocommunications Assembly, Geneva, Switzerland, 1997.

31 Schwering, Felix K.; Violette, Edmond J.; and Espeland, Richard H., "Millimeter-Wave Propagation in Vegetation: Experiments and Theory.", *IEEE Transactions on Geoscience and Remote Sensing*, Vol. 26, No. 3, pp. 355-367, May 1988.

32 Majeed, Mohamed and Tjuatja, Saibun, "An Improved Propagation Model for Wireless Communications.", 1995 IEEE International Conference on Communications. Converging Technologies for Tomorrow's Applications. ICC '96. Conference Record (Cat. No. 96CH35916), p. 3 vol. Xxxix+1848, 292-296 vol.1.

33 Al-Nuaimi, M.O. and Stephens, R.B.L, "Measurements and Prediction Model Optimization for Signal Attenuation in Vegetation Media at Centimeter Wave Frequencies .", *IEE Proc.-Microw. Antennas Propag.*, Vol. 145, No. 3, June 1998.

34 Seville, A., "Vegetation Attenuation: Modeling and Measurements at Millimetric Frequencies.", 10th International Conference on Antennas and Propagation (Conf. Publ. No. 436), p. 2 vol. (xxxiii+553+396), 5-8 vol. 2.

35 Stanford Telecom, "Presentation on Wireless Broadband Distribution Systems.", 1998.

36 Gray, Douglas, “Hewlett-Packard Presentation, Optimal Cell Deployment for LMDS Systems.”, Wireless Broadband TeleStrategies Conference, Washington, DC, July 15, 1996

37 Hewlett-Packard Company, “HP Application Note 1296, LMDS-The Wireless Interactive Broadband Access Service”, 1997.

38 Gray, Douglas A., “A Broadband Wireless Access System at 28GHz.”, 0-7803-4194-5/97 IEEE Wireless Communications Conference 1997, 1997.

39 Papazian, P.B.; Jones, D.L.; Espeland R.H., “Wideband Propagation Measurements at 30.3GHz through a Pecan Orchard in Texas. ”, U.S. Department of Commerce, NTIA Report 92-287, September 1992.

40 Hewlett-Packard Company, “HP ESG-D Series RF Signal Generators Option UN8 Product Overview”, 1998.

41 Hewlett Packard Company, “Product Note HP 89400-8, Using vector modulation analysis in the integration troubleshooting and design of digital RF communications systems”, 1994.

42 Timothy Pratt, private communication.

Edward P. Manning

Edward Manning served four years in the U.S. Army working for the Intelligence Security Command (INSCOM). After his military experience, Ed received a Bachelor of Science in Electrical Engineering from Penn State University. He spent 1 ½ years working in industry prior to attending Virginia Tech for graduate studies. While at Virginia Tech, Ed worked as a Graduate Research Assistant for both the Center for Wireless Telecommunications (CWT) and Communication Network Services (CNS). Ed's professional interests are in the planning, design, and implementation of wireless systems.